1190452 (5909045)
ROBINSON,RGR/ ELECTRI

All rights reserved

INFORMATION TO ALL USERS
The quality of this reproduction is dependent upon the quality of the copy submitted.

In the unlikely event that the author did not send a complete manuscript
and there are missing pages, these will be noted. Also, if material had to be removed,
a note will indicate the deletion.

Published by ProQuest LLC (2017). Copyright of the Dissertation is held by the Author.

All rights reserved.
This work is protected against unauthorized copying under Title 17, United States Code
Microform Edition © ProQuest LLC.

ProQuest LLC.
789 East Eisenhower Parkway
P.O. Box 1346
Ann Arbor, MI 48106 - 1346

THE ELECTRICAL PROPERTIES OF GOLD AND TANTALUM THIN FILMS AFTER ARGON ION IMPLANTATION

R. G. R. ROBINSON, B.Sc. DUNELM 1943

540905

Foreward by I.H. Wilson (Supervisor)

This thesis has been assembled by myself from papers found at his home after the tragic death of Graham Robinson, known to us all as Gray. His experimental work was nearly complete and he had finished the chapters on experimental procedure and the results for his thesis. The other main document available to us was his transfer report and parts of this are reproduced in the appropriate chapters. The work falls into two parts - argon bombardment of gold films, and argon bombardment of tantalum films. The transfer report refers only to the former and so comments by myself (in italics) will be included where necessary. Extracts from other material will be included where appropriate. The main results of the work on gold films has already been published.[1]

Contents

	Page
Abstract	1
1 Introduction	4
2 Theory	7
2.1 Introduction	7
2.2 The effect of sputtering on the conductivity of thin films	8
2.2.1 Ion bombardment	8
2.2.2 Electrical resistance	9
2.2.3 Tantalum films (unknown density)	10
2.3 Strain sensitivity	11
2.3.1 Longitudinal gauge factor	13
2.3.2 Transverse gauge factor	14
2.4 The temperature coefficient of strain gauge factor β	14
2.5 Theoretical value of the temperature coefficient of resistance α	15
2.6 Statistical methods	17
3 Experimental Techniques	18
3.1 Thin films	18
3.1.1 Substrate Preparation	18
3.1.2 Gold Films	18
3.1.3 Tantalum Films	18
3.1.4 Electrode Pads	19
3.1.5 Ion Bombardment	19
3.2 Measurements	20

Contents (continued)

3.2.1 Resistance Measurement 20

3.2.2 Temperature Control and Measurement 23

3.2.3 Temperature Coefficient of Resistance 25

3.2.4 Strain-Gauge Factor 27

3.3 Anodising 31

3.4 Vacuum Annealing 34

4 Results 37

4.1 Gold Films 38

4.1.1 Sheet Resistance 38

4.1.2 Resistivity 40

4.1.3 Annealing 40

4.1.4 Temperature Coefficient of Resistance 46

4.1.5 Strain-Gauge Coefficient of Resistance 46

4.1.6 Temperature Coefficient of Strain-Gauge Factor 52

4.1.7 S.E.M. Microscope Examination 52

4.1.8 Microprobe Analysis 55

4.2 Tantalum Films Before Bombardment 55

4.2.1 Sheet Resistance 57

4.2.2 Temperature Coefficient of Resistance 57

4.2.3 Strain-Gauge Coefficient of Resistance 62

4.3 Bombarded Tantalum Films 67

4.3.1 Resistance 67

4.3.2 Temperature Coefficient of Resistance 71

4.3.3 Strain-Gauge Factor 75

4.3.4 Annealing 75

4.3.5 Depth profiling by anodization 80

Contents (continued)

5 Discussion of results 87

5.1 Gold films 87

5.1.1 Strain gauge coefficient (γ) 87

5.1.2 Tunnelling 88

5.1.3 Metallic conduction 89

5.1.4 The temperature coefficient of resistance (α) 90

5.1.5 The temperature coefficient of strain gauge factor (β) 91

5.1.6 The structure of the bombarded films 92

5.1.7 The resistance ageing effect 93

5.1.8 The drop in resistance for doses below 2×10^{15} ions cm^{-2} 95

5.2 Tantalum films 95

5.2.1 The as-deposited films 95

5.2.2 The effect of argon bombardment on resistivity 96

5.2.3 Changes in T.C.R. as a result of argon bombardment 97

5.2.4 Changes in strain gauge factor as a result of argon bombardment 98

5.2.5 Resistance ageing 98

6 Conclusions 100

6.1 Argon bombardment of gold films 100

6.2 Argon bombardment of tantalum films 102

7 References 104

8 Appendices 106

ABSTRACT

Evaporated gold and tantalum films have been bombarded with argon ions. In the case of gold films this resulted in an increase of the sheet-resistance by sputter etching to a maximum of 40 kΩ/□ . The strain-gauge coefficient of resistance (γ) (i.e. the fractional change in resistance per unit strain) was measured for films with a wide range of sheet-resistance, and was found to be almost invariant with an average of 2.6. This contrasts greatly with the published values of γ of up to 100 for thin island-structure evaporated films of similar sheet-resistance.

The temperature coefficient of strain-gauge factor (β) was found to be similar in magnitude but opposite in sign to the temperature coefficient of resistivity (α), which was measured as $+12 \times 10^{4}/^{0}C$.

The measured values of γ, β and α agree well with values calculated assuming metallic conduction modified by reduction of the electron mean-free-path. We, therefore, conclude that a connected metallic layer still exists at very high values of sheet-resistance.

ABSTRACT (continued)

In the case of tantalum films (that contain 30 atomic per cent oxygen) conduction was found to be by a combination of metallic and activated tunnelling. In the latter case there is some evidence for an increase in importance of this mechanism with oxygen concentration and for the existence of at least two activation energies.

After bombardment with low doses of argon the resistivity (ρ) and also α shifted markedly towards values expected of very pure tantalum films, probably as a result of radiation enhanced diffusion and preferential sputtering of oxygen combined with re-arrangement of the film to form large precipitates of b.c.c. tantalum.

There was aso a significant increase in γ (from an average of 3 up to 5.2) at similar doses, possibly as a result of changes in the microstructure increasing the importance of strain induced changes in the metallic conduction paths in the film..

The metallic phase appears to be metastable as ρ increases with time (up to two years) at room temperature, probably due to reaction with oxygen near the film/substrate interface.

For higher doses ρ drops (but not in a way explainable by sputter etching) α changes from a large positive value to a small negative one, and γ drops towards a value of 2 which is the predicted value for Ta on glass.

ABSTRACT (continued)

These results indicate that a single phase, stable, low sputtering rate compound is formed, probably by reaction with the glass substrate. This compound has a mixture of activated tunnelling and metallic conduction with the strain gauge factor apparently determined by the metallic component of conduction.

Some preliminary attempts at electrical depth profiling of the bombarded tantalum films by anodization are reported and the results support the models proposed above.

1. Introduction

This work is part of a programme aimed at understanding the effects of ion bombardment on the electrical properties of thin metal films.

Measurement of strain-gauge coefficient of resistance, henceforth called strain-gauge factor, was undertaken because it provides information on conduction mechanisms that are dominant in the implanted thin films, and because work on active ion implantation of active metal films has indicated that this technique might be used to produce useful devices.[2,3]

Argon bombardment of gold films was chosen for the first study because of the inert nature of ion and target, and because the sputtering characteristics are reasonably well understood. In addition evaporated gold films have shown a very large difference in strain-gauge factor (γ) (two orders of magnitude) between structures of the connected type (metallic conduction) and discontinuous island structures (tunnelling conduction).[4,5]

The strain gauge factor is defined by; $\gamma \equiv (\delta R/R)/(\delta \ell/\ell)$ where R is the resistance and ℓ is the length of the conductor.

Continuous 200 Å evaporated gold films on glass substrates have been bombarded with 40 keV argon ions to increase the sheet-resistance by several orders of magnitude, into the region where

thin evaporated films would be discontinuous. The values of γ and α(the temperature coefficient of resistance or T.C.R.) and also the temperature coefficient of the strain-gauge factor (β), were measured.

In the second study the same (inert) ion was used but a chemically reactive film, tantalum, was used in order to determine the effects on strain-gauge factor of structural changes observed by other workers at Surrey[6,7,8] on similar films. A large amount of data was accumulated on the properties of the 'as deposited' films (resistivity, T.C.R., activation energy for conduction, strain-gauge factor and stability), as well as determination of the effects of argon bombardment on these properties.

A first attempt was made at determining electrical properties as a function of depth by anodic oxide profiling. Although the latter was not completely successful it provided the ground-work that lead to a very successful technique being developed by other workers at Surrey.[8]

2. Theory

2.1 Introduction

This section is a compilation of the relationships devised by Gray. These are used in the results section for comparison with experimental results.

2.2 The effect of sputtering on the conductivity of thin films

Consider 1 cm^3 of pure gold. Its mass is 19.3 g, and its relative mass is $\frac{19.3}{197}$ mole.

The number of atoms contained in 1 cm^3, is, by Avogadro's Number,

$$\frac{19.3}{197} \times 6.025 \times 10^{23}, = 59 \times 10^{21} \text{ atoms.}$$

Thus the number of gold atoms per unit atomic area in a 1 cm length is, on average,

$$\sqrt[3]{59 \times 10^{21}} = 3.893 \times 10^{7} ;$$

and the average number per unit atomic area in the thickness of a 240 Å film is

$$240 \times 10^{-8} \times 3.893 \times 10^{7} = 93.5 \text{ atoms.}$$

The mean linear distance between atoms is 2.57 Å .

2.2.1 Ion Bombardment

A monatomic layer of gold 1 cm^2 in area would contain,

$$(3.893 \times 10^{7})^2 = 15.15 \times 10^{14} \text{ atoms.}$$

Let the number of conducting atoms affected by the ion bombardment be S atoms/ion. [Note: this is similar to the sputter rate which, for gold, is 10 atoms/ion with argon ions at 40 keV.]

The number of ions required to remove, by sputtering, the number of atoms equivalent to a monatomic layer of gold is, therefore,

$$\frac{15.15 \times 10^{14}}{S} \text{ ions.cm}^{-2} ;$$

and this would involve an electric charge of

$$\frac{15.15 \times 10^{14}}{S} \times 1.60 \times 10^{-19} \text{ coulomb/cm}^2$$

$$= \frac{242}{S} \ \mu\text{C.cm}^{-2} . \qquad \text{--------- } 2.1$$

The charge to remove atoms equivalent to a film of mean thickness 240-Å would be

$$\frac{22620}{S} \ \mu C.cm^{-2}$$

2.2.2 Electrical Resistance

The resistivity of gold in bulk is

$$= 2.285 \times 10^{-6} \ \Omega \text{ cm, (at } 30^{\circ}\text{C),}$$

and the resistance of a slab, of thickness t, length ℓ and breadth b is

$$R = \rho \frac{\ell}{bt} \quad \Omega$$

When the slab is of square format ℓ = b, and the resistance

$$R = \frac{\rho}{t} \quad \Omega/\square .$$

The Conductance of such a slab, of thickness 240 Å, is

$$G = \frac{1}{R} = \frac{240 \times 10^{-8}}{2.285 \times 10^{-6}}$$

$$= 1.05 \text{ siemen/square (at } 30^{\circ}\text{C).}$$

Under argon-ion bombardment the film thickness (and hence the film conductance) will be reduced.

Consider such a film after ion bombardment with charge C coulomb. The mean film thickness remaining will be

$$\frac{t\left(\frac{22620}{S} - C\right)}{\frac{22620}{S}} = \frac{t\ (22620 - SC)}{22620} \quad \text{cm.}$$

The conductance would be

$$G = \frac{t\ (22620 - SC)}{22620\rho_F} \quad S/\square \qquad \text{----------- } 2.2$$

which is shown in figure 4.3 for three values of S.

The resistance of the film would be

$$R = \frac{22620\ \rho_F}{t\ (22620 - SC)} \quad \Omega/\square \qquad \text{----------- } 2.3$$

2.2.3 Tantalum films (unknown density)

$$\text{Atoms/cm}^3 = \frac{D}{(Wt)} \times No \qquad \text{Atoms/cm} = \sqrt[3]{\frac{DNo}{(Wt)}}$$

$$\text{linear spacing} = \sqrt[3]{\frac{Wt}{D \times No}} \quad \text{cm}$$

$$\text{Atoms/cm}^2 \text{ monolayer} = \left[\frac{D\ No}{(Wt)}\right]^{2/3}$$

$$\text{Ions needed to remove a monolayer} = \frac{I}{S}\left[\frac{D\ No}{(Wt)}\right]^{2/3}$$

Ions needed to remove thickness t

$$= \frac{I}{S}\left[\frac{D\ No}{(Wt)}\right]^{2/3} \times \frac{t}{\left[\frac{Wt}{D\ No}\right]^{1/3}}$$

$$= \frac{I}{S}\left[\frac{D\ No}{(Wt)}\right] \times t \quad \text{Ions/cm}^2$$

$$N = \frac{D}{S} \times \frac{No}{\left[AtWt\right]} \times t$$

$$N = \frac{D}{S} \times \frac{6.025 \times 10^{23}}{180.95} \times 750 \times 10^{-8} \quad \text{Ions/cm}^2$$

$$= \frac{D}{S} \times 0.250 \times 10^{17} \quad \text{Ions/cm}^2$$

By experiment this $= 3 \times 10^{17}$ Ions/cm^2
determined by extrapolation of the resistance versus dose curve

$$\therefore \quad 0.25 \frac{D}{S} = 3 \qquad \therefore \frac{D}{S} = \underline{12}$$

$$N = \frac{D}{S} \times 0.25 \times 10^{17} = 3 \times 10^{17} \quad \text{Ions/cm}^2$$

Film sheet resistance during bombardment

$$R_S = \frac{\rho}{t} \times \frac{N}{(N - n)} \qquad \text{------------ 2.4}$$

2.3 Strain Sensitivity γ.

Under tensile elastic deformation the change in resistance of a thin film is given by

$$\frac{dR}{R} = \frac{d\ell}{\ell} = \frac{db}{b} - \frac{dt}{t} + \frac{d\rho}{\rho} .$$

Poisson's ratio for unconstrained dimensions would give

$$db = dt = -\sigma \frac{d\ell}{\ell} , \text{ and}$$

Parker and Krinsky[4] have shown that this leads to a Strain-Gauge Coefficient of Resistance of

$$\gamma = \frac{dR/R}{d\ell/\ell} = 1 + 2\sigma + \frac{d\rho/\rho}{d\ell/\ell} . \qquad \text{---------- 2.5}$$

The dimensions (apart from the thickness) of thin films, however, may be assumed to be the same as those of the substrate, so that the width b is constrained by the contraction experienced by the substrate; that is

$$\frac{db}{b} = -\sigma_s \frac{d\ell}{\ell} ,$$

a circumstance which gives rise to a differential lateral tensile strength of amount

$$\sim (\sigma_f - \sigma_s) \frac{d\ell}{\ell} ;$$

which, in turn, causes a further lateral strain in the direction of the film thickness and a stress reaction in the direction of the applied strain.

Consider the three principal strains in an isotropic medium (the film);

$$\varepsilon_1 = \frac{p_1}{E} - \sigma_f \frac{(p_2 + p_3)}{E} = \frac{p_s}{E_s} ;$$

$$\varepsilon_2 = \frac{p_2}{E} - \sigma_f \frac{(p_1 + p_3)}{E} = \frac{-\sigma_s p_s}{E_s} ;$$

$$\varepsilon_3 = \frac{p_3}{E} - \sigma_f \frac{(p_1 + p_2)}{E} ;$$

where ε_1 = strain in the direction of the length ℓ and the applied stress p_1 ,

ε_2 = strain in the direction of the width b and the differential lateral stress p_2 ,

ε_3 = strain in the direction of the thickness t and the lateral stress p_3 , (=0),

E = Young's modulus for the film material,

E_s = Young's modulus for the substrate,

p_s = the stress applied to the substrate by the bending rig.

By combining the above three equations and applying the known end-conditions, ε_3 may be obtained in terms of ε_1 and Poisson's ratios for film and substrate,

$$\varepsilon_3 = \sigma_f \frac{(1 - \sigma_s)}{(1 - \sigma_f)} \varepsilon_1 ;$$

or

$$\frac{dt}{t} = - \sigma_f \frac{(1 - \sigma_s)\, d\ell}{(1 - \sigma_f)\, \ell} .$$

This leads to values for the strain-gauge coefficients of resistance.

$$\gamma = \frac{dR/R}{d\ell/\ell} = 1 + \sigma_s + \sigma_f \frac{(1 - \sigma_s)}{(1 - \sigma_f)} + \frac{dp/p}{d\ell/\ell} \qquad \text{------- 2.6}$$

This is similar to the result of Verma[10]

2.3.1 <u>Longitudinal Gauge Factor</u> γ_b

Change of resistance is measured in the direction ($\pm\ell$) of the applied strain.

The resistance $R_\ell = \rho \dfrac{\ell}{bt}$,

so that

$$\frac{\partial R}{R\ell} = \frac{\partial \rho}{\rho} - \frac{\partial t}{t} + \frac{\partial \ell}{\ell} - \frac{\partial b}{b} .$$

Using the relationship derived above, the longitudinal strain-gauge coefficient of resistance is;

$$\gamma_\ell = \frac{\partial R/R_\ell}{\partial \ell/\ell} = +(1+\sigma_s) + \sigma_f \frac{(1-\sigma_s)}{(1-\sigma_f)} + \frac{\partial \rho/\rho}{\partial \ell/\ell} \qquad \text{-------- 2.7}$$

2.3.2 Transverse Gauge Factor γ_b

In this case change of resistance is measured in the direction ($\pm b$) at right-angles to the direction ($\pm\ell$) of the applied strain.

The resistance $R_b = \rho \dfrac{b}{\ell\, t}$,

so that

$$\frac{\partial R}{R_b} = \frac{\partial \rho}{\rho} - \frac{\partial t}{t} - \frac{\partial \ell}{\ell} + \frac{\partial b}{b} .$$

again, using the same relationships, the transverse strain-gauge coefficient of resistance is formulated as,

$$\gamma_b = \frac{\partial R/R_b}{\partial \ell/\ell} = -(1+\sigma_s) + \sigma_f \frac{(1-\sigma_s)}{(1-\sigma_f)} + \frac{\partial \rho/\rho}{\partial \ell/\ell} \qquad \text{--------- 2.8}$$

It is assumed that the films are isotropic, and that,

$$\rho_b = \rho_\ell = \rho .$$

2.4 The temperature coefficient of strain-gauge factor β

The temperature coefficient of resistance (T.C.R.) is defined as

$$\alpha = \frac{1}{R}\frac{\partial R}{\partial T} .$$

Writing the temperature coefficient of strain-gauge factor as

$$\beta = \frac{1}{\gamma}\frac{\partial\gamma}{\partial T} \ ;$$

we have

$$\beta = \frac{1}{\frac{\partial R/R}{\partial\ell/\ell}}\frac{\partial}{\partial T}\left[\frac{\partial R/R}{\partial\ell/\ell}\right] \ ;$$

and

$$\beta = \frac{1}{\partial R/\partial\ell}\frac{\partial^2 R}{\partial\ell\partial T} + \frac{1}{\ell}\frac{\partial\ell}{\partial T} - \frac{1}{R}\frac{\partial R}{\partial T} \ .$$

The first term is a temperature coefficient of the rate of change of resistance with length - which should be invariant: the second term is the coefficient of linear expansion, which may be neglected as being two orders of magnitude below the third term: the third term is the T.C.R. This result has been obtained by Witt and Coutts[11],

$$\beta = -\alpha \qquad \text{---------- 2.9}$$

2.5 Theoretical value of the temperature coefficient of resistance α

We will derive a value of α assuming metallic conduction in the film that is limited by the reduction in electron mean free path caused by the proximity of the film surfaces.

It has been suggested[12] that the average free path length is given by

$$\bar{\lambda} = \frac{3t}{4} + \frac{t}{2}\ \ell n\left[\frac{\lambda_B}{t}\right]$$

where t is the film thickness and λ_B is the bulk mean free path.

The relative conductivity is then given by

$$\frac{\sigma}{\sigma_B} = \frac{\bar{\lambda}}{\lambda_B} = \frac{3t}{4\lambda_B} + \frac{t}{2\lambda_B}\ \ell n\left[\frac{\lambda_B}{t}\right]$$

where σ_B is the bulk conductivity. This expression has to be modified to account for diffuse scattering at boundaries[13,14], giving the relation

$$\frac{\sigma}{\sigma_B} = \frac{3t}{4\lambda_B} (1 + 2_p) \{\ln \left(\frac{\lambda_B}{t}\right) + 0.4228\}$$

- - - - - - - - - - 2.10

where p is the fraction of incident electrons specularly reflected and $p^2 << 1$. Using an extension of Matthiessen's rule, the resistivity of the film ρ_f is the sum of components due to lattice scattering (ρ_L), scattering by defects and impurities (ρ_D) and surface scattering (ρ_s). The bulk resistivity ρ_B is just composed of the first two components since ρ_s is assumed to be negligible.

The T.C.R. is defined as

$$\alpha = \frac{1}{R} \frac{dR}{dT} = \frac{1}{\rho} \frac{d\rho}{dT}$$

As a first approximation one can say that ρ_D and ρ_s do not depend strongly on temperature so that for a continuous, homogeneous film;

$$\alpha_f = \frac{1}{\rho_f} \frac{d\rho_f}{dT} = \frac{1}{\rho_f} \frac{d\rho_L}{dT}$$

and

$$\alpha_B = \frac{1}{\rho_B} \frac{d\rho_B}{dT} = \frac{1}{\rho_B} \frac{d\rho_L}{dT}$$

Then

$$\frac{\alpha_f}{\alpha_B} = \frac{\rho_B}{\rho_f} = \frac{\sigma}{\sigma_B}$$

Using Heavens'[12] approximate solution for eqn.2.10 for $t << \lambda_B$,

$$\alpha_f = \alpha_B \{\ln \left(\frac{\lambda_B}{t}\right) + 0.4228\}^{-1}$$

Now the sheet resistivity $R_s = \rho_f/t$ so that

$$\alpha_f = \alpha_B \{\ln \left(\frac{\lambda_B R_s}{\rho_f}\right) + 0.4228\}^{-1} \qquad ---------- 2.11$$

This model includes a large number of assumptions, and it may be more realistic to take into account scattering at grain boundaries.

2.6 Statistical Methods

The measurements made in the course of this strain-gauge evaluation include unpredictable errors, and although an attempt was made to minimise their occurrence the graphs show their presence only too clearly.

It is assumed that these errors are random in occurrence and magnitude, and that they have a Normal probability distribution. It follows, therefore, that Standard Deviations may be calculated for suitable quantities such that the probability of the quantity lying within the range

mean value ± 1 S.D. is 0.68,

or mean value ±1.96 S.D. is 0.95,

or mean value ± 2.58 S.D. is 0.99.

It is usually satisfactory to take the range ± 1.96 S.D. as defining the 95% confidence limits.

3. Experimental Techniques

3.1 Thin Films

Films were vacuum evaporated onto soda-glass substrates approximately 1 mm thick. High temperature annealing was not employed. It was therefore hoped that no problems would be encountered from out-diffusion of sodium and other metal ions from the substrate. For gold films 3" x 1" glass was used whilst for tantalum both 1" x 1" squares and 3" x 0.2" strips were used. A few tantalum films were laid onto mica and some onto alumina substrate: these were used for sheet resistance and TCR measurements but no significant difference was noted as a result of their use.

3.1.1 Substrate Preparation

The substrate was cleaned by gentle abrasion in hot detergent solution. By rinsing in hot water and hot distilled water, and with a final rinse in de-ionised water. Drying was carried out on a lamina-flow bench, and only those substrates that dried without cloudiness to give clear specula reflections were used for film deposition.

3.1.2 Gold Films

Gold was evaporated from a tungsten wire spiral electrically heated in a vacuum of between 1×10^{-6} and 2×10^{-6} torr. The substrate temperature was that of the equipment ambient.

Films were laid down having a thickness within the range 200 Å to 300 Å. This was measured after evaporation by Talystep Indicator. But thickness was monitored during some evaporation runs using a quartz crystal thickness monitor oscillating at about 250 Khz, whilst for other runs the resistance of a test film was monitored, and evaporation was stopped when this had reached a resistance of 10 Ω.

3.1.3 Tantalum Films

Tantalum was evaporated by electron-beam heating in an ultra-high vacuum system pumped by an oil diffusion pump and fitted with a

liquid nitrogen cold trap. A titanium sublimation pump was available, enabling a pressure of 5 x 10^{-9} torr to be reached at the start of each evaporation run. During evaporation the pressure (and temperature) rose and after about five minutes had reached an indicated level of about 10^{-6}, at which point the run was usually interrupted for cooling.

Film thickness measurements made after unloading the evaporator indicated consistently a rate of deposition of tantalum of 50 Å per minute, and this rate was used to estimate film thickness during the subsequent evaporation runs.

3.1.4 Electrode Pads

Each film had gold electrodes formed at either end to define the film length and to enable electrical connections to be made. The gold pads were evaporated in vacuo through masks, after a preliminary flash evaporation of a titianium "glue" layer. The resulting electrodes were robust enough to allow connecting leads to be soft-soldered into place.

The masks used for the gold and tantalum films are shown in Figures 3.1 and 3.2 respectively.

3.1.5 Ion Bombardment

The ion bombardment was carried out in a 500 keV heavy ion accelerator with sector-magnet mass-analysis and closed loop voltage control using the mass defining slits. Uniformity of dose was achieved by electrostatic scanning of the beam on a raster equivalent to double the area of the beam defining aperture. Uniformity is estimated at better than 1%, beam convergence is estimated to be less than 0.2°. The ion dose was monitored by measuring the charge collected by the target. An electrostatic field was used to suppress secondary electrons. The target chamber was pumped by liquid nitrogen trapped diffusion pump with a cold finger (liquid nitrogen) mounted close to the target. Typical operating pressure was 5 X 10^{-7} torr.

3.2 Measurements

All electrical measurements were conducted with the specimens at atmospheric pressure.

The effect of the unimplanted ends on the resistivity, TCR and strain gauge factor of implanted gauges was corrected for by using formulae derived by M. R. Moulding (transfer report 1977) and reproduced here as appendix 3.

3.2.1 Resistance Measurement

An equal-arm Wheatstone Bridge circuit was used for measuring film resistance, the DC supply being 2 V for most films so as to limit the power dissipation to 2 mW/cm^2 and so avoid thermal errors. For high resistance films the bridge ratio arms were unequal and the supply could be increased to 10 V.

Mask for electrode areas.

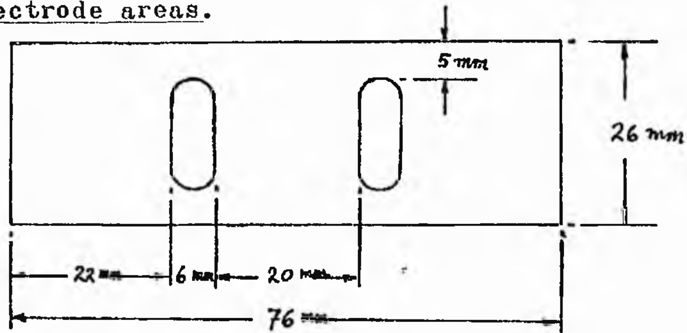

Mask for strain-gauge film.

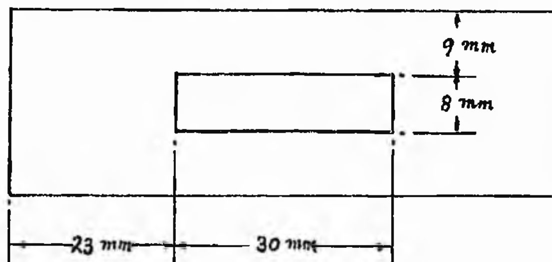

Ion bombardment mask.

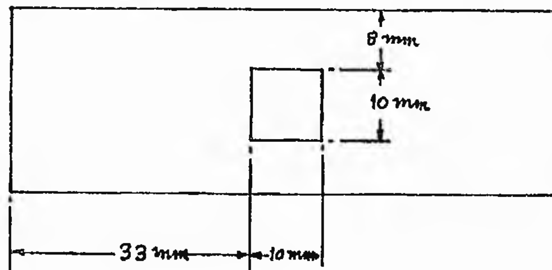

Specimen strain-gauge.

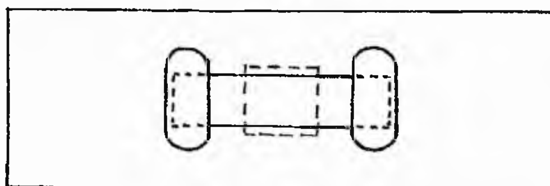

FIG. 3.1 MASKS FOR GOLD FILMS.

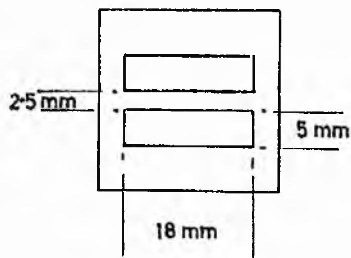

Tantalum films

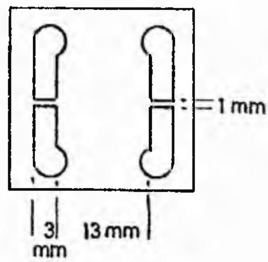

Gold electrodes

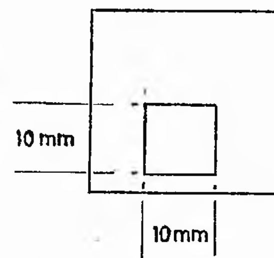

Bombardment window

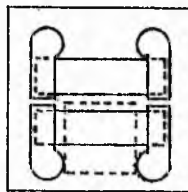

1" × 1"
Composite film

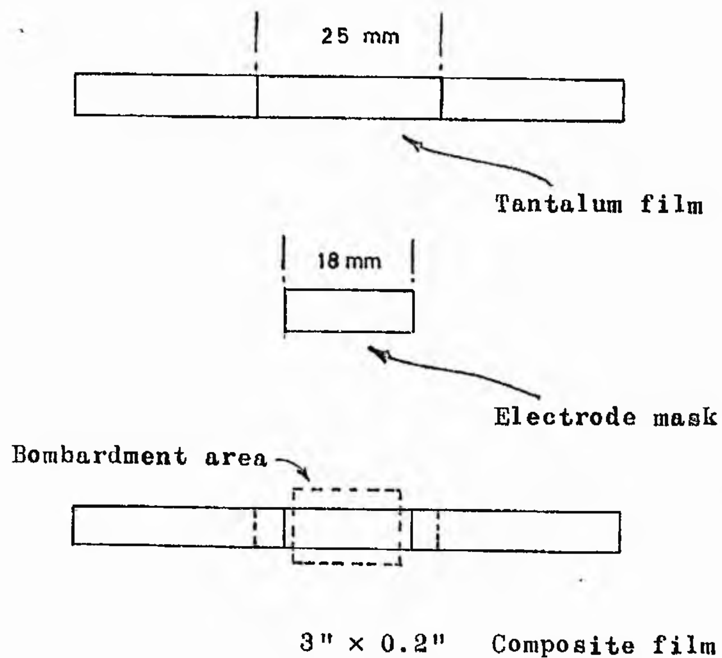

3" × 0.2" Composite film

FIG. 3.2 MASKS FOR TANTALUM FILMS

For the measurement of the gold films a centre-zero micro-ammeter was used as balance detector (+-100 μA range), and a series of spot measurements was made for each run. In the case of the tantalum films an x-y plotter was available and this allowed a continuous record to be made of the measurements.

Before use the films were annealed at room temperature for a minimum time of one week, and also at 120° C for two hours.

3.2.2 Temperature Control and Measurement

In order to avoid errors due to temperature variation during the measurement of strain-gauge factor the temperature must be held constant. The use of glass as the substrate limits the maximum safe strain to about 250 PPM and the change of resistance this gives is, in the case of gold films, the equivalent of a temperature change of less than one half degree celsius. Thus, for there to be no more than a 5% error in strain-gauge factor from this cause the temperature must not vary by more than 0.02° C during straining. This is difficult to achieve over protracted periods but seems possible for the duration of one strain run.

The four-point straining rig was positioned inside a fan-blown environmental chamber in such a way that strain could be applied, and measured, from the outside. The schematic arrangement of this equipment is shown in Figure 3.3. Temperature could be tightly controlled by a closed-loop servo over the range 20° C to 120° C using a filamentary air-heating element and a filamentary tungsten resistor as the sensor. The temperature was measured with an iron-constantan thermocouple soldered to a copper vane of 2 sq.cm. placed in the air stream of the chamber, and with the cold junction kept in melting ice. The thermal

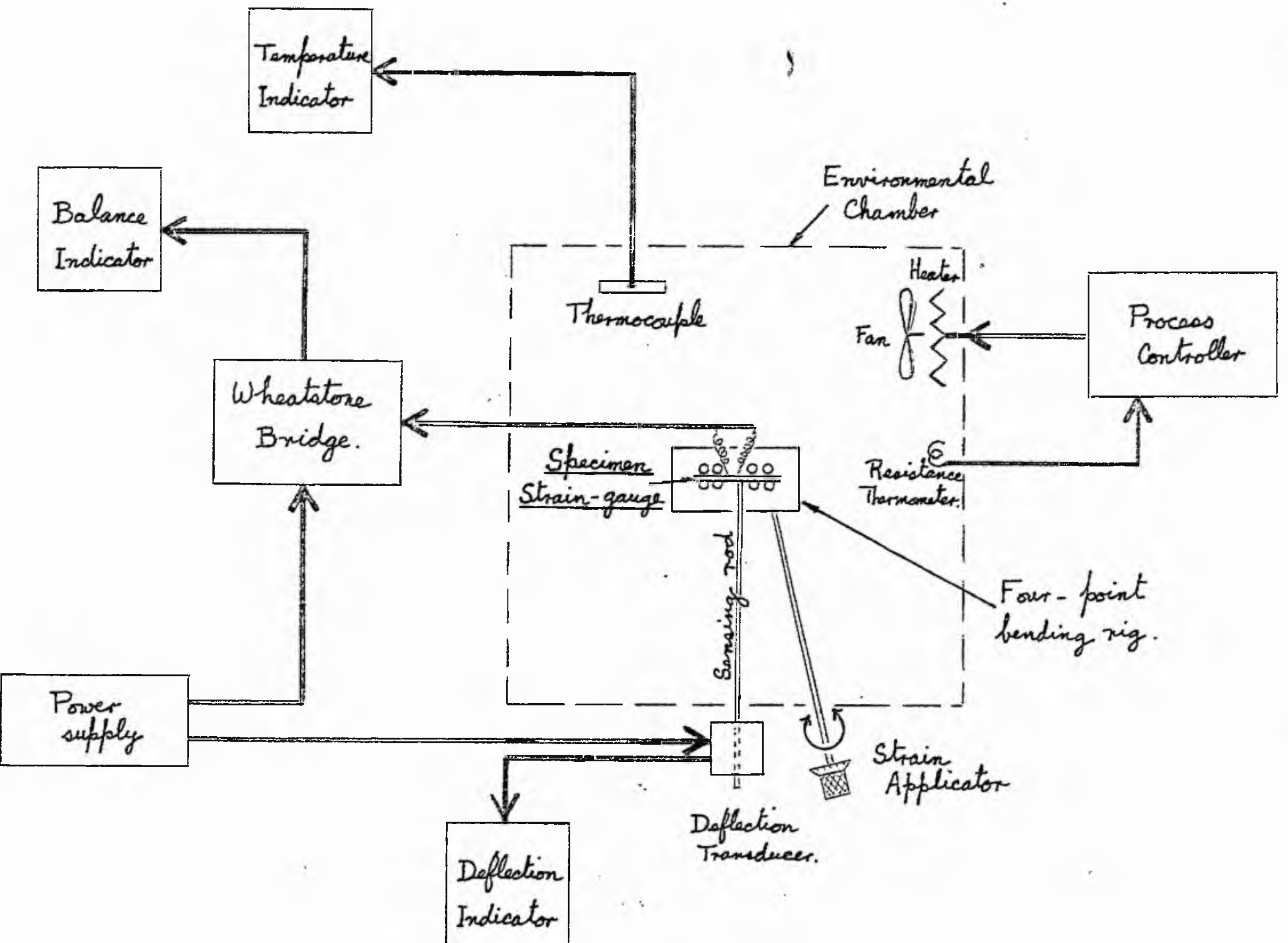

FIG. 3.3 SCHEMATIC ARRANGEMENT OF THE EQUIPMENT

EMF was read on a moving coil indicator. Temperature control was possible, but to a reduced accuracy, over the extended range -20° C to + 150° C with the aid of auxiliary cooling or heating.

The environmental chamber was also used for making TCR measurements.

3.2.3 Temperature Coefficient of Resistance

In the case of the gold films precise measurements of resistance were made at about twelve spot temperatures between room temperature and 120° C both for rising and for falling temperature. The results were corrected for end effects in the case of bombarded films by a simple computer routine, and were displayed as a graph plot for a visual check on high temperature stability: a simple line fitting procedure was used to obtain the TCR and the sheet resistance at 30° C.

Most of the tantalum films were measured with the aid of an x-y plotter, vertical deflection being the out-of-balance output of the Wheatstone Bridge and horizontal deflection the thermocouple EMF. The procedure adopted here was to heat the chamber to about 120° C, to start the x-y plot, and to allow the chamber to cool slowly over a period of about an hour. Half way through the period water cooling was started so as to maintain a more or less constant cooling rate down to room temperature. The resistance scale was calibrated each time by altering the bridge balance point and marking the change on the plot, and the temperature scale was calibrated once and for all with the thermo junction in steam. A best-fit straight line was drawn through the plot, and this was subsequently corrected for end effects to give the TCR and sheet resistance at 30° C. Figure 3.4 shows a typical TCR run for a tantalum film.

A few tantalum films were measured over the extended temperature range -190° C to + 110° C. These films were mounted within an aluminium

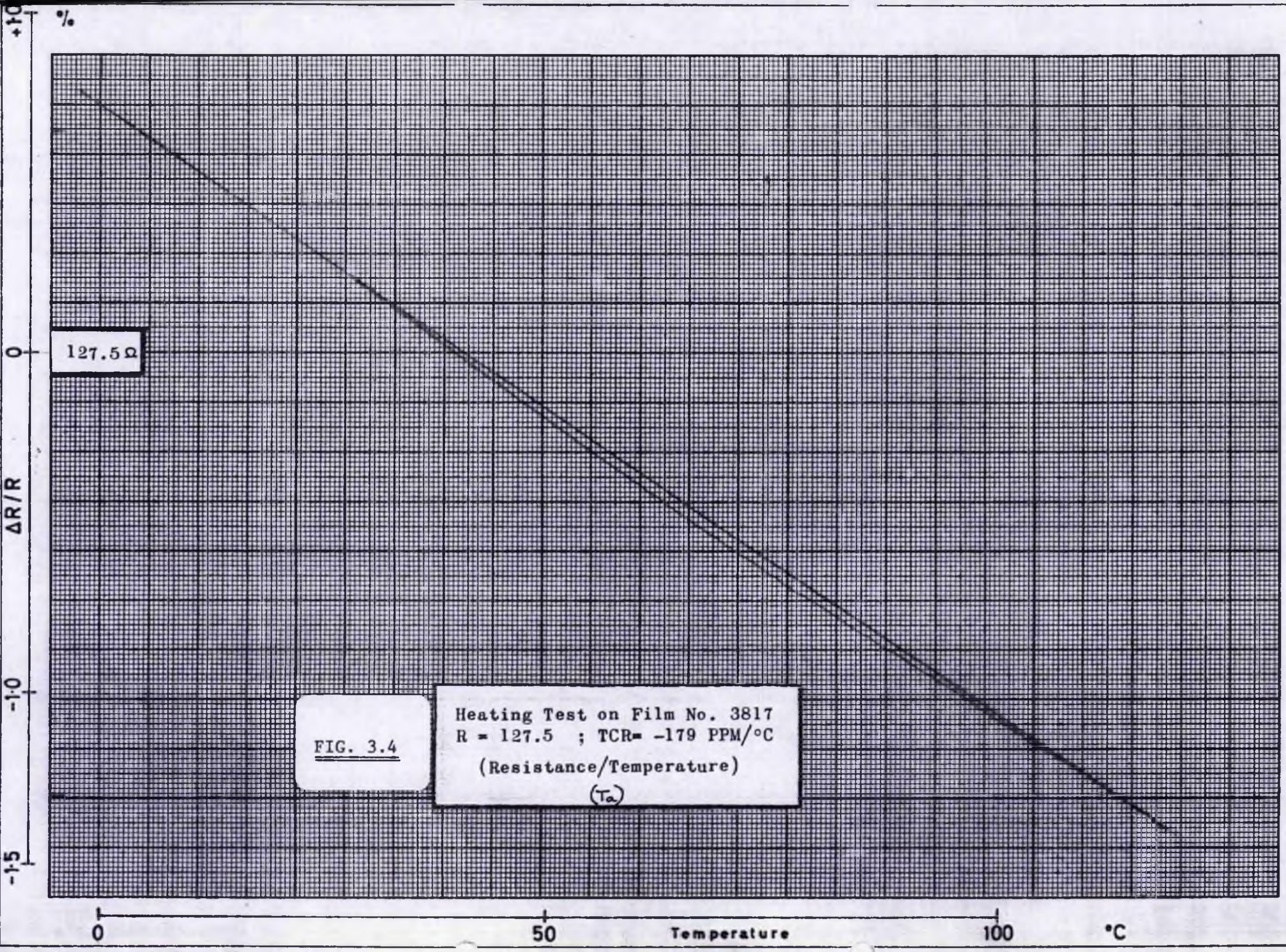

%
+1·0
0
ΔR/R
-1·0
-1·5
127.5 Ω
FIG. 3.4
Heating Test on Film No. 3817
R = 127.5 ; TCR= -179 PPM/°C
(Resistance/Temperature)
(Ta)
0
50
Temperature
100
°C

block narrow enough to pass through the neck of an ordinary picnic dewar flask and also through an aperture into the environmental chamber; see Figure 3.5. The flask was half filled with liquid nitrogen and the block was carefully lowered into it so as to cool the films to -195° C. The block was then raised so that the temperature would rise slowly, to reach 0° C after about four hours. Temperature was again measured by thermocouple and moving coil indicator, and resistance by Wheatstone Bridge. Spot measurements were made at approximately 10° C intervals, and when the temperature had reached about $+ 5^{\circ}$ C the block was transferred to the environmental chamber, and heating was applied in steps to $+ 110^{\circ}$ C. The results were corrected for end effect and were plotted (R v.T) and (log R v.1/T). Typical outputs of data for these plots are shown in Table 3.1 and plotted in Figure 3.6.

3.2.4 Strain-Gauge Factor

The substrates were loaded into the four-point bending rig positioned inside the environmental chamber, see Figure 3.7. Strain was calculated from a measurement of substrate deflection, made mid-way between the two fixed posts of the bender. Using a differential transformer transducer. With the maximum safe strain for 1 mm thick glass substrate applied by the rig ($\pm 250 \times 10^{-6}$) the deflection obtained was 0.1 mm and the transducer output was $\pm$ 118 millivolt.

For gold films the transducer output was measured on a centre-zero millivoltmeter having a backing-off facility. A number of spot readings of resistance and deflection were taken as the strain was applied; then the results were corrected for end effects, were displayed in graphical form, and a straight line established through them to give the strain-gauge factor. All these calculations and the plots were

FIG. 3.5

and

FIG. 3.7

missing.

TABLE 3.1 Argon-Ion Bombardment of Tantalum Films

NO. 1203. (Before bombardment)

'A'	20.500	36.200	51.300	65.500	81.000	95.000	108.000	°C
	124.568	124.423	124.191	124.059	123.896	123.926	123.607	Ω
'B'	20.500	36.200	51.300	65.500	81.000	95.000	108.000	°C
	124.094	123.893	123.723	123.545	123.382	123.212	123.085	Ω

FILM LENGTH = 13.0 mm BREADTH = 5.0 mm IMPLANTED LENGTH = 0.0 mm FILM THICKNESS = 800. Å
ION DOSE = 0. μC·cm⁻²

NITS = 1. RES AT 0 DEG C = 0.1247E 03
S.E. OF RESIST = 0.8328E-02
NITS = -1. RES AT 0 DEG C = 0.1243E 03
S.E. OF RESIST = 0.4671E-02
HORIZ SCALE = 0.2000E-03 VERT SCALE = 0.2000E-02
NITS = 4. COORDS OF AXES = 0.2414E-02 0.4810E 01
HORIZ SCALE = 0.2000E-03 VERT SCALE = 0.2000E-02
NITS = 4. COORDS OF AXES = 0.2414E-02 0.4810E 01

'A' SHEET RESIST AT 30 DEG C = 0.4766E 02 Ω/□
TCR = -0.8944E-04
'B' SHEET RESIST AT 30 DEG C = 0.4766E 02 Ω/□
TCR = -0.9289E-04

ACTIVATION ENERGY = 0.8730E-03 eV

ACTIVATION ENERGY = 0.9049E-03 eV

NO. 1203. (After bombardment)

'A'	14.200	30.500	44.500	59.200	74.000	89.200	104.100	88.000	72.200	62.500	°C
	47.800	32.000									
	124.034	123.836	123.652	123.482	123.319	123.150	122.981	123.167	123.327	123.434	Ω
	123.612	123.809									
'B'	14.200	30.500	44.500	59.200	74.000	89.200	104.100	88.000	72.200	62.500	°C
	47.800	32.000									
	117.187	117.178	117.142	117.124	117.110	117.108	117.100	117.109	117.134	117.140	Ω
	117.160	117.193									

FILM LENGTH = 13.0 mm BREADTH = 5.0 mm IMPLANTED LENGTH = 10.0 mm FILM THICKNESS = 800. Å
ION DOSE = 6700. μC·cm⁻²
($42 \cdot 10^{15}$ ions·cm⁻²)

NITS = -1. RES AT 0 DEG C = 0.1241E 03
S.E. OF RESIST = 0.3729E-02

'A', SHEET RESIST AT 30 DEG C = 0.4762E 02 Ω/□
TCR = -0.9375E-04

CORRECTED

'B'	88.568	88.602	88.604	88.626	88.651	88.690	88.722	88.688	88.670	88.650
	88.631	88.621								

NITS = -1. RES AT 0 DEG C = 0.8855E 02
S.E. OF RESIST = 0.3455E-02
HORIZ SCALE = 0.2000E-03 VERT SCALE = 0.2000E-03
NITS = 4. COORDS OF AXES = 0.2465E-02 0.4483E 01
HORIZ SCALE = 0.2000E-03 VERT SCALE = 0.2000E-03
NITS = 5. COORDS OF AXES = 0.2465E-02 0.4483E 01

'B', SHEET RESIST AT 30 DEG C = 0.4429E 02 Ω/□
TCR = 0.1764E-04 (IMPLANTED)

ACTIVATION ENERGY = 0.8855E-03 eV

ACTIVATION ENERGY = [-0.1754E-03 (IMPLANTED)]

ARRHENIUS PLOT 1201

x 10^2

LOG$_e$(RESISTANCE) OHMS

1·18155
1·17966
1·17760
1·17540
1·17415
1·17183

1·06500 0·88800 0·74000 0·58400 0·45000 0·29000 0·15700 x 10^2

RECIPROCAL TEMPERATURE —— (marked °C)

NON-BOMBARDED FILMS, 850 Å

SHEET RESISTANCE AT 30 °C 'A'-FILM 'B'-FILM
= 45·4 Ω/□ ; 45·5 Ω/□
TCR = -105 PPM ; -132 PPM
Ɛ = ·0010 eV ; ·0013 eV

x 10^3 ARRH 1201

LOG$_e$(RESISTANCE) OHMS

1·57672
1·57478
1·57351
1·57297
1·57140
1·57129
1·56956
1·56919
1·56787
1·56694
1·56623
1·56500
1·56467
1·56300

1·04009 0·98000 0·80200 0·76000 0·68200 0·60000 0·56100 0·44800 0·32600 0·20100 0·09300 x 10^2

RECIPROCAL TEMPERATURE (T^{-1}) —— (marked – °C)

'B'- FILM AFTER ION BOMBARDMENT

ION DOSE = 200 × 10^{15} IONS·cm^{-2} A^+
SHEET RESISTANCE = 790 Ω/□ AT 30°C
TCR = −91 PPM ; Ɛ = 0·0008 eV

FIG. 3.6

carried out using a digital computer. Each strain run was completed within a time span of about two minutes so as to minimise temperature errors (see Section 3.2.2), and the results from four runs in tension and four in compression were averaged to obtain the final strain-gauge factor. A typical computer plot for a gold strain-gauge is shown in Figure 3.8.

For the tantalum films the x-y plotter was available, and this was used to display Wheatstone Bridge out-of-balance vertically and transducer output horizontally. A typical strain run for a tantalum film is shown in Figure 3.9., where the film was strained from tension to compression and back again as a check on temperature drift. The resistance scale was established by altering the bridge balance point, the slope of the best straight line drawn through the plot being used to calculate the strain-gauge factor after end corrections had been applied. The correction for the unbombarded section of bombarded gauges necessary in order to determine the true value of γ was done using formulae similar to those derived by M. R. Moulding (transfer report 1977) Appendix .

3.3 Anodising

Some of the tantalum films were examined in layers by progressive anodic oxidation. A strong solution of acetic acid was used as the electrolyte (50% glacial acetic acid in water), and a platinum foil of 2.5 sq. cm. was the counter electrode. A difficulty encountered in this work is that of insulating the submerged electrode and defining the anodised portion of the film. This was overcome here by the use of a generous layer of apiezon wax applied over the electrode and its lead so as partially to cover the tantalum film and to leave the required window exposed.

The anodic potential was increased in steps of approximately 2 V from a source current limited to 25 μA. At each step the film was withdrawn from the electrolyte, washed in several changes of distilled water, dried, and placed in the environmental chamber for the resistance and TCR

NO. 026, 60 DEG C, 1000 UC/SQCM

TENSION

505.800 505.750 505.700 505.650 505.600 505.550 505.500

-0.05 0.00 0.05

COMPRESSION

505.450 505.420 505.400 505.390 505.350 505.320 505.300 505.280 505.250

-0.05 0.00 0.05

FIG. 3.8

Strain measurement of an Argon-bombarded Gold Film.
(Electrical Resistance/ Substrate Deflection)

AG 20.VIII.77

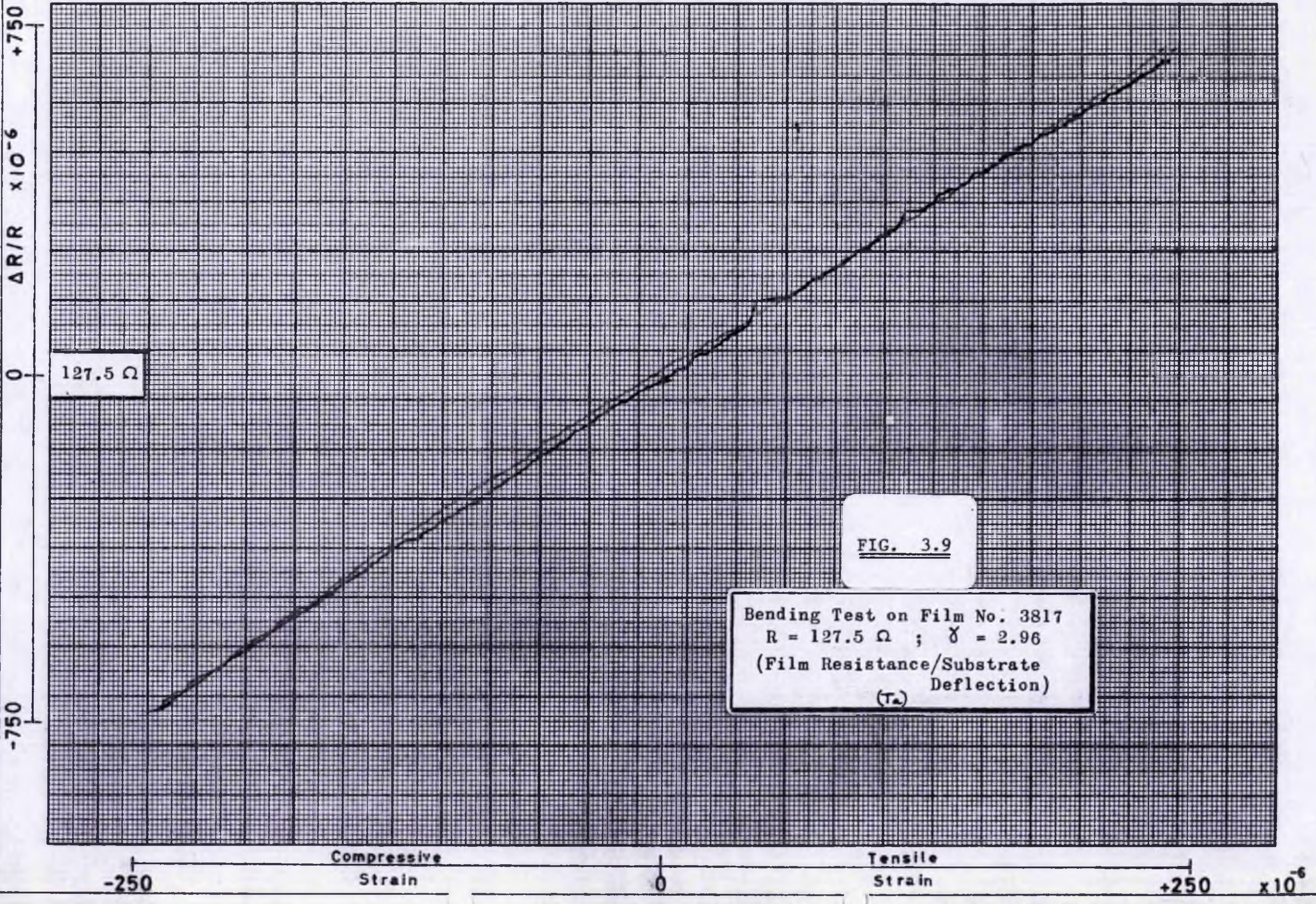

FIG. 3.9

Bending Test on Film No. 3817
R = 127.5 Ω ; γ = 2.96
(Film Resistance/Substrate Deflection)

to be measured. Anodising was continued at increasing potential until the film became open circuit. The results of a typical run are listed in Table 3.2.

3.4. Vacuum Annealing

A number of tantalum films were annealed isothermally in vacuo at temperarures up to 300^0C.

The films were loaded onto a sliding platform. This was positioned at the cool end of a metals research vacuum furnace and kept there until the pressure was reduced below 10^{-4} Torr. The platform was then pushed into the hot region of the furnace for one hour, by which time the pressure was usually better than 5×10^{-5} Torr. The platform was then withdrawn to cool for half an hour, and then unloaded.

At each step in the annealing, the sheet resistance of the films was measured. This was done using a four-point probe because of the impracticability of using soft-soldered joints. The probe spacing was 1.0 mm and a current of 1 mA was used for measuring the low resistance films and 0.1 mA for those with high resistance.

The temperature was increased in steps of 50^0 C from 150^0 C to 300^0 C.

TABLE 3.2 Anodisation of 800-Å Tantalum Film

	Plain Film					Argon-Ion Bombarded			
	VOLTAGE	J	CONDUCTANCE (MHO)	TCR (PPM)		VOLTAGE	L	CONDUCTANCE (MHO)	TCR (PPM)
1203 A	000 V	4	0.2112E-01	-0.1111E-03	1203 B	000 V	4	0.2287E-01	-0.6148E-05
1203 A	002 V	4	0.2093E-01	-0.1086E-03	1203 B	002 V	4	0.2235E-01	0.1559E-06
1203 A	003 V	4	0.2077E-01	-0.1029E-03	1203 B	003 V	4	0.2206E-01	-0.1938E-05
1203 A	005 V	4	0.2033E-01	-0.1037E-03	1203 B	005 V	4	0.2143E-01	0.3628E-05
1203 A	007 V	4	0.1983E-01	-0.1061E-03	1203 B	007 V	4	0.2082E-01	-0.2834E-05
1203 A	010 V	4	0.1901E-01	-0.1084E-03	1203 B	010 V	4	0.1988E-01	-0.1044E-04
1203 A	013 V	4	0.1833E-01	-0.1149E-03	1203 B	013 V	4	0.1895E-01	-0.9216E-05
1203 A	016 V	4	0.1752E-01	-0.1188E-03	1203 B	016 V	4	0.1776E-01	-0.1600E-04
1203 A	019 V	4	0.1700E-01	-0.1194E-03	1203 B	019 V	4	0.1708E-01	-0.2034E-04
1203 A	022 V	4	0.1627E-01	-0.1276E-03	1203 B	022 V	4	0.1616E-01	-0.2731E-04
1203 A	026 V	4	0.1520E-01	-0.1313E-03	1203 B	026 V	4	0.1499E-01	-0.3408E-04
1203 A	030 V	4	0.1404E-01	-0.1390E-03	1203 B	030 V	4	0.1384E-01	-0.4595E-04
1203 A	032 V	8	0.1288E-01	-0.1379E-03	1203 B	032 V	8	0.1262E-01	-0.5172E-04
1203 A	033 V	4	0.1279E-01	-0.1500E-03	1203 B	033 V	4	0.1254E-01	-0.5624E-04
1203 A	034 V	4	0.1261E-01	-0.1489E-03	1203 B	034 V	4	0.1237E-01	-0.5692E-04
1203 A	035 V	4	0.1231E-01	-0.1484E-03	1203 B	035 V	4	0.1208E-01	-0.5731E-04
1203 A	036 V	4	0.1210E-01	-0.1468E-03	1203 B	036 V	4	0.1187E-01	-0.5744E-04
1203 A	038 V	4	0.1167E-01	-0.1429E-03	1203 B	038 V	4	0.1147E-01	-0.5937E-04
1203 A	041 V	4	0.1110E-01	-0.1450E-03	1203 B	041 V	4	0.1084E-01	-0.6588E-04
1203 A	045 V	4	0.1033E-01	-0.1342E-03	1203 B	045 V	4	0.1000E-01	-0.6981E-04
1203 A	047 V	4	0.9633E-02	-0.1376E-03	1203 B	047 V	4	0.9219E-02	-0.8059E-04
1203 A	048 V	4	0.9169E-02	-0.1219E-03	1203 B	048 V	4	0.8268E-02	-0.8395E-04
1203 A	049 V	4	0.9155E-02	-0.1407E-03	1203 B	049 V	4	0.8186E-02	-0.9044E-04
1203 A	054 V	4	0.9144E-02	-0.1454E-03	1203 B	054 V	4	0.8092E-02	-0.8855E-04
1203 A	060 V	4	0.8971E-02	-0.1393E-03	1203 B	060 V	4	0.7885E-02	-0.8401E-04
1203 A	070 V	4	0.7571E-02	-0.6637E-04	1203 B	070 V	4	0.5438E-02	-0.9207E-04
1203 A	080 V	4	0.5149E-02	0.3421E-04	1203 B	080 V	4	0.3787E-02	-0.9410E-04
1203 A	090 V	4	0.5118E-02	-0.9852E-04	1203 B	090 V	4	0.3390E-02	-0.1109E-03
1203 A	100 V	4	0.4901E-02	-0.6283E-04	1203 B	100 V	0	0.0000E 00	0.0000E 00
1203 A	109 V	4	0.4766E-02	-0.9463E-04	1203 B	109 V	0	0.0000E 00	0.0000E 00
1203 A	118 V	4	0.3402E-02	0.1945E-04	1203 B	118 V	0	0.0000E 00	0.0000E 00
1203 A	126 V	0	0.0000E 00	0.0000E 00	1203 B	126 V	0	0.0000E 00	0.0000E 00

TABLE 3.2 Anodisation of 850-Å Tantalum Film

Plain Film					Argon-Ion Bombarded				
	VOLTAGE	J	CONDUCTANCE (MHO)	TCR (PPM)		VOLTAGE	L	CONDUCTANCE (MHO)	TCR (PPM)
1201 A	000 V	4	0.2294E-01	-0.1504E-03	1201 B	000 V	4	0.1204E-02	-0.9597E-04
1201 A	002 V	4	0.2276E-01	-0.1494E-03	1201 B	002 V	4	0.1138E-02	-0.1080E-03
1201 A	003 V	4	0.2258E-01	-0.1480E-03	1201 B	003 V	4	0.1102E-02	-0.1024E-03
1201 A	005 V	4	0.2217E-01	-0.1396E-03	1201 B	005 V	4	0.1023E-02	-0.1027E-03
1201 A	007 V	4	0.2175E-01	-0.1440E-03	1201 B	007 V	4	0.9270E-03	-0.1150E-03
1201 A	010 V	4	0.2110E-01	-0.1494E-03	1201 B	010 V	4	0.8076E-03	-0.1021E-03
1201 A	013 V	4	0.2045E-01	-0.1501E-03	1201 B	013 V	4	0.6729E-03	-0.1012E-03
1201 A	016 V	4	0.1963E-01	-0.1491E-03	1201 B	016 V	4	0.5040E-03	-0.1035E-03
1201 A	019 V	4	0.1911E-01	-0.1510E-03	1201 B	019 V	4	0.4085E-03	-0.9736E-04
1201 A	022 V	4	0.1839E-01	-0.1539E-03	1201 B	022 V	4	0.3339E-03	-0.1069E-03
1201 A	026 V	4	0.1737E-01	-0.1503E-03	1201 B	026 V	4	0.2358E-03	-0.1009E-03
1201 A	030 V	4	0.1624E-01	-0.1512E-03	1201 B	030 V	4	0.1454E-03	-0.3870E-03
1201 A	032 V	8	0.1514E-01	-0.1586E-03	1201 B	032 V	8	0.5718E-04	-0.8717E-04
1201 A	033 V	4	0.1506E-01	-0.1691E-03	1201 B	033 V	4	0.5221E-04	-0.3235E-03
1201 A	034 V	4	0.1487E-01	-0.1682E-03	1201 B	034 V	4	0.4720E-04	-0.2807E-03
1201 A	035 V	4	0.1455E-01	-0.1671E-03	1201 B	035 V	4	0.4254E-04	-0.9823E-04
1201 A	036 V	4	0.1432E-01	-0.1630E-03	1201 B	036 V	4	0.3969E-04	-0.9617E-04
1201 A	038 V	4	0.1384E-01	-0.1622E-03	1201 B	038 V	4	0.3495E-04	-0.9552E-04
1201 A	041 V	4	0.1310E-01	-0.1610E-03	1201 B	041 V	4	0.2819E-04	-0.9762E-04
1201 A	045 V	4	0.1222E-01	-0.1491E-03	1201 B	045 V	4	0.1927E-04	-0.8748E-04
1201 A	047 V	4	0.1152E-01	-0.1531E-03	1201 B	047 V	4	0.1150E-04	0.5008E-03
1201 A	048 V	4	0.1108E-01	-0.1400E-03	1201 B	048 V	4	0.7942E-05	-0.3390E-03
1201 A	049 V	4	0.1106E-01	-0.1545E-03	1201 B	049 V	4	0.7975E-05	0.3361E-03
1201 A	054 V	4	0.1105E-01	-0.1570E-03	1201 B	054 V	0	0.0000E 00	0.0000E 00
1201 A	060 V	4	0.1095E-01	-0.1555E-03	1201 B	060 V	4	0.7258E-05	-0.1196E-03
1201 A	070 V	4	0.9310E-02	-0.8996E-04	1201 B	070 V	4	0.6378E-05	-0.7629E-04
1201 A	080 V	4	0.6633E-02	0.2108E-04	1201 B	080 V	0	0.0000E 00	0.0000E 00
1201 A	090 V	4	0.6588E-02	-0.1091E-03	1201 B	090 V	0	0.0000E 00	0.0000E 00
1201 A	100 V	4	0.6345E-02	-0.7496E-04	1201 B	100 V	0	0.0000E 00	0.0000E 00
1201 A	109 V	4	0.6169E-02	-0.1061E-03	1201 B	109 V	0	0.0000E 00	0.0000E 00
1201 A	118 V	4	0.4852E-02	0.4114E-05	1201 B	118 V	0	0.0000E 00	0.0000E 00
1201 A	126 V	0	0.0000E 00	0.0000E 00	1201 B	126 V	0	0.0000E 00	0.0000E 00

4. Results

The electrical properties of the metal films made as described above in section 3, have been measured for different levels of bombardment with argon ions. In this work all ion bombardment was carried out using argon.

The electrical properties investigated are:

Sheet Resistance,

Temperature Coefficient of Resistance,

Strain-Gauge Coefficient of Resistance.

4.1 Gold Films

All the gold films were made by evaporation 'in vacuo' onto glass substrate; the film thickness being controlled (see 3.1.2) so as to produce films of approximately 12 ohms resistance.

4.1.1 Sheet Resistance

The sheet resistance of the gold film at evaporation was, on average, 4.8 ohm/sq + - 0.6 ohm/sq, measured at 30° C. Multiplication by the film thickness shows an apparent resistivity of 11.5 microhm-cm. (The resistivity of bulk gold is 2.25 microhm-cm.)

The effect of ion bombardment on the sheet resistance of a single 240 - Å gold film is shown in Figure 4.1. Here the resistance of a particular film is plotted against bombardment dose at different stages during the ion bombardment. The main feature is the dramatic increase in sheet resistance that occurs at a bombardment dose of 6.5×10^{-15} ions/cm^2 (corresponding to 1050 μC/cm^2). It is at this level of bombardment that the film goes open circuit, so that only a small increase in bombardment effects a large change.

Initially on bombardment the sheet resistance drops slightly with increasing ion dose, reaching -40% at 1.5×10^{15} ions/cm^2. Beyond this dose the resistance rises steadily through two orders of magnitude. For argon-ion bombardment above 6.5×10^{15} ions/cm^2 the resistance rises rapidly to an open-circuit condition.

The continuous curve shown in Figure 4.1 is a"best fit" line calculated using equn.2.3 for assumed values of sputter rate and initial resistivity, and is based on the premise that the film is uniformly thinned as the bombardment proceeds. The curve which most closely fits the observed points is that for a sputter rate of 20 atoms/ion and an initial resistivity of 22.5 microhm-cm.

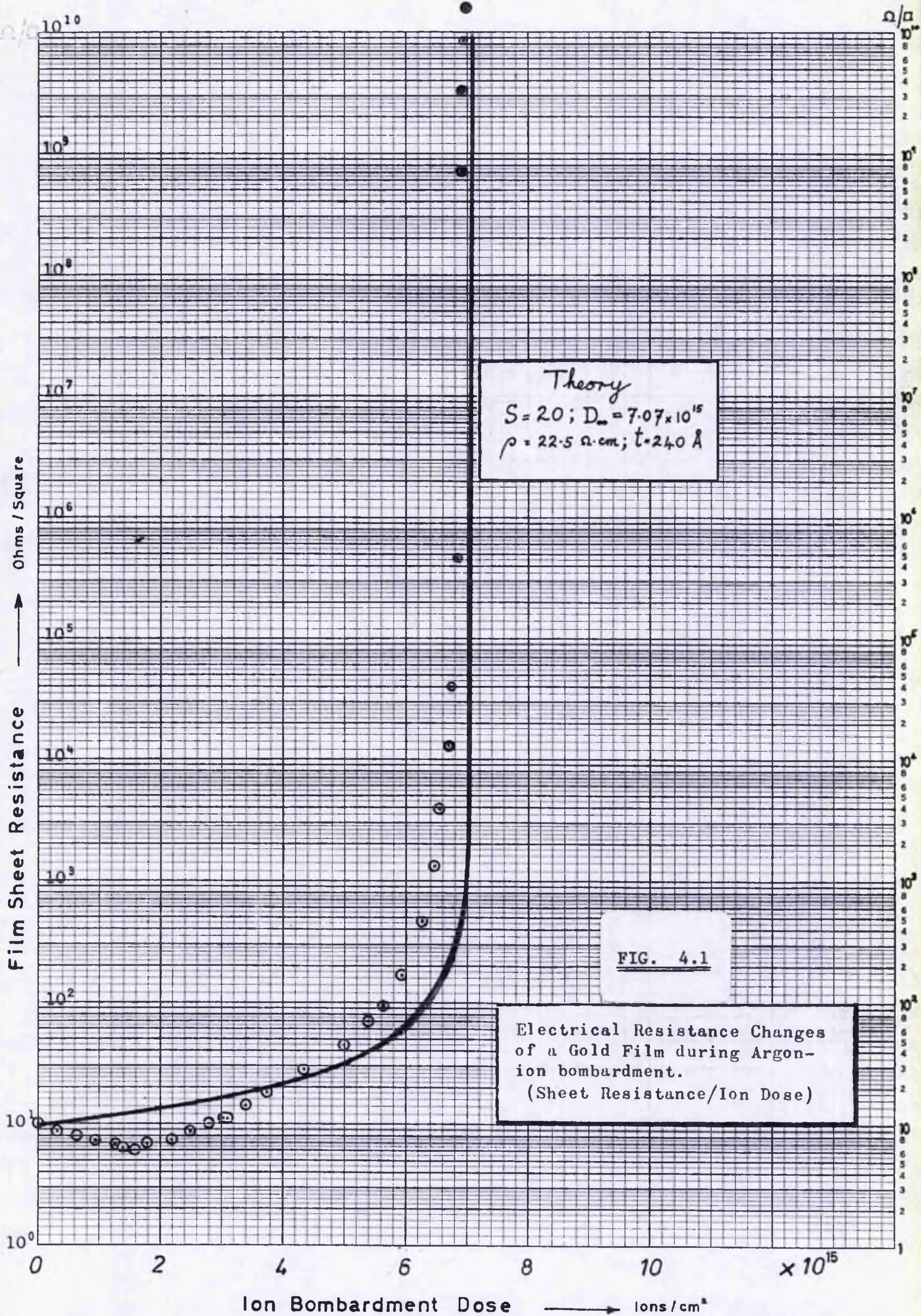

FIG. 4.1

Electrical Resistance Changes of a Gold Film during Argon-ion bombardment.
(Sheet Resistance/Ion Dose)

4.1.2 Resistivity

The effective resistivity of the film during argon bombardment may be calculated from the sheet resistance/bombardment dose relationship plotted in Figure 4.1 by assuming the film thickness to vary inversely as the dose. This calculated result is plotted in Figure 4.2 against bombardment dose.

The initial resistivity of this film was 24 $\mu\Omega$.cm., but dropped gradually to 12 $\mu\Omega$.cm. at a bombardment dose of 1.9 x 10^{15}ions/cm^2. On further bombardment the resistivity progressively increased until the film became effectively open-circuit.
In Figure 4.3 is shown the variation of conductivity with ion dose with theoretical curves for three values of sputtering rate. The relationship between volume resistivity and sheet resistance is shown in Figure 4.4.

4.1.3 Annealing

The isothermal annealing of gold films at room temperature is shown in Figures 4.5, and 4.6. Figure 4.5 shows the resistance change for a film bombarded to a resistance of 100 ohms. No significant change occurred over a period of about 200 hours (~1 week), but after this the resistance increased steadily and reached 2000 ohms after 1000 hours. Beyond this period the resistance remained practically constant. During the rapid resistance change the slope of the line (on the log/log scale) is 2, indicating a second-order dependance with time.

Annealing curves for several more films are given in Figure 4.6. The resistances have been normalised to the values obtaining at the end of the ion bombardment. It is characteristic of all films that the resistance remained constant for about 200 hours, increased during the next 200 or 300 hours, and thereafter remained relatively unchanged for several thousand hours.

The extent of the resistance change has been observed to be as much

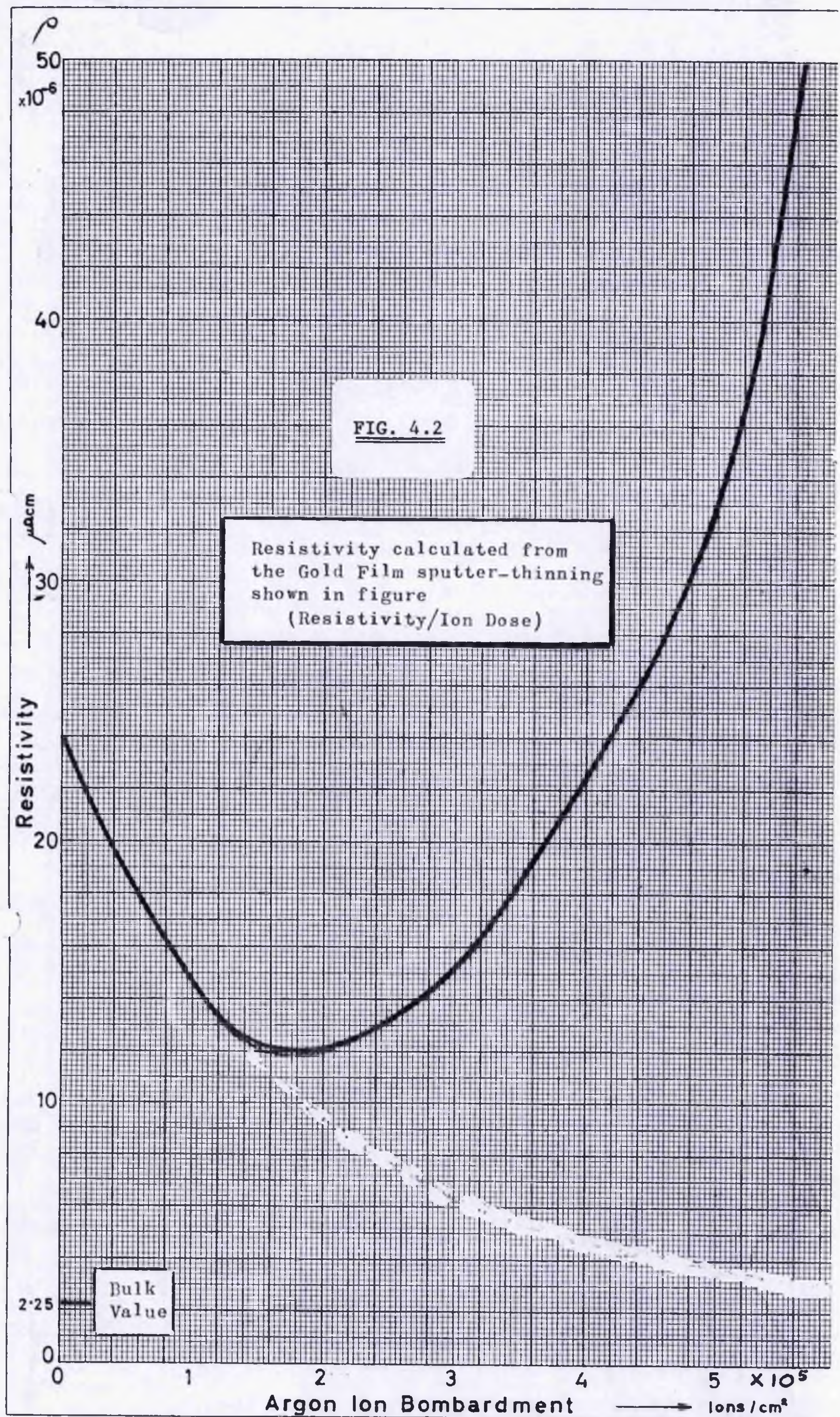

FIG. 4.2

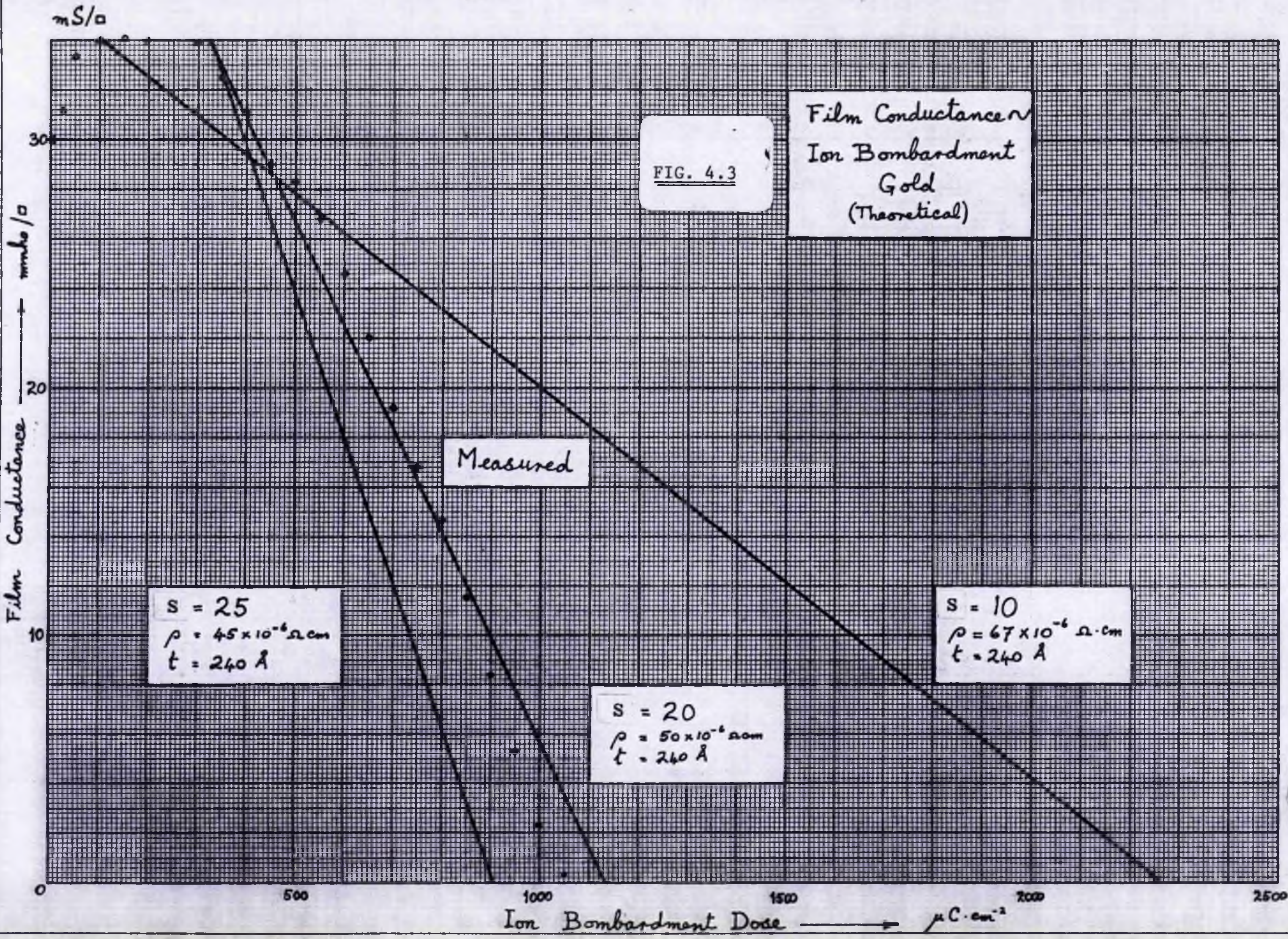

FIG. 4.3
Film Conductance ~ Ion Bombardment
Gold
(Theoretical)
Measured
S = 25
ρ = 45 x 10⁻⁶ Ω cm
t = 240 Å
S = 20
ρ = 50 x 10⁻⁶ Ω cm
t = 240 Å
S = 10
ρ = 67 x 10⁻⁶ Ω·cm
t = 240 Å
mS/□
Film Conductance → mho/□
Ion Bombardment Dose → μC·cm⁻²
0
10
20
30
500
1000
1500
2000
2500

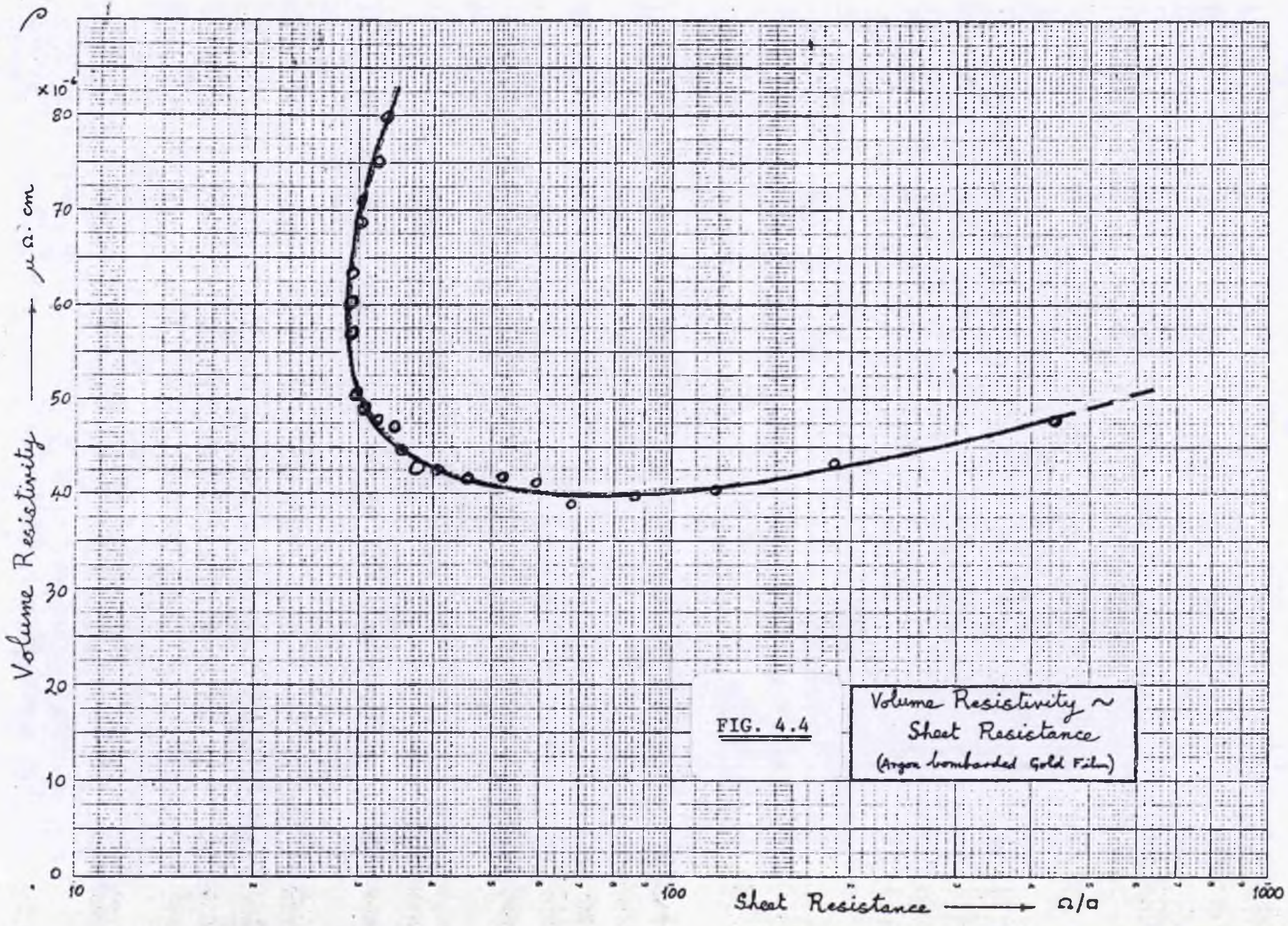

FIG. 4.4

FIG. 4.5

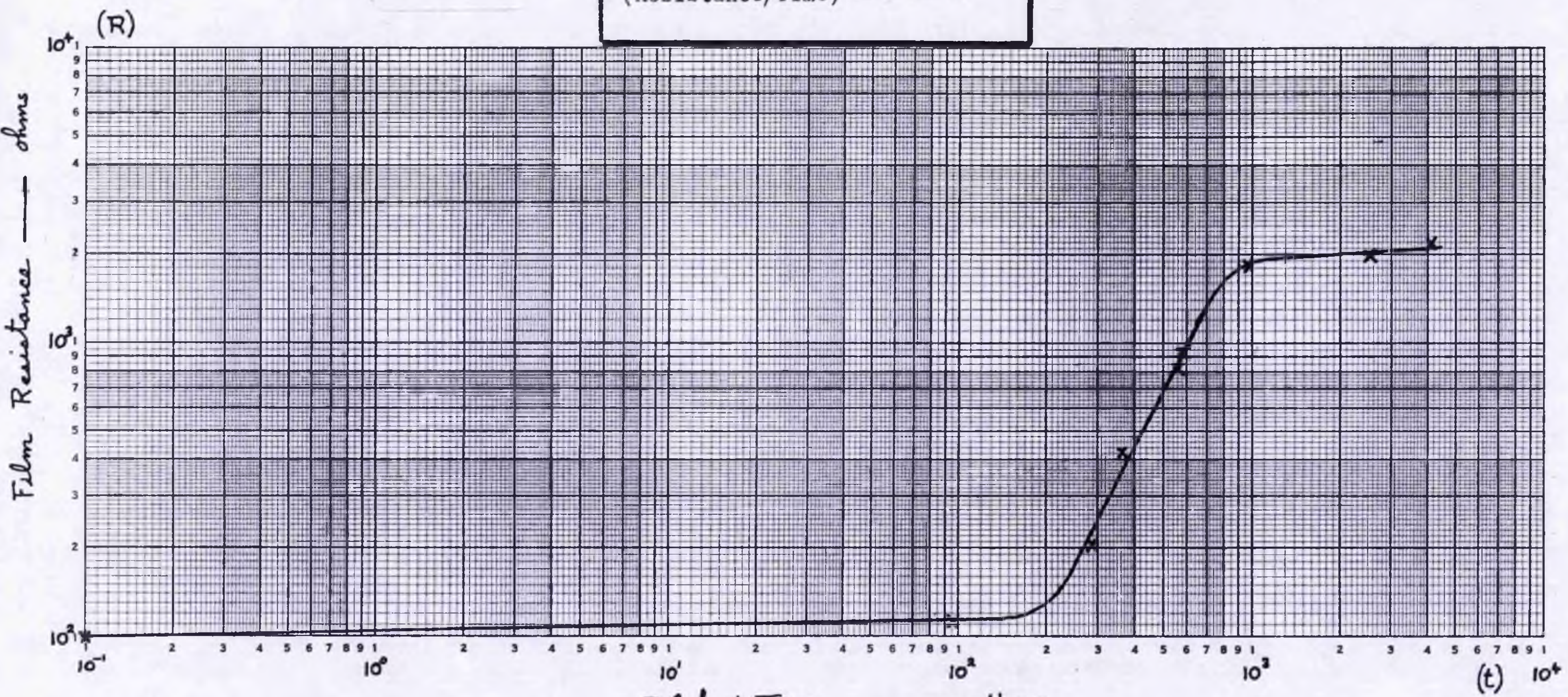

Room-temperature Annealing of an Ion-bombarded Gold Film. (Resistance/Time)

FIG. 4.6

Isothermal Annealing at Room Temperature of Ion-bombarded Gold Films.
(Normalised Resistance/Time)

as x40 and as little as x1.1, but the high resistance films become open-circuit eventually, after about 5000 hours.

The resistance changes for 12 films are given in Table 4.1.

4.1.4 Temperature Coefficient of Resistance

The temperature coefficient of resistance (TCR) of the sputtered films was measured after annealing for two weeks at room temperature and two hours at 120° C, and is plotted against their sheet resistance in Figure 4.7(a,b). In the main the TCR's all lie between 1000 parts per million per degree C and 1500 PPM/°C, though there is some indication of an increase in TCR at low sheet resistance (above 10 ohms/square). The average TCR of ion-bombarded gold films having sheet resistances between 3 ohms/square and 4×10^4 ohms/square is +1175 PPM/°C + - 95 PPM/°C.

The theoretical curve is based on equn.2.11 for the TCR of thin films, using MPF = 800 Å, resistivity = 50 μΩ.cm and TCR of bulk gold = 4000 PPM/°C.

Values of TCR for 15 specimens are given in Table 4.2. It can be seen from this and Fig. 4.7(b), that for the 35 MΩ/square specimen we have a negative value.

4.1.5 Strain-Gauge Coefficient of Resistance

The strain-gauge coefficients of the sputter-etched gold films, measured after annealing, are shown in Figure 4.8 plotted against their sheet resistance. Those having low sheet resistance (< 6 ohm/sq) are for films measured before bombardment, although the sheet resistances extend from less than 3 ohms/square to more than 4×10^4 ohms/square the resulting strain-gauge coefficients show no corresponding variation. The average value of strain-gauge coefficient for all gauges is $\gamma = 2.58 \pm 0.07$.

The straight horizontal line drawn at $\gamma = 2.43$ is developed from the theoretical relationship given in equn. 2.6.

TABLE 4.1

NO.	AT BOMBARDMENT RESISTANCE (Ω)	AT BOMBARDMENT DATE	AT BOMBARDMENT DOSE (μCcm^{-2})	AT BOMBARDMENT RESISTANCE (Ω) A	DATE	TIME LAPSE (Hrs)	RESISTANCE (Ω) B	RELATIVE RESISTANCE B/A	DATE	TIME LAPSE (Hrs)	RESISTANCE (Ω) C	RELATIVE RESISTANCE C/A	DATE	TIME LAPSE (Hrs)	RESISTANCE (Ω) D	RELATIVE RESISTANCE D / A
020	10.8	18.I.73	1220	10 000	9.II.73	528	54 150	5.41	11.VII.73	4224	52 400	5.24	2.III.74	9766	0/C	
021	11.0	18.I.73	1036	3 080	9.II.73	528	37 100	12.1	11.VII.73	4224	38 750	12.6	2.III.74	9766	88 400	28.7
023	10.75	17.I.73	780	92	2.II.73	584	128	1.41	11.VII.73	4248	127	1.38	2.III.74	9790	142.3	1.6
024	11.77	17.I.73	980	1 070	2.II.73	384	1568	1.47	11.VII.73	4248	1657	1.55	2.III.74	9790	1630	1.52
025	14.18	17.I.73	640	32	2.II.73	384	37.7	1.18	11.VII.73	4248	39	1.22	2.III.74	9790	36.7	1.15
026	13.68	17.I.73	1000	290	9.II.73	552	456.9	1.58	11.VII.73	4248	550	1.9	2.III.74	9790	485	1.67
035	6.3	1.XII.73	1650	192	29.XII.73	360	211	1.1	2.III.74	2160	205.5	1.07				
038	8.9	5.IX.73	—	98.5	9.IX.73	96	112	1.14	17.IX.73	288	201.8	2.05	20.IX.73	360	429	4.35
					28.IX.73	562	834	8.45	29.IX.73	576	944	9.6	15.X.73	960	1844	18.8
					20.XII.73	2544	1977	20.1	24.II.74	4128	2219	22.5	2.III.74	4272	2252	22.9
042	11.6	1.XII.73	300	150	24.XII.73	552	3069	20.5	2.III.74	2160	5248	35				
043	46.8	1.XII.73	250	124	26.XII.73	600	1131	9.15	2.III.74	2160	1255	10.1				
044	9.5	1.XII.73	1360	153	27.XII.73	624	5375 (10226)	35.2	2.III.74	2160	13 053 (annealed)	85.3				
047	5.2	1.XII.73	750	800	16.XII.73	360	1224	1.53	2.III.74	2160	1271	1.59				

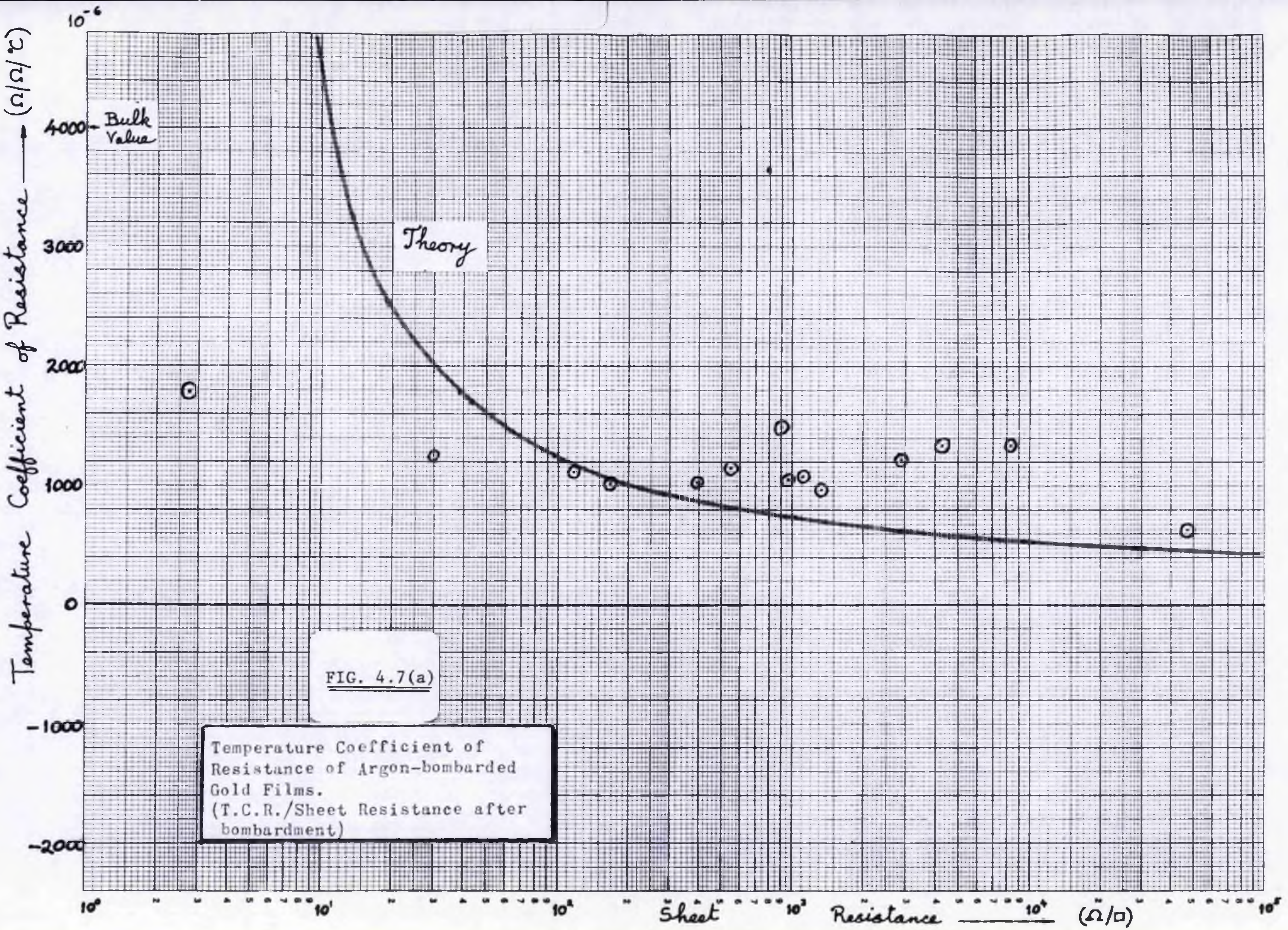

FIG. 4.7(a)

Temperature Coefficient of Resistance of Argon-bombarded Gold Films. (T.C.R./Sheet Resistance after bombardment)

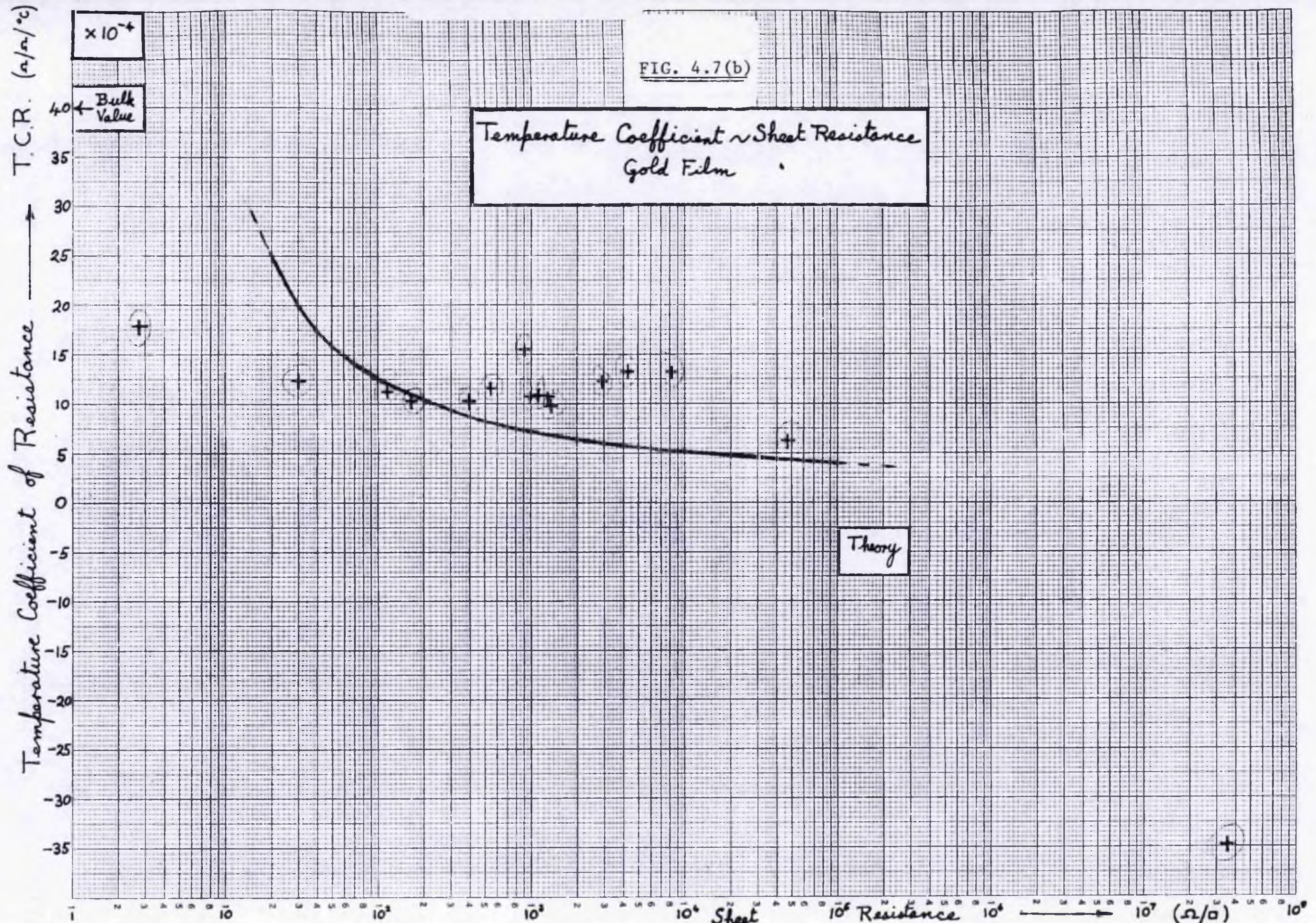
FIG. 4.7(b)
Temperature Coefficient ~ Sheet Resistance
Gold Film
Theory
× 10⁻⁴
Bulk Value
T.C.R. (Ω/Ω/°C)
Temperature Coefficient of Resistance
Sheet Resistance (Ω/□)
40
35
30
25
20
15
10
5
0
-5
-10
-15
-20
-25
-30
-35
1
10
10²
10³
10⁴
10⁵
10⁶
10⁷
10⁸

TABLE 4.2

Specimen Number	010	021	023	024	025	020	035	035	038	038	042	043	044	044	047
Substrate thickness (mm)	.835	.87	.85	.85	.88	.875	.908	.908	.96	.96	.89	.89	.883	.883	.885
Bombardment window (mm sq)	10	10	10	10	10	10	—	10	14	14	10	10	10	10	10
Ion dose ($\mu C\ cm^{-2}$)	1505	1036	780	980	640	1000	Nil	1650	—	—	800	250	1360	1360	750
Sheet resistance	35.0 MΩ/□	46.7 kΩ/□	116.5Ω/□	1325Ω/□	30.0Ω/□	395Ω/□	2.75Ω/□	189Ω/□	545Ω/□	1140Ω/□	2920Ω/□	905Ω/□	4300Ω/□	8300Ω/□	980Ω/□
T.C.R. ($\times 10^{-4}$)	-34.8	6.10	11.2	9.77	12.5	10.2	17.9	10.2	11.5	10.7	12.2	15.5	13.4	13.3	10.6
Temperature (°C)	STRAIN-GAUGE COEFFICIENT OF RESISTANCE, (S.G.C.R)														
-20	—	—	3.71	2.85	—	2.78	2.63	2.58	2.08	—	—	—	—	—	—
-10	—	—	—	2.82	2.85	—	2.86	2.47	2.49	—	—	—	—	—	—
0	—	—	—	2.97	2.77	—	2.53	2.64	2.04	—	—	—	—	—	—
10	—	—	—	3.94	3.04	3.72	2.34	2.71	2.04	2.02	2.81	2.81	2.21	2.19	—
20	—	—	—	2.68	2.97	2.60	2.49	2.60	1.93	2.16	3.03	3.02	2.29	2.29	—
30	—	—	—	2.48	2.74	2.61	2.28	2.58	1.92	2.05	2.72	2.62	2.43	2.14	—
40	—	—	—	2.43	2.90	2.60	2.52	2.56	1.95	2.09	2.50	2.54	2.57	2.18	—
50	—	—	—	2.53	2.69	2.74	2.66	2.58	1.93	2.07	2.90	2.80	—	2.10	—
60	—	—	—	2.38	2.68	2.61	2.56	2.64	2.0	2.06	—	2.50	—	2.16	—
70	—	—	—	2.56	2.52	2.68	2.40	—	1.96	2.03	—	—	—	—	—

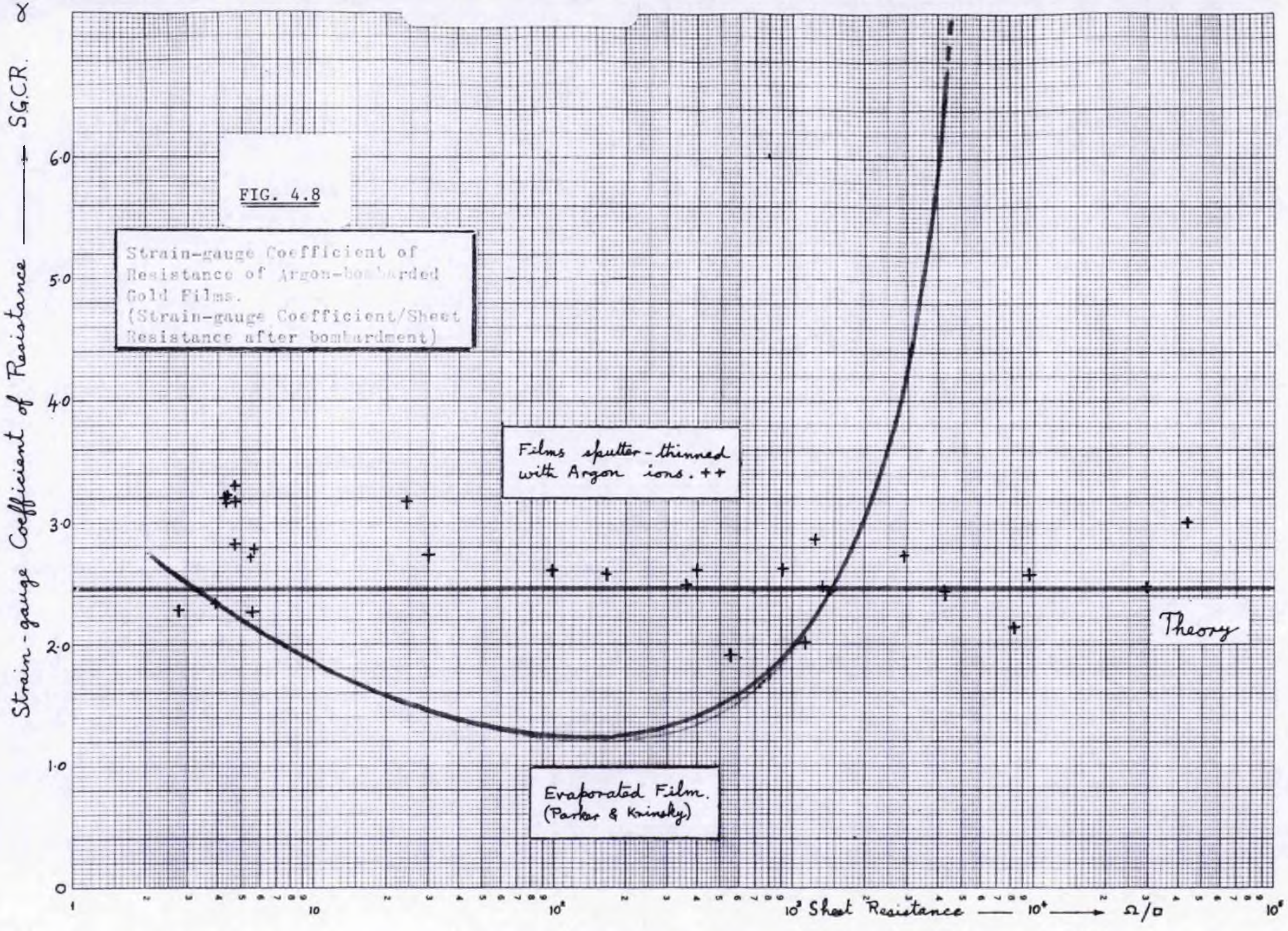

FIG. 4.8

Strain-gauge Coefficient of Resistance of Argon-bombarded Gold Films. (Strain-gauge Coefficient/Sheet Resistance after bombardment)

The curved line is taken from the work of Parker and Krinsky,[4] and shows the variation in γ with sheet resistance found by them for evaporated thin gold films (without ion bombardment). They found that the strain-gauge factor of this type of film has a minimum value of $\gamma = 1.2$ at $R_s = 150$ ohms/square, that it rises to the bulk value ($\gamma = 4.48$) for low sheet resistances (thicker films), and that it rises steeply towards $\gamma = 100$ for films having R_s greater than about 2×10^5 ohms/square.

4.1.6. Temperature Coefficient of Strain-Gauge Factor

Measurements were made by strain-gauge factor at different temperatures, with the result shown in Figure 4.9. Because no significant variation of γ was found with change in R_s due to ion bombardment, measurements are included of films having had different ion bombardment doses. The very large scatter in the strain-gauge measurements arises from difficulties in controlling the bending of the specimens in the environmental chamber.

A simple line-fitting routine was used to obtain the temperature coefficient of strain-gauge factor of $\rho = -1590$ PPM/$^\circ$C + - 1100 PPM/$^\circ$C, and an average value for γ of 2.58 at 30° C. This result is statistically significant.

4.1.7 S.E.M. Microscopic Examination

The structure of the bombarded gold films has been examined under the scanning electron microscope at a magnification of X14000. Unbombarded films show a smooth featureless surface; but after bombardment this is found covered with irregularly shaped dark areas (substrate). Figure 4.10 shows micrographs of four films at different bombardment levels.

At a dose of 4×10^{15} ions/cm^2 (Film No. 25) the micrographs shows thin fissures in the film surface: the resistance of this film had been

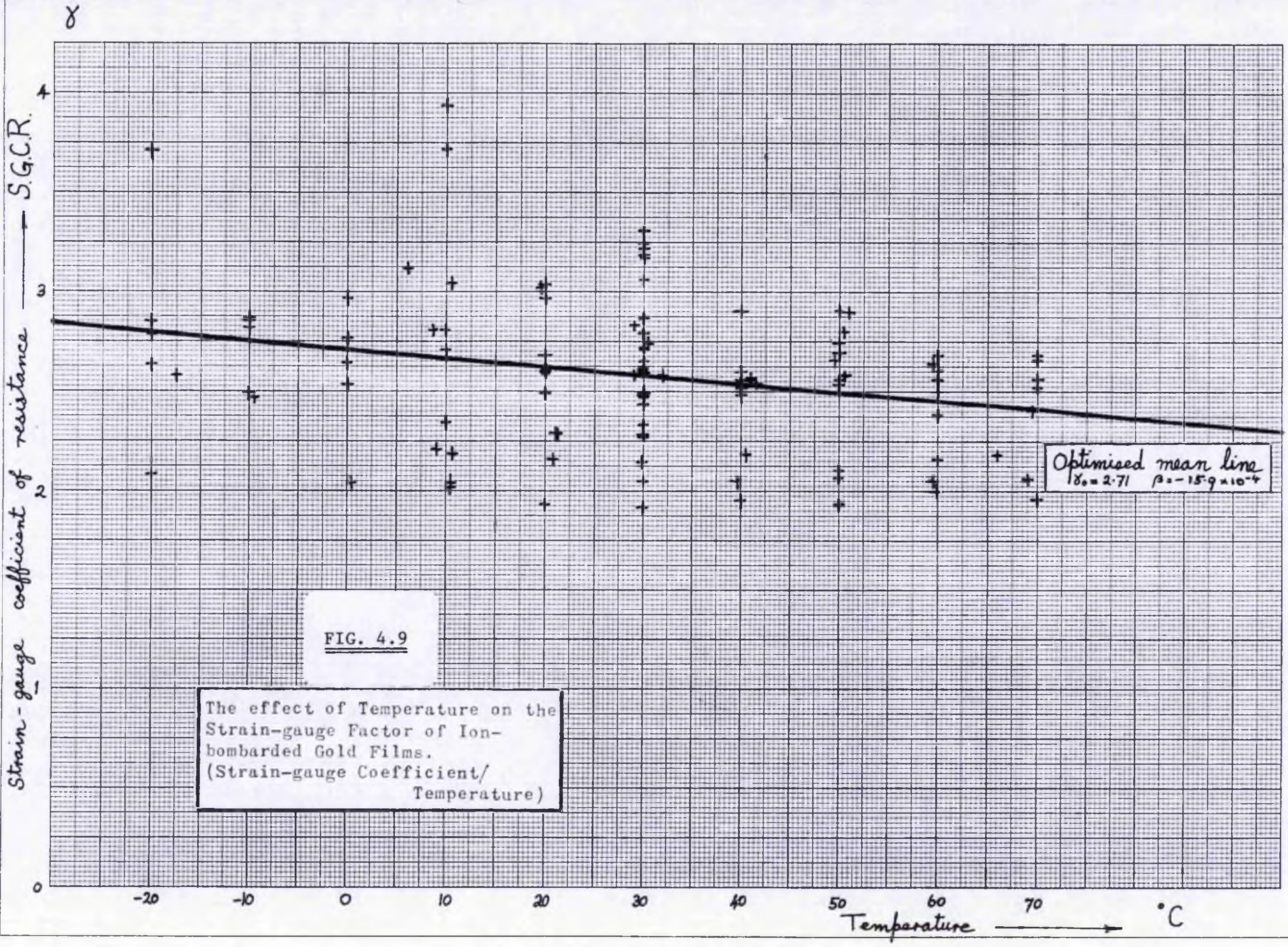

FIG. 4.9

The effect of Temperature on the Strain-gauge Factor of Ion-bombarded Gold Films. (Strain-gauge Coefficient/Temperature)

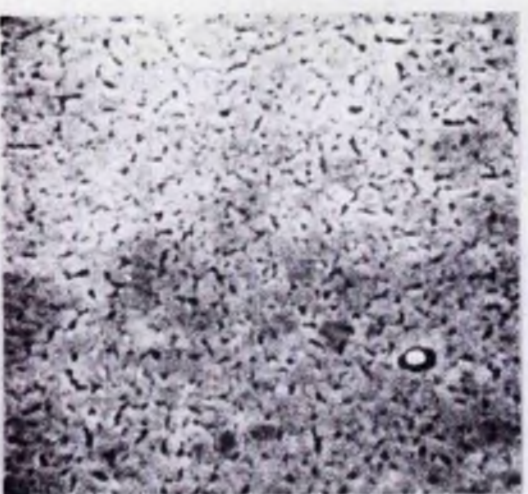

No. 25 R_s = 30Ω/□, 4 × 10^{15} Ions/cm^2

Magnification
× 14k

Tilt 35°

→| 1 μm |←

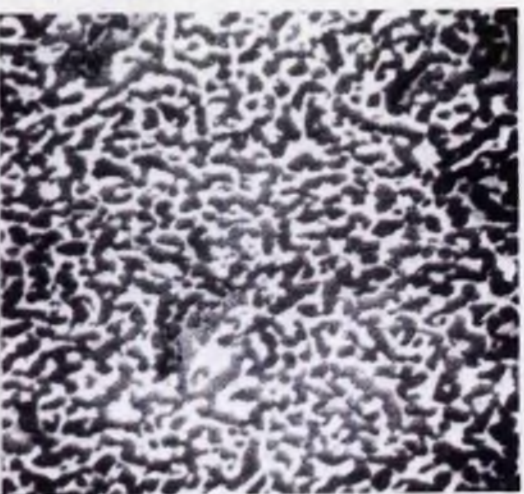

No. 26 R_s = 290Ω/□, 6.2 × 10^{15} Ions/cm^2

No. 47 R_s = 980Ω/□, 4.7 × 10^{15} Ions/cm^2

FIG. 4.10

GOLD FILM

S.E.M. MICROGRAPHS

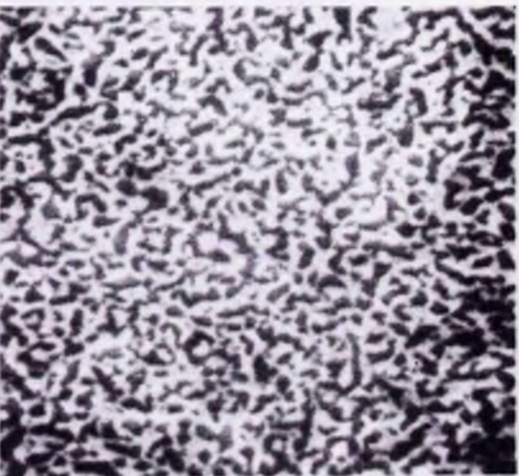

No. 21 R_s = 99 kΩ/□, 6.5 × 10^{15} Ions/cm^2

increased by ion bombardment to 30 ohm/sq. A second film (No.47) bombarded to 4.7×10^{15} ions/cm^2 , had a sheet resistance of 980 ohm/sq. The fissures in this had thickened about five times without a significant increase in their length, though the mean spacing of the damage sites was the same as in the first case.

Film No.26 had been bombarded to 6.2×10^{15}ions/cm^2 . Here the areas of damage (dark areas) covered more than half the film surface and the remaining metal had taken on a spongiform appearance. The resistance of this film seems unually low (being 290 ohm/sq) since film No. 21, bombarded to 6.5×10^{15} ions/cm^2 had a sheet resistance of 99 kilohm/sq. In this film also the appearance was spongiform, though having a finer texture than that of No. 26.

4.1.8 Microprobe Analysis

An examination was made of the light and dark areas shown in the micrographs, using x-ray analysis in a C.S.I. microprobe analiser. Film No. 26 was used for this(bombardment was 4.7×10^{15} ions/cm^2): the spectrograms are shown in Figure 4.11. The trace on the left was made with the probe on a light area, and it shows a well defined gold response of about one-half that obtained for silicon. On the right is the trace for a dark area, which has no gold peak but shows correspondingly similar values for sodium, silicon and calcium.

This result demonstrates that the light areas of the micrographs are gold film and that the dark areas are holes in the film through which the soda glass substrate is observed.

With the probe directed to an unbombarded part of the film the response peaks for gold and for silicon were of equal amplitude.

4.2 Tantalum Films before Bombardment

The tantalum films used for strain measurement were all deposited

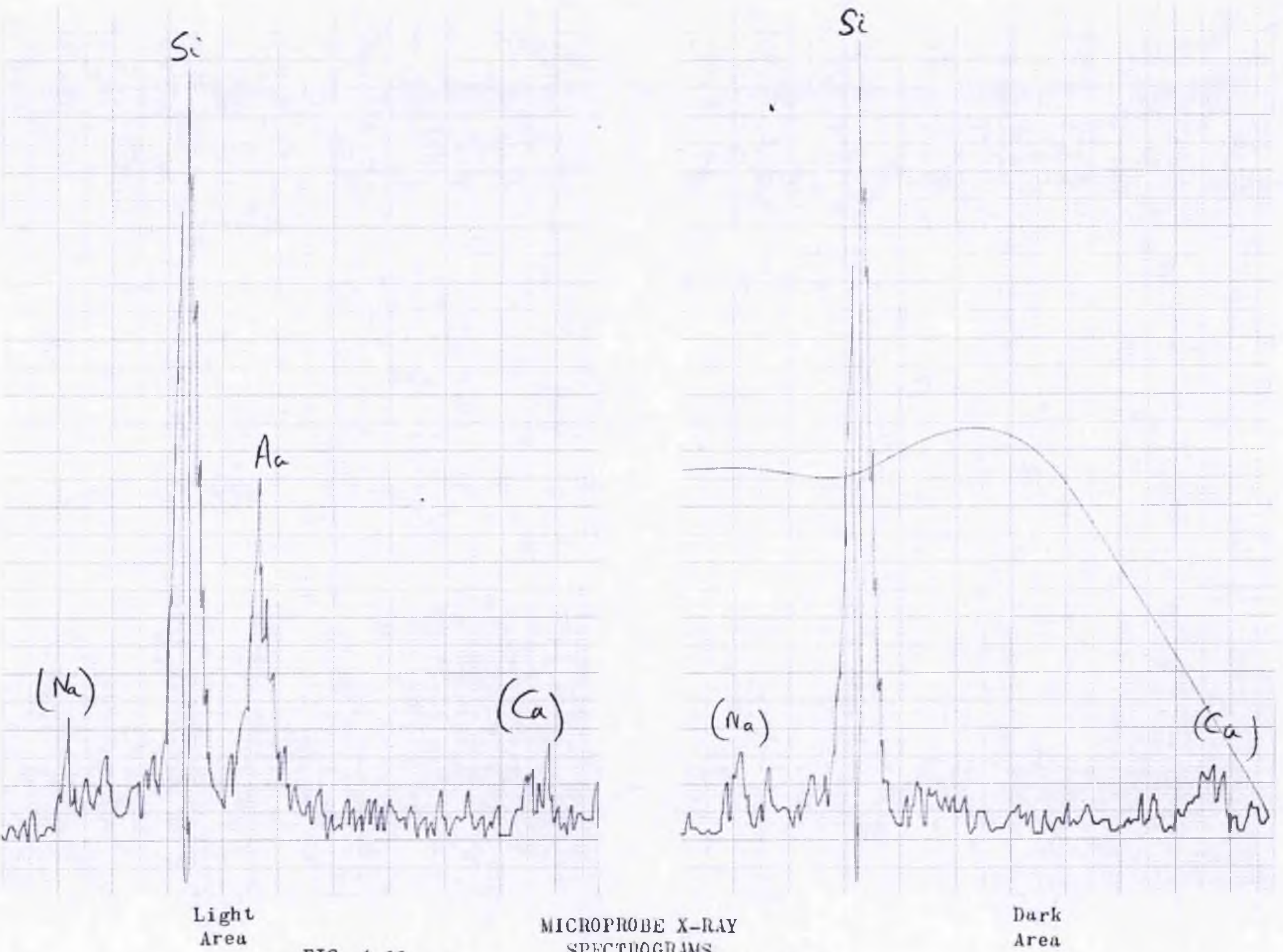

FIG. 4.11 MICROPROBE X-RAY SPECTROGRAMS (R_s = 980 Ω/□, 4.7 × 10^{15} ions/cm^2)

onto glass substrates, but a few others - used for sheet resistance and TCR measurement - were deposited onto alumina and a few onto mica substrates, no noticeable difference was observed in their use.

4.2.1 Sheet Resistance

The variation of sheet resistance with film thickness was explored within the thickness range 50 Å to 2600 Å, and was found to extend from R_s = 80 KΩ/sq to R_s = 14Ω/sq respectively. A plot of this result is given in Figure 4.12. The sheet resistance varies inversely with film thickness, being asymptotic to a line ρ = 360 μΩ.cm for the thicker films and rising steeply above this line at film thicknesses below 100 Å.

The corresponding variation of resistivity with film thickness has been calculated for the mean sheet resistance line (shown dotted in Figure 4.12) and is given in Figure 4.13. This shows that for film thickness above 400 Å the resistivity is sensibly constant, being 380 μΩ.cm for T = 2500 Å and 400 μΩ.cm for T = 400 Å. Below this thickness the resistivity rises rapidly, and reaches 2500 μΩ.cm at T = 50 Å.

4.2.2. Temperature Coefficient of Resistance

The TCR of evaporated tantalum film measured between room temperature and about 120° C is very small, and is practically constant for films of greater thickness than 200 Å. The average TCR of these films is -150 PPM/° C. Films of lesser thickness show a progressively greater negative TCR, 50-Å films having a TCR of -1800 PPM/ °C. This is shown in Figure 4.14. The transition (around T = 150 Å) between large negative TCR and a constant, small TCR is quite abrupt.

TCR plotted against sheet resistance is given in Figure 4.15. The region of constant TCR extends from R_s = 14 Ω/sq to R = 9 K Ω/sq.

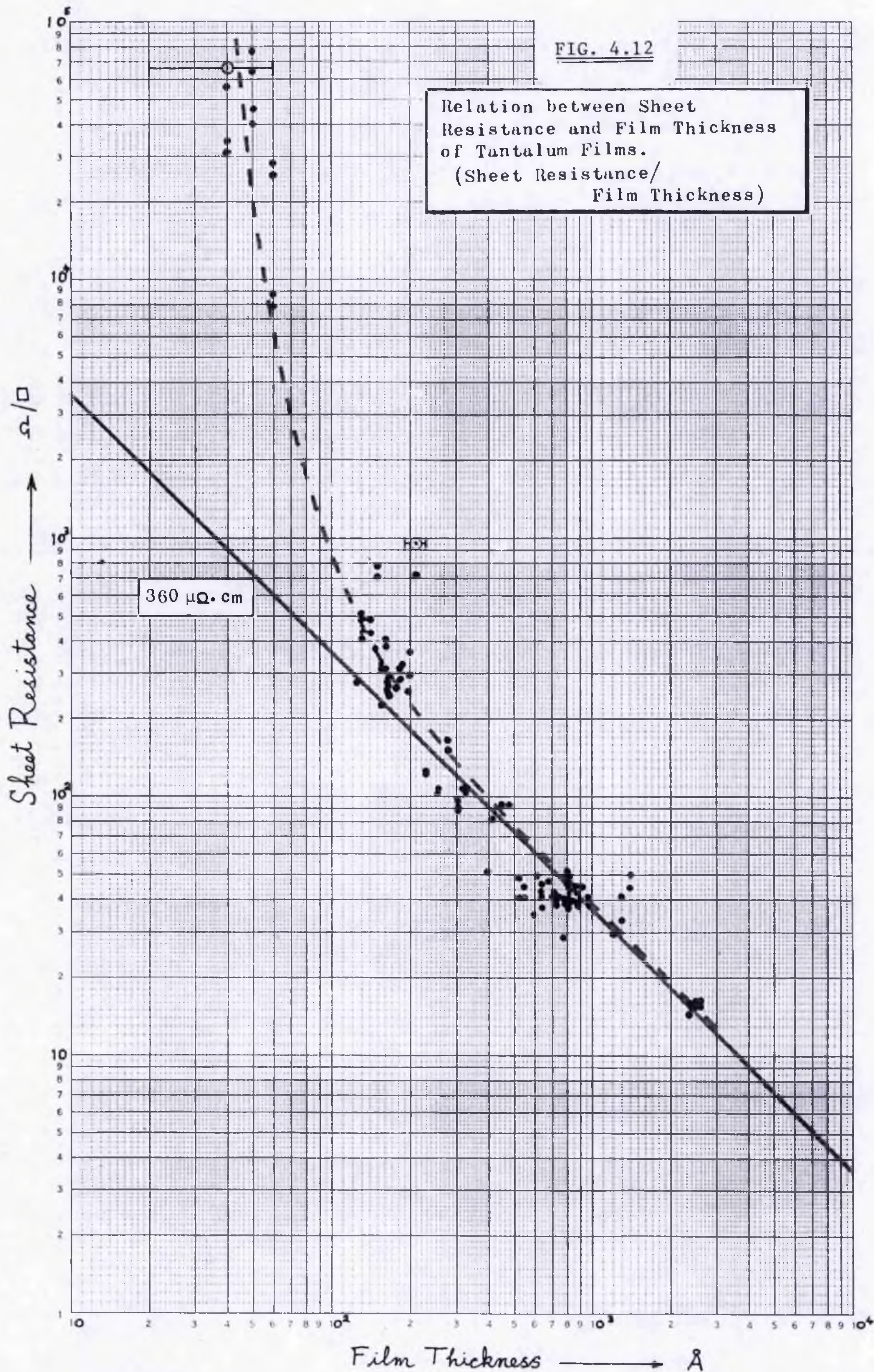
FIG. 4.12
Relation between Sheet Resistance and Film Thickness of Tantalum Films.
(Sheet Resistance/ Film Thickness)
360 μΩ.cm
Sheet Resistance → Ω/□
Film Thickness → Å

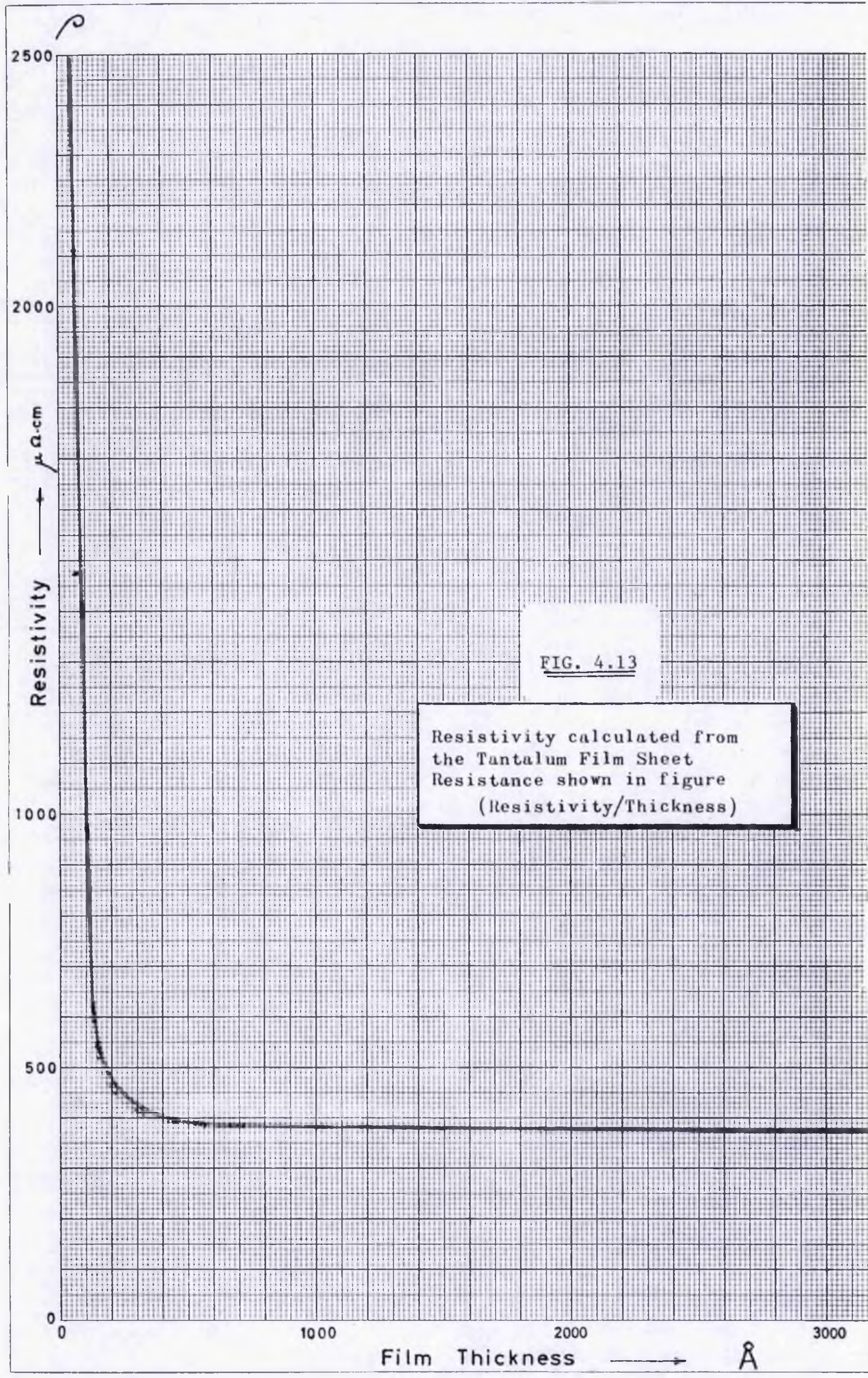
ρ
2500
2000
1000
500
0
Resistivity ——→ μ Ω-cm
0
1000
2000
3000
Film Thickness ——→ Å
FIG. 4.13
Resistivity calculated from
the Tantalum Film Sheet
Resistance shown in figure
(Resistivity/Thickness)

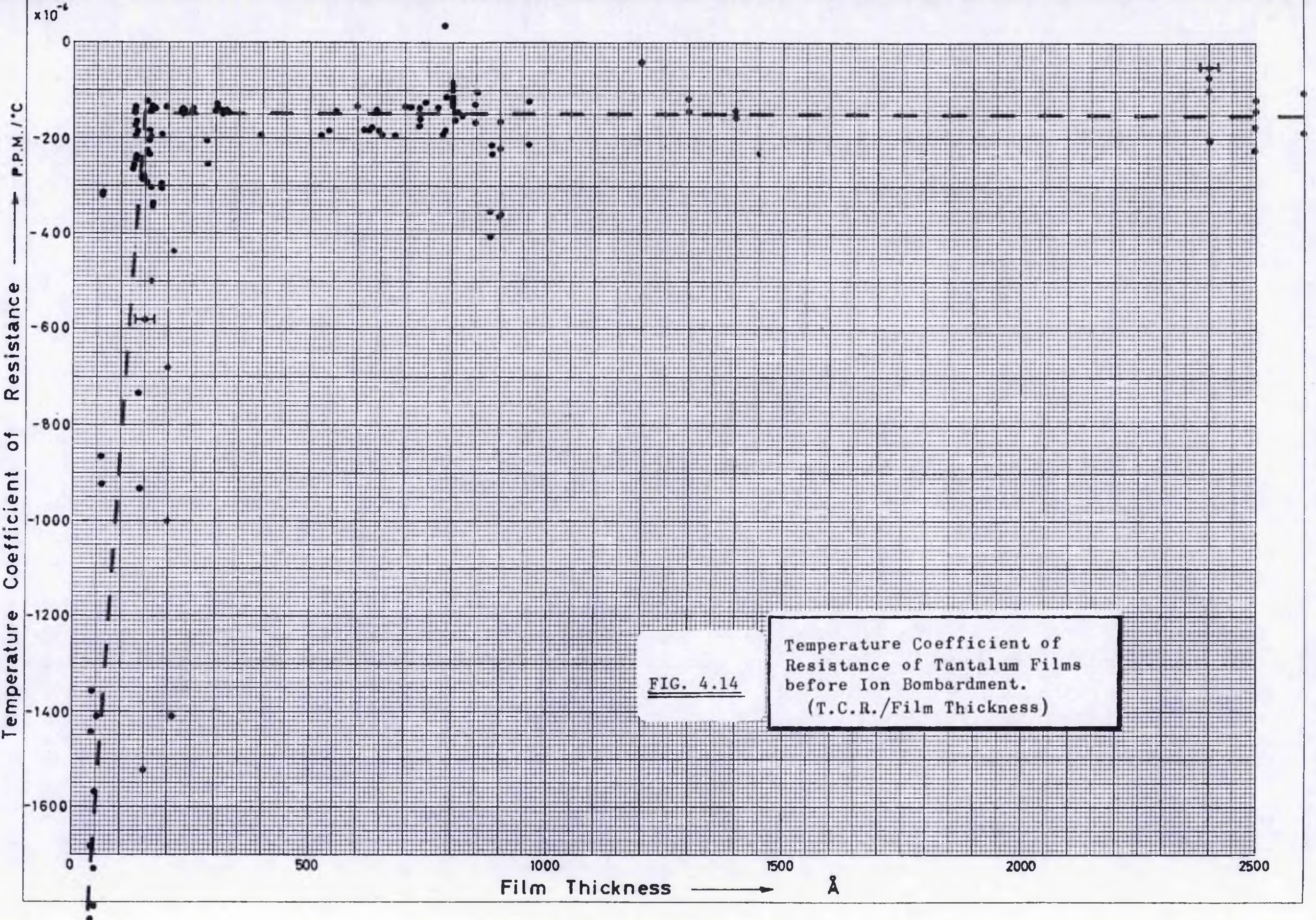
x 10^-6
0
-200
-400
-600
-800
-1000
-1200
-1400
-1600
Temperature Coefficient of Resistance
P.P.M./°C
0
500
1000
1500
2000
2500
Film Thickness
Å
FIG. 4.14
Temperature Coefficient of Resistance of Tantalum Films before Ion Bombardment.
(T.C.R./Film Thickness)

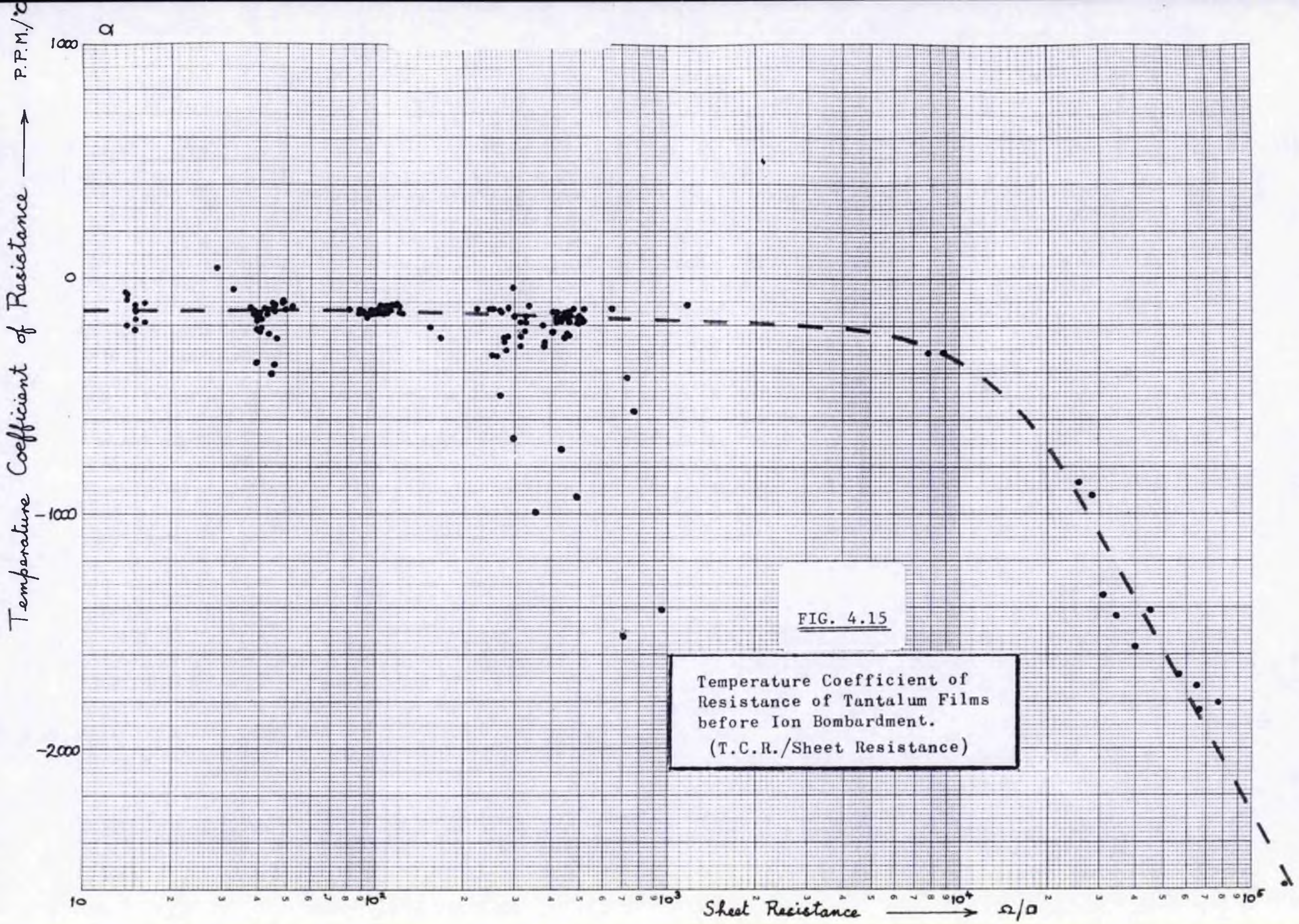

FIG. 4.15

Temperature Coefficient of Resistance of Tantalum Films before Ion Bombardment. (T.C.R./Sheet Resistance)

At greater sheet resistance the TCR becomes larger and more negative, but the transition is not abrupt.

A few films with sheet resistance below 1000 Ω/sq have TCR greater than usual, but this seems to be abnormal.

The resistance of one film (No.3706, T = 730 Å) has been observed over the temperature range -195° C to + 110° C, see Figure 4.16. By treating this result as a second order relationship the following expression is obtained:

$$R_s = 40.9(1 - 144 \times 10^{-6} T + 0.28 \times 10^{-6} T^2) \ \Omega/\text{sq.}$$

Extrapolation indicates a minimum sheet resistance of 40.1 Ω/sq. occurring at a temperature of 257° C.

An Arrhenius plot from these resistance/temperature measurements is given in Figure 4.17. Three activation levels are evidence in this; at temperatures below -130° C an activation energy of 0.23×10^{-3} eV; between -130° C and -35° C a level of 0.51×10^{-3} eV; and for temperatures above -35° C a level of 1.04×10^{-3} eV . These activation energies stand approximately in the ratios 1:2:4.

The activation energies of all films are shown plotted against sheet resistance in Figure 4.18. The energies were measured over the temperature range room temperature to about 120° C. Although there is a general trend towards higher activation energy at greater sheet resistance, there is a considerable spread in the energy values, extending over about one order of magnitude.

4.2.3 Strain-Gauge Coefficient of Resistance

Strain-gauge measurements were made on tantalum films evaporated to a nominal thickness of 750 Å : those used had sheet resistances between 30 Ω/□ and 50 Ω/□. Under simple four-point bending up to a value of about 250 micro-strain, the strain-gauge effect was linear, with an average coefficient of γ = 3.04 and standard error 0.15 (5%). No significant change in γ was observed with sheet resistance, see Figure 4.19.

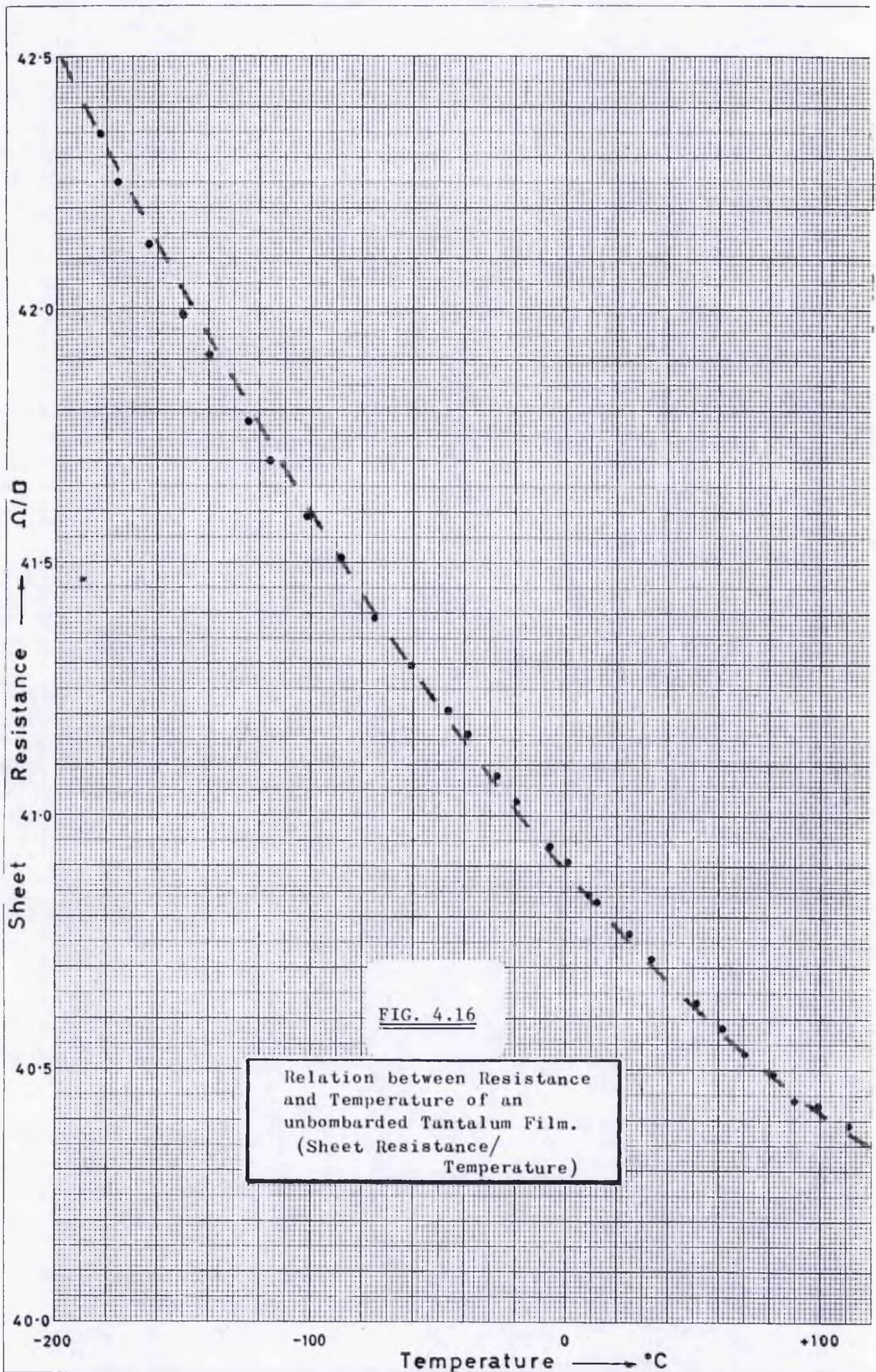

FIG. 4.16

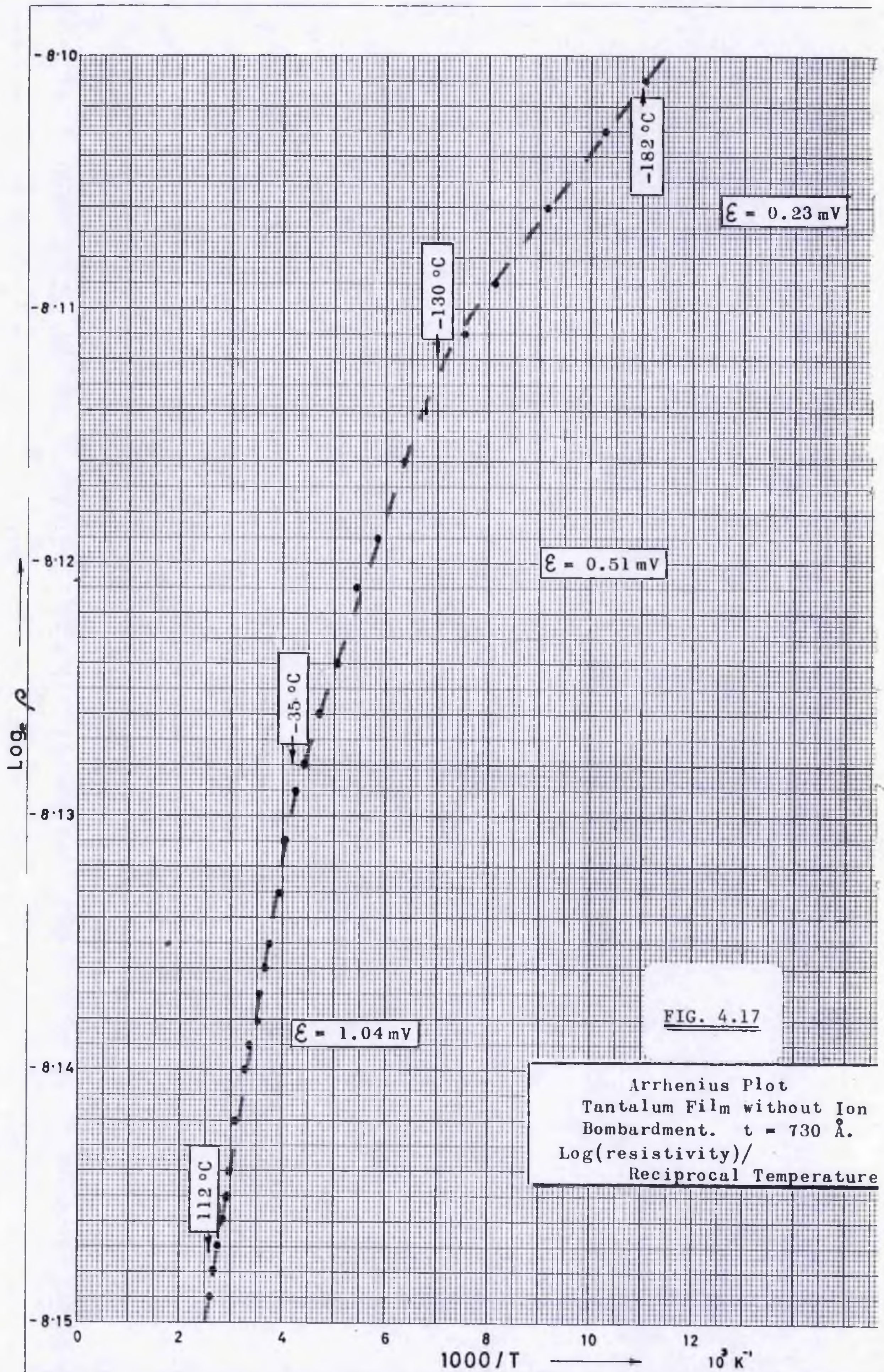

FIG. 4.17

Arrhenius Plot
Tantalum Film without Ion Bombardment. t = 730 Å.
Log(resistivity)/
Reciprocal Temperature

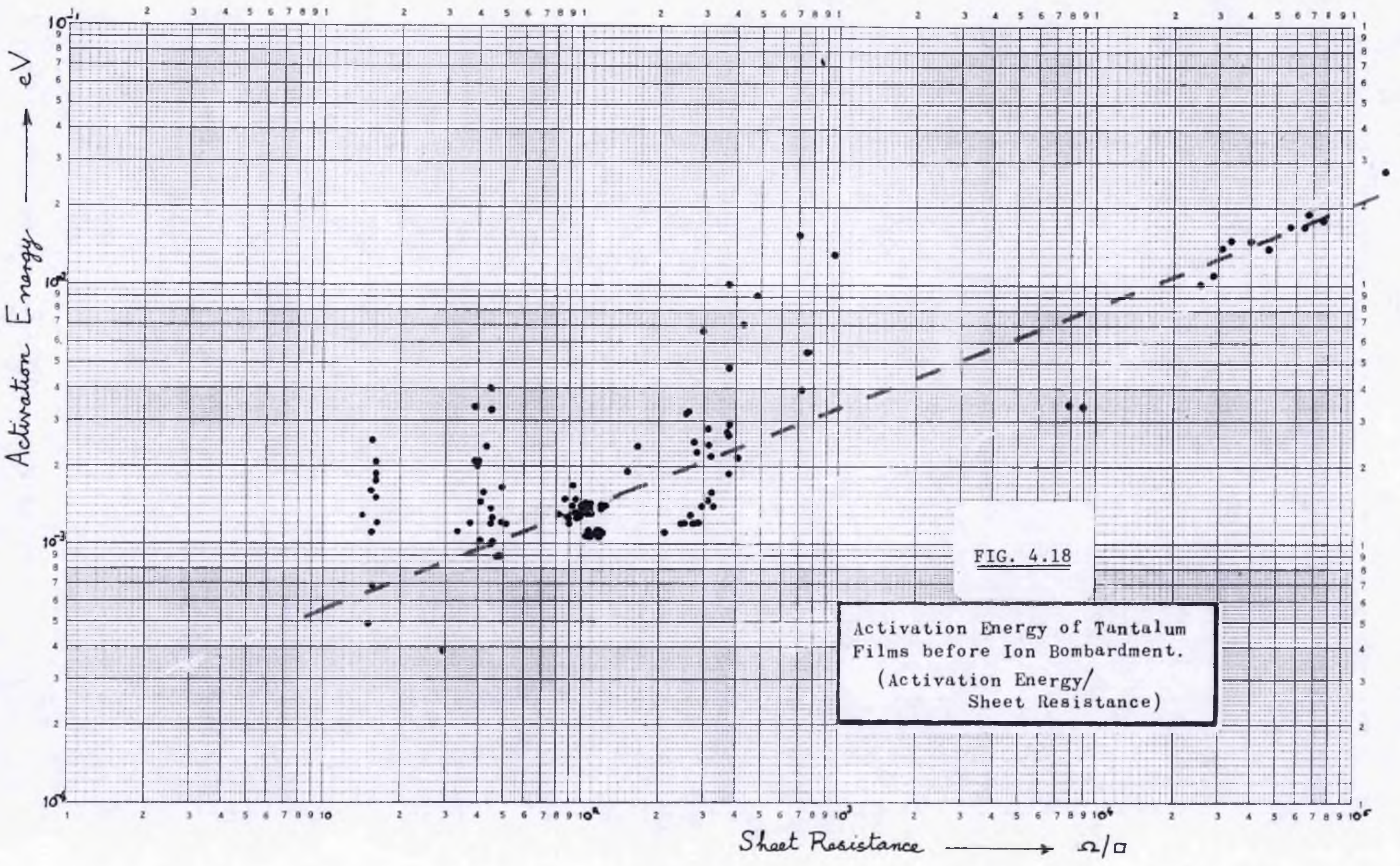

FIG. 4.18

Activation Energy of Tuntalum Films before Ion Bombardment. (Activation Energy/ Sheet Resistance)

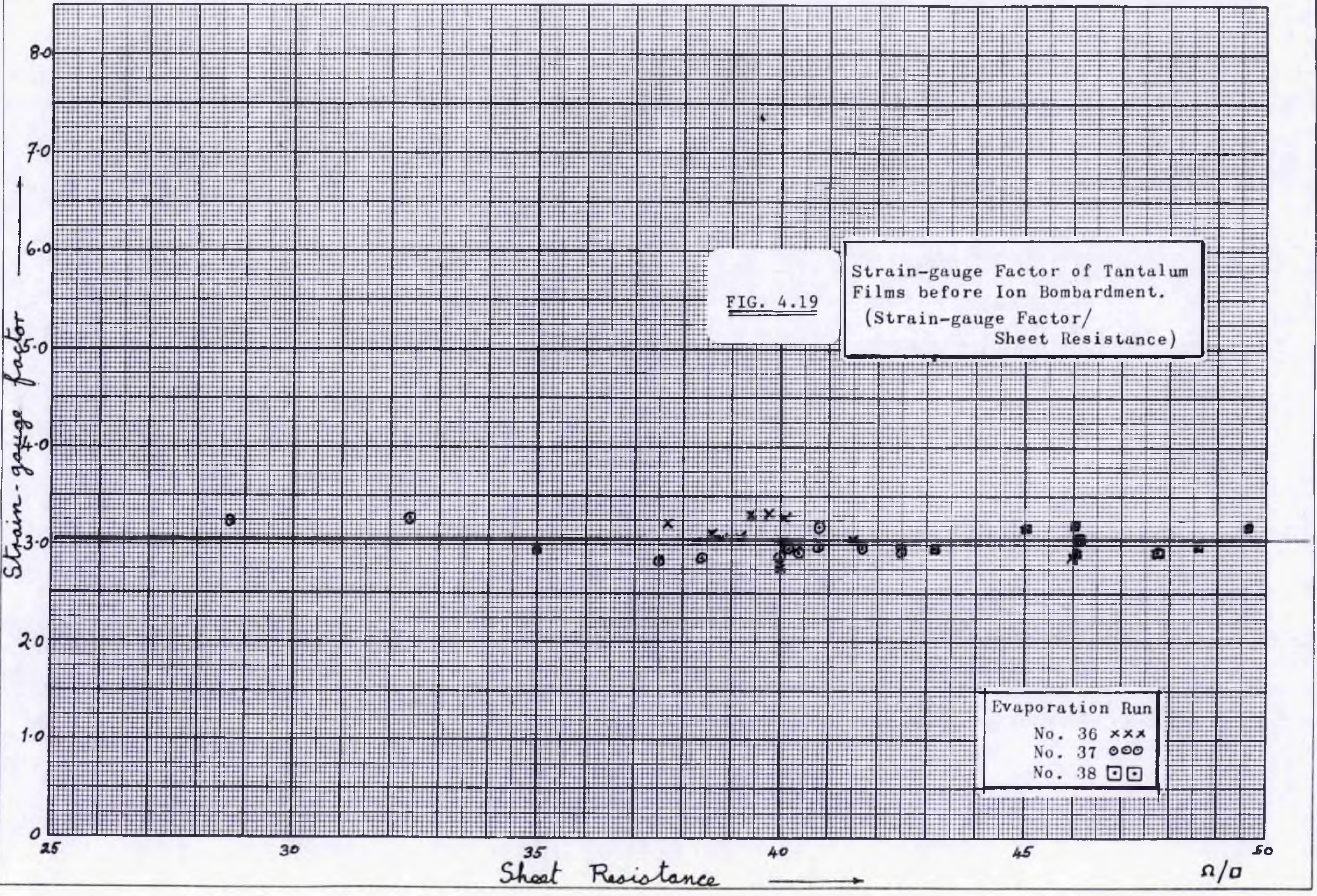

FIG. 4.19

Strain-gauge Factor of Tantalum Films before Ion Bombardment. (Strain-gauge Factor/ Sheet Resistance)

Strain-gauge factor was used as a measure of the repeatability of the evaporated tantalum films. Figure 4.20 shows histograms of γ for three different evaporation runs and also for the combined result. The mean γ obtained in each evaporation run is within 3% of the average value for γ quoted above for all runs combined, and generally is very much closer than this.

A cumulative frequency diagram for the same films is shown in Figure 4.21.

4.3 Bombarded Tantalum Films

The films previously used for strain-gauge measurements were then subjected to argon-ion bombardment at 50 KeV. The projected range of such ions in β - tantalum is 210 Å[16], so that nearly all the beam energy was absorbed within the film thickness, nominally of 750 Å. The maximum dose used was 2.8×10^{17} ions/cm^2.

4.3.1 Resistance

The effect of ion bombardment on the resistance of tantalum films was similar to its effect on gold films. Initially bombardment reduced the resistance but as it proceeded the resistance was increased until eventually the film became open circuit. At a dose of 0.6×10^{17} ions/cm^2 the sheet resistance was reduced to 50% of its original value (40 $\Omega/\square$), and this was followed by a steady rise in resistance that reached 6000 $\Omega/\square$ at 2.6×10^{17} ions/cm^2 (see Figure 4.22). All the films bombarded with doses greater than 2.8×10^{17} ions/cm^2 were found to be open circuit upon measurement.

Shown as a continuous line is the result of simple sputtering theory (equn.2.4).

The minimum ion dose needed to remove a given film completely is related to this value, but a contributary cause of increased resistance must be the oxidation that follows breaking the vacuum. Thus it may be

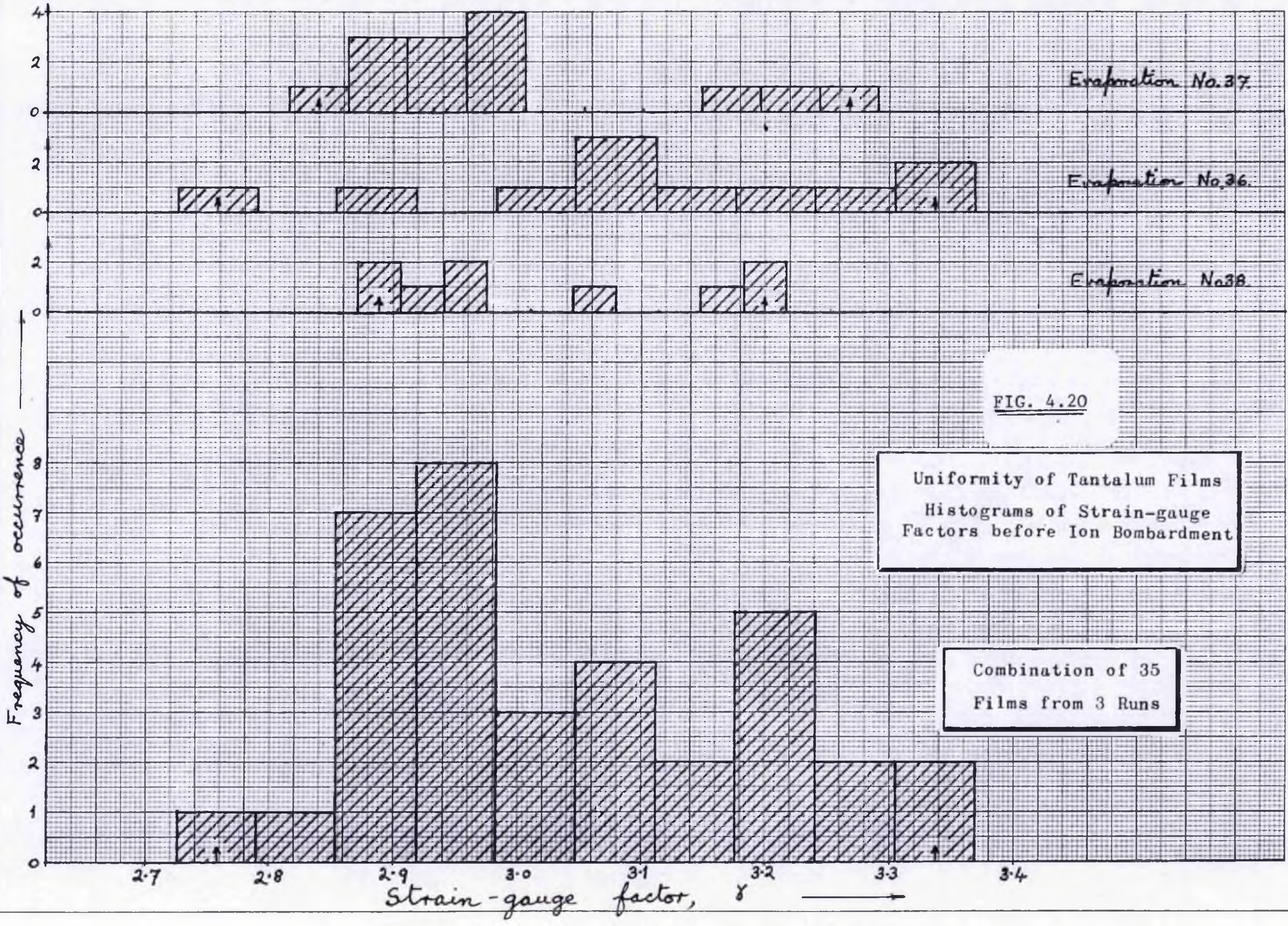

FIG. 4.20

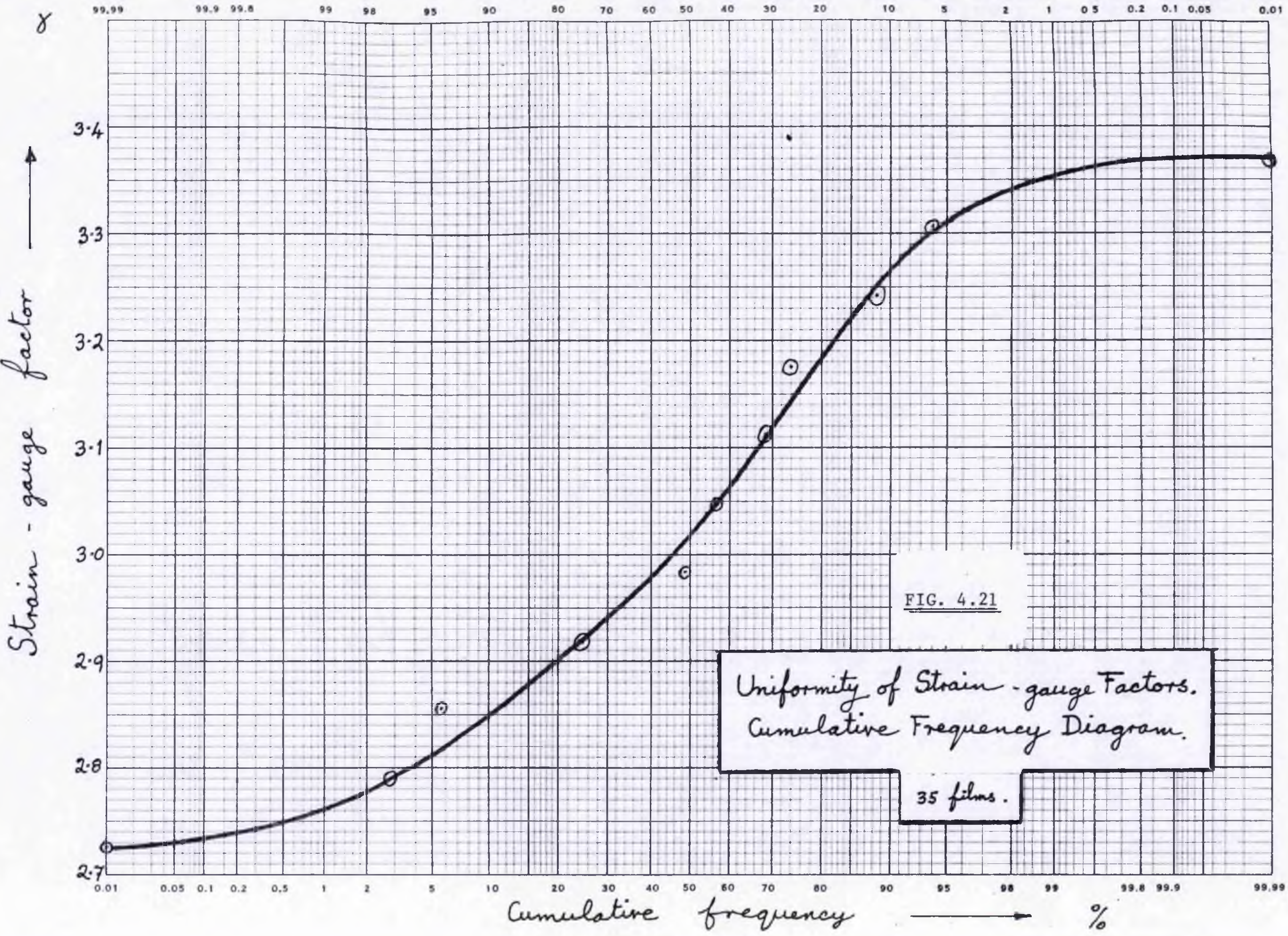

FIG. 4.21
Uniformity of Strain-gauge Factors.
Cumulative Frequency Diagram.
35 films.
Strain - gauge factor γ
3·4
3·3
3·2
3·1
3·0
2·9
2·8
2·7
Cumulative frequency %
0.01 0.05 0.1 0.2 0.5 1 2 5 10 20 30 40 50 60 70 80 90 95 98 99 99.8 99.9 99.99

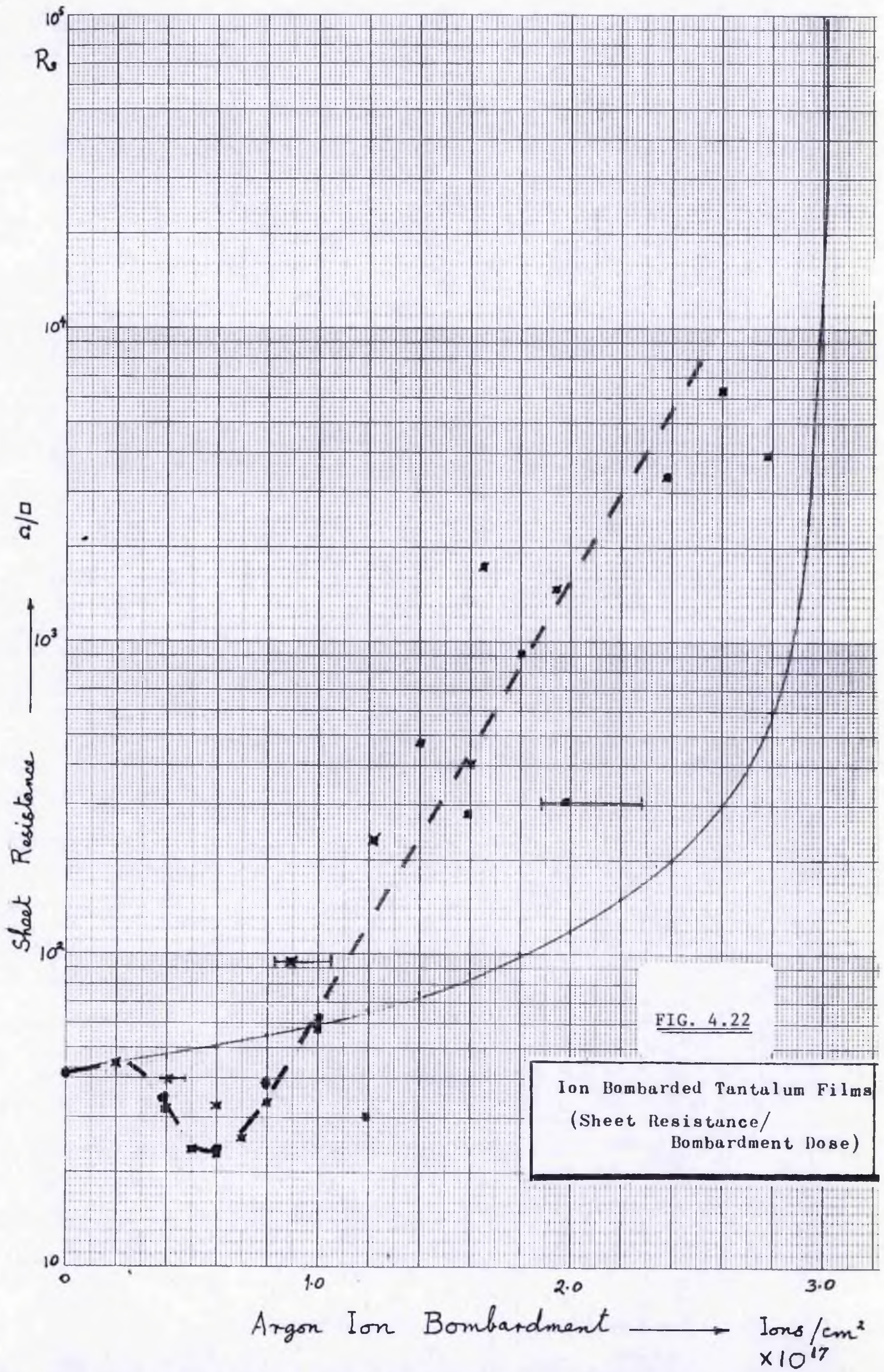

FIG. 4.22

Ion Bombarded Tantalum Films
(Sheet Resistance/
Bombardment Dose)

assumed that a dose of 3.0 x 10^{17} ions/cm^2 is required to sputter such films right through. Assuming this and also that sputtering uniformly reduces the film thickness, values for film resistivity were calculated and plotted against ion dose; Figure 4.23. The initial resistivity was 360 μΩ.cm before bombardment, which was reduced to 160 μΩ.cm at 0.6 x 10^{17} ions/cm^2 and thereafter increased steadily towards infinity at a dose of 3 x 10^{17} ions/cm^2 .

The resistivity of bulk tantalum is 13.9 μΩ.cm at 30° C.

4.3.2 <u>Temperature Coefficient of Resistance</u>

Figure 4.24 shows the TCR of tantalum films plotted against ion bombardment dose: TCR was measured between room temperature and + 120°C.

Films bombarded with a dose greater than 1.3 x 10^{17} ions/cm^2 showed constancy in TCR; the value being close to -100 PPM/°C. This was slightly less than the TCR of unbombarded films of -150 PPM/°C.

Between 0.2 x 10^{17} and 1.2 x 10^{17} ions/cm^2 bombardment raises the TCR considerably. In this region the curve forms a cusp, centred at 0.6 x 10^{17} ions/cm^2 , which extends into positive TCR values. The largest TCR value encountered so far is + 420 PPM/° C.

The resistance of four films having representative values of bombardment within the dose range established above was measured over the temperature range boiling point of nitrogen to the boiling point of water. The graphs of the non-bombarded film have already been reported, see Figures 4.16 and 4.17, but all the results accord well with measurements made only above room temperature. Table 4.3 shows the principal results for these films. Negative TCR is shown both by the non-bombarded and by the heavily bombarded film (with dose = 2.6 x 10^{17} ions/cm^2); the TCR of the bombarded film being slightly the lesser (-127PPM/°C as against -160PPM/°C before bombardment.) The two films with bombardment doses within the transition

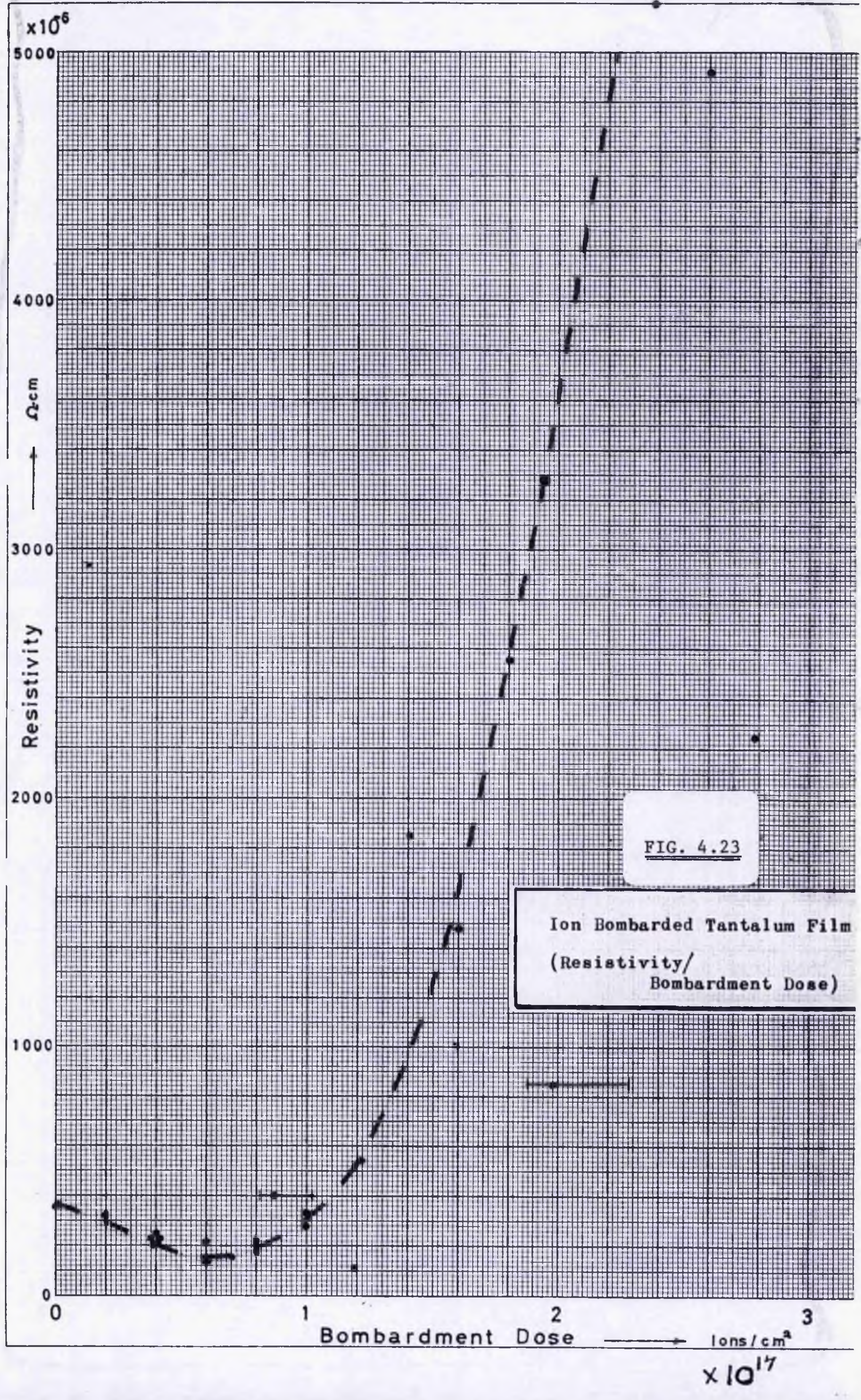
x10⁻⁶
5000
4000
3000
2000
1000
0
Resistivity → Ωcm
0
1
2
3
Bombardment Dose → Ions/cm²
x 10¹⁷
FIG. 4.23
Ion Bombarded Tantalum Film
(Resistivity/
Bombardment Dose)

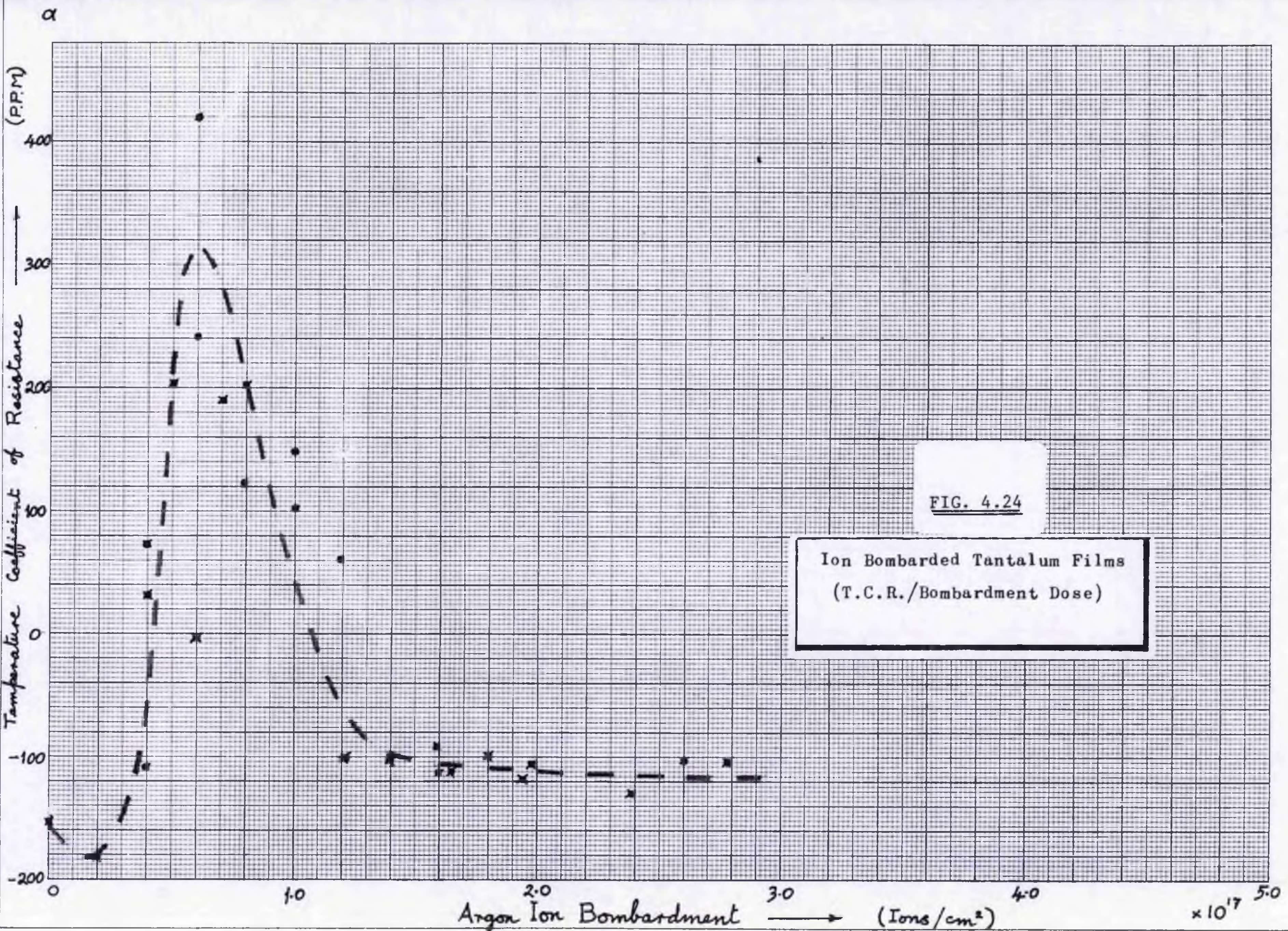

FIG. 4.24

Ion Bombarded Tantalum Films

(T.C.R./Bombardment Dose)

region both show positive TCR with values similar to those given above in Figure 4.24., and they show considerably linearity in their resistance~temperature plots; the standard error being only about one part in 10^4 in each case. Arrhenius plots were made for these films and were found to have a linear region at each end of the temperature scale

FILM NUMBER	3706	3610	3714	3703
BOMBARDMENT DOSE ($\times 10^{17}$ IONS/CM^2)	NIL	0.6	0.8	2.6
SHEET RESISTANCE ($\Omega/\square$ 30° C)	40.8	28.6	36.8	7330
TCR (PPM/$^\circ$C)	-160	+177	+175	-127
ACTIVATION ENERGY				
T < -130°C (meV)	0.25	-0.24	-0.22	0.20
T > -35°C (meV)	1.02	-1.41	-1.51	0.90

Table 4.3 Tantalum Film Resistance Measurements over the Temperature Range -195°C to $+110^\circ$ C.

connected by a curved transition. In the case of the non-bombarded film three linear regions were evident (see section 4.2.2. and Figure 4.17).The ratio of the activation energy at high temperature to that at low temperature is about 4:1 for the negative TCR films.

4.3.3 Strain-Gauge Factor

The Strain-Gauge factors found for non-bombarded tantalum films averaged $\gamma = 3.04$. A plot of strain-gauge factor of films bombarded with different ion dose levels is given in Figure 4.25. It shows a transition region between doses of 0.3×10^{17} ions/cm^2 and 1.3×10^{17} ions/cm^2 in which γ increased to a maximum value of about 5.2 and then returned to about 3.0. This is followed by a linear region in which γ was reduced as bombardment proceeded, being 2.2 at a dose of 2.8×10^{17} ions/cm^2.

4.3.4 Annealing

After manufacture all the films were kept for about one week (at room temperature) before any measurements could be made. Additionally this isothermal annealing period was followed by heating to about 130° C for two or three hours so as to stabilise the resistance and prevent drift during the TCR runs. The bombarded films were also heat stabilised at 130°C before use.

The long-term history of four bombarded films has been followed over a period of two years. This annealing was carried out at room temperature without the heat ageing, except that two of the films were annealed at 130°C after 2000 hours. These results are shown in Figures 4.26 and 4.27.

Figure 4.26 shows changes in the resistance of two films bombarded with doses in the transitional region, i.e. 0.6×10^{17}ions/cm^2 and 0.8×10^{17} ions/cm^2 respectively. The resistance continued to rise with time lapse, and after 2000 hours had increased by two orders of magnitude. This was the case for both films.

The change in resistance of the films reported in Figure 4.27 on the other hand, amounted only to a rise of 10% in 2000 hours. These films had been bombarded with 0.98×10^{17}ions/cm^2 & 1.1×10^{17}ions/cm respectively.

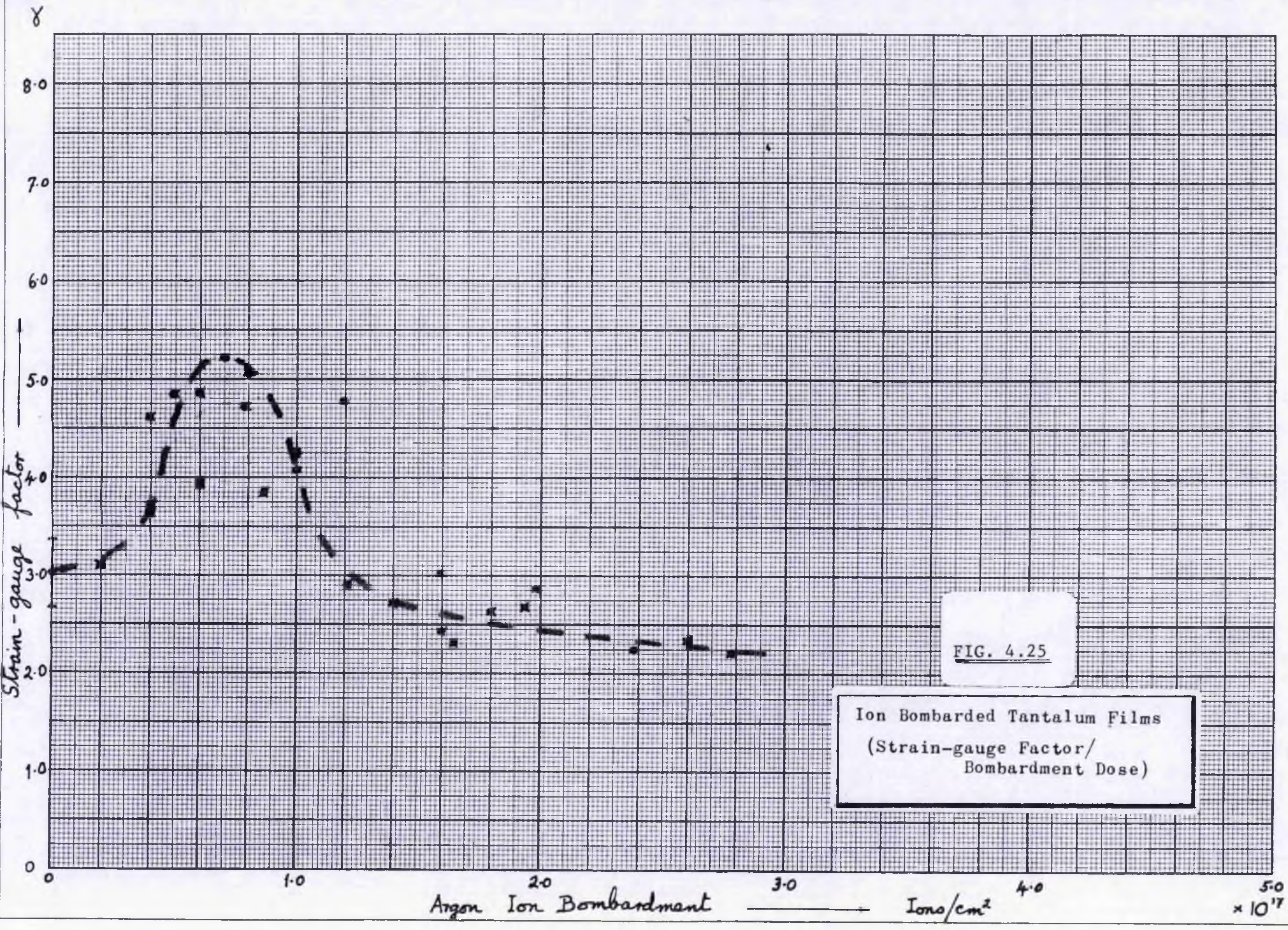

FIG. 4.25

Ion Bombarded Tantalum Films
(Strain-gauge Factor/
Bombardment Dose)

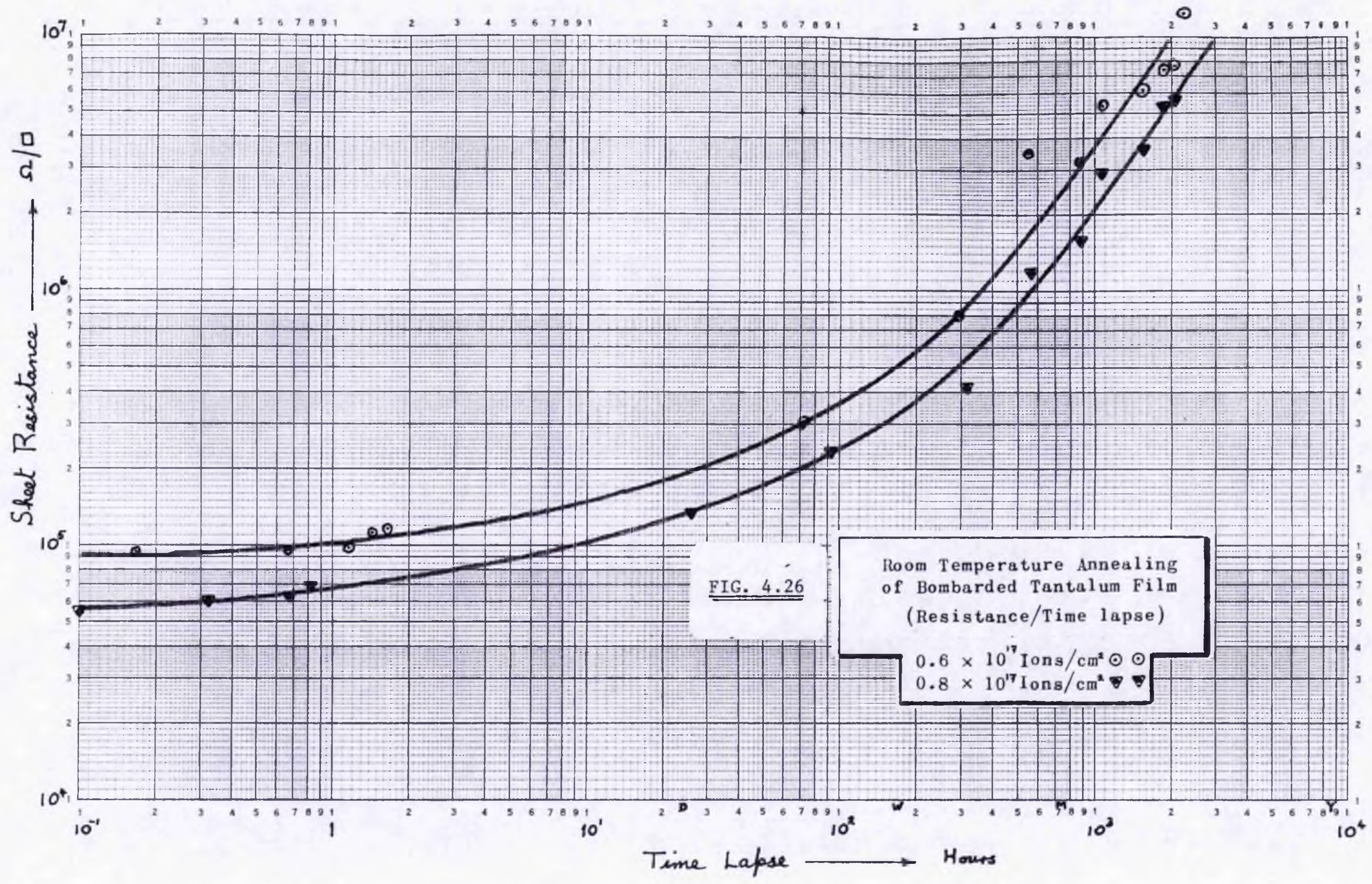

FIG. 4.26

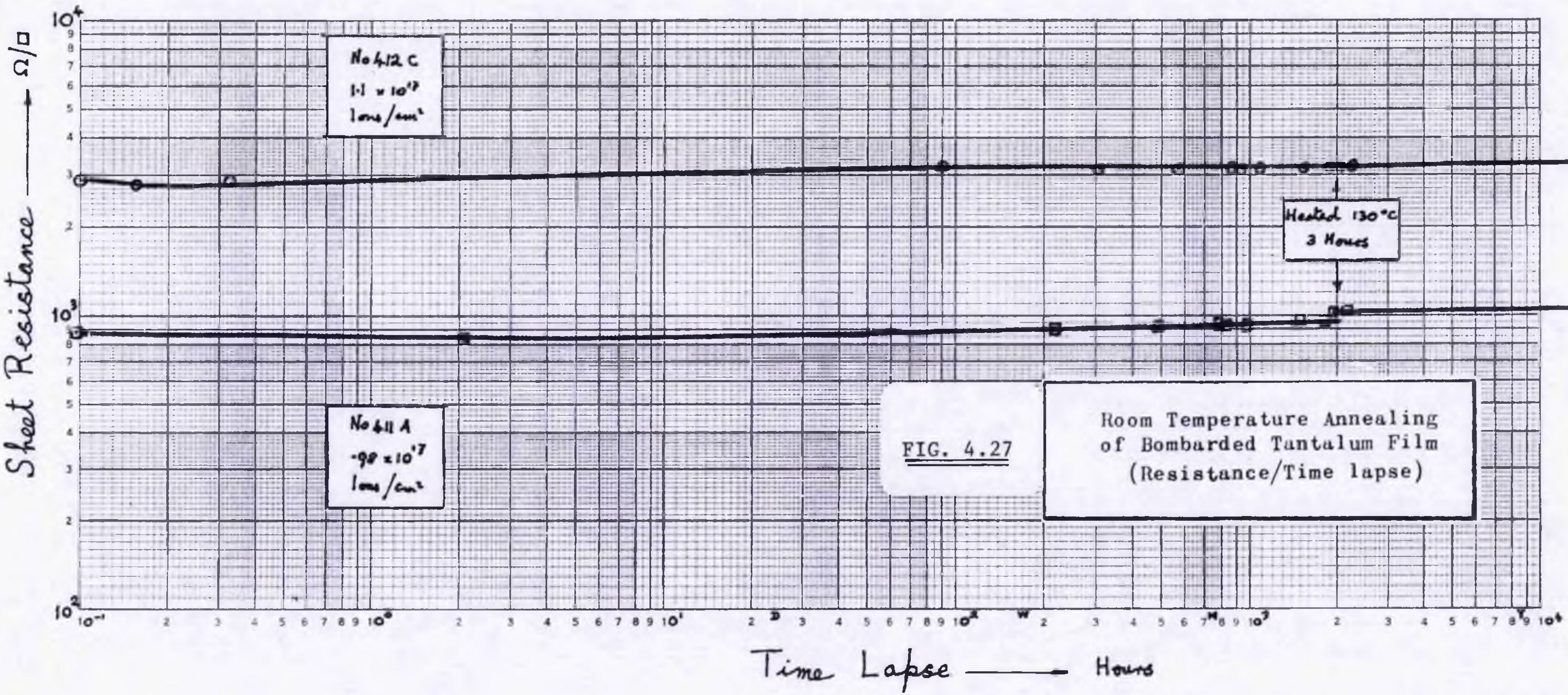

FIG. 4.27

Room Temperature Annealing of Bombarded Tantalum Film (Resistance/Time lapse)

After the heat aging one film had not changed at all and the resistance of the other had increased by a further 7%. At the end of 18000 hours (two years) an additional 4% increase was observed in the resistance of both films.

4.3.5. Depth Profiling by Anodization

Shown in Figure 4.28 a,b and c are the results of incremental anodic profiling of an unbombarded tantalum film and one bombarded to a dose of 0.35 x 10^{17} *ions/*cm^{-2} *. This was an early attempt to use this technique and there is a large scatter of values, probably resulting from drifts of resistance between measurements (time between measurement steps could vary from a few minutes to a weekend). One can tell from these measurements (assuming that the anodization rate stayed constant) that the bombarded film was thinner, both films appear to have a region of uniform conductivity near the surface with lower conductivity near the substrate. From the TCR plot it appears that the unbombarded film is fairly uniform, whilst the bombarded film has a region of very positive TCR (remember the curve is an integral one), falling to the original value as the substrate is approached).*

Similar results for a dose of 2 x 10^{17} *ions/*cm^{-2} *are shown in Figure 4.29. The bombarded film is much thinner and of lower conductivity and lower (negative) TCR, but the electrical properties appear to vary little with depth.*

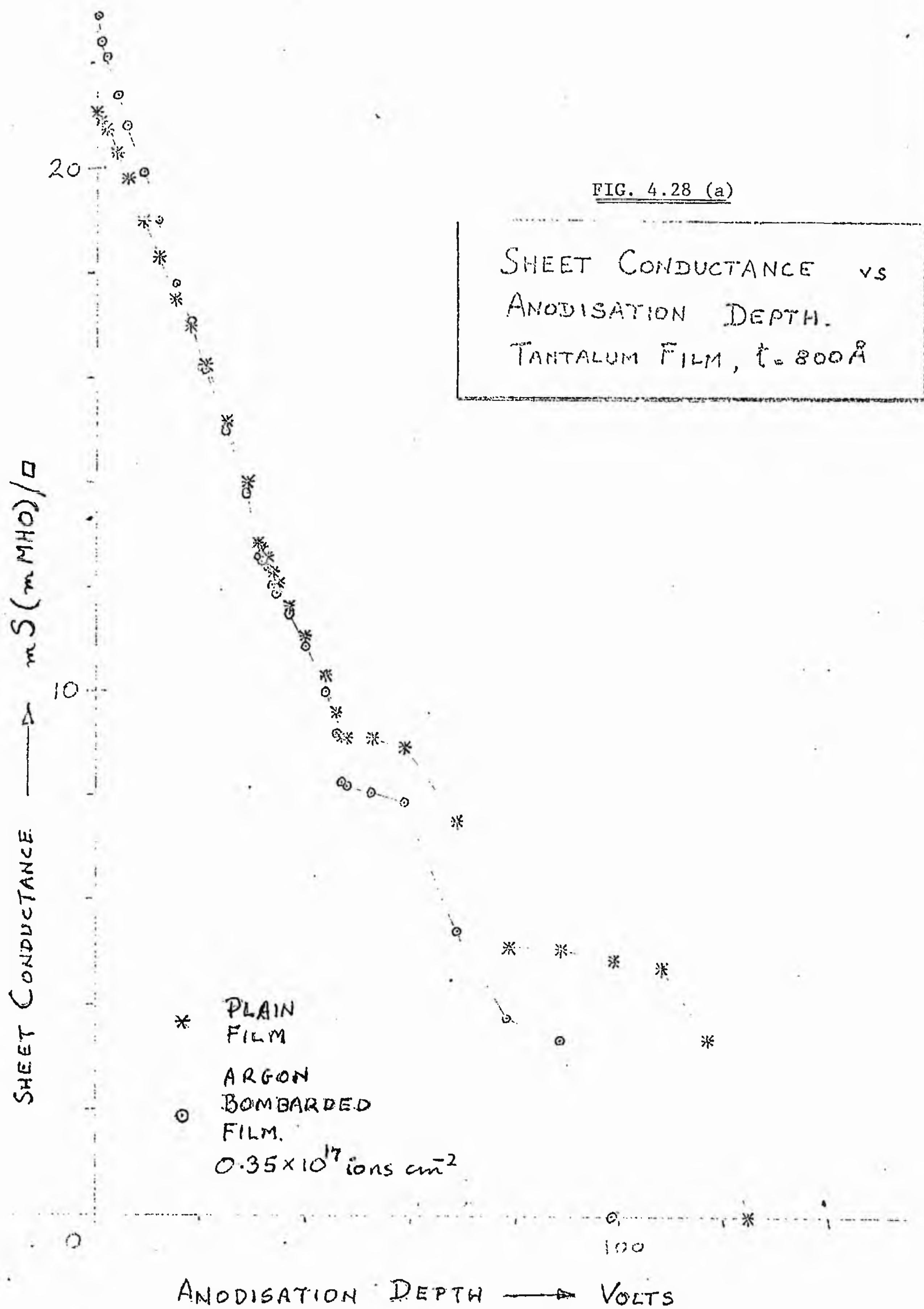
FIG. 4.28 (a)
SHEET CONDUCTANCE vs ANODISATION DEPTH. TANTALUM FILM, t = 800Å
SHEET CONDUCTANCE → mS (mMHO)/□
20
10
0
100
ANODISATION DEPTH → VOLTS
* PLAIN FILM
⊙ ARGON BOMBARDED FILM. 0·35×10^17 ions cm^-2

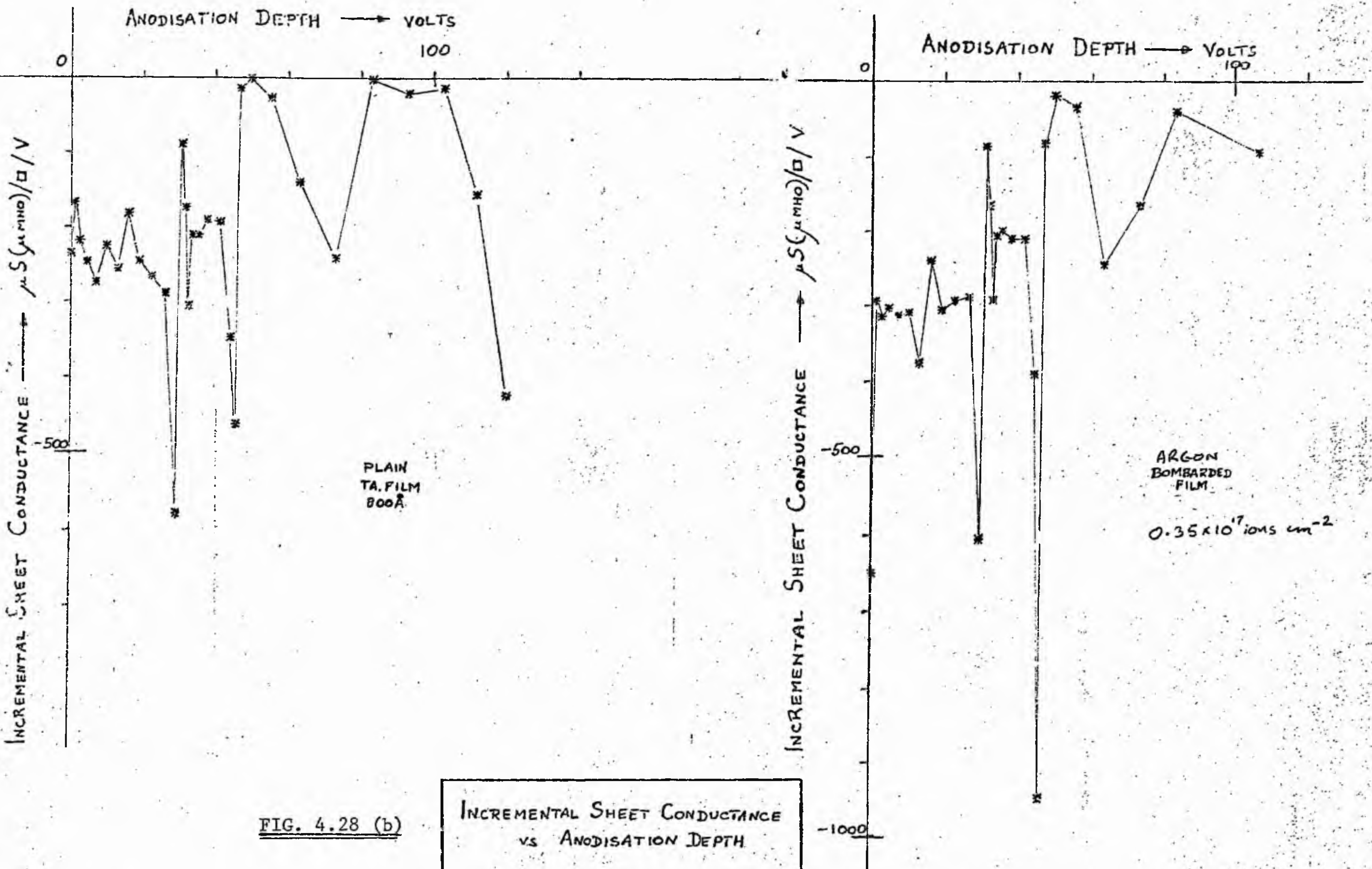

Incremental Sheet Conductance vs Anodisation Depth

FIG. 4.28 (b)

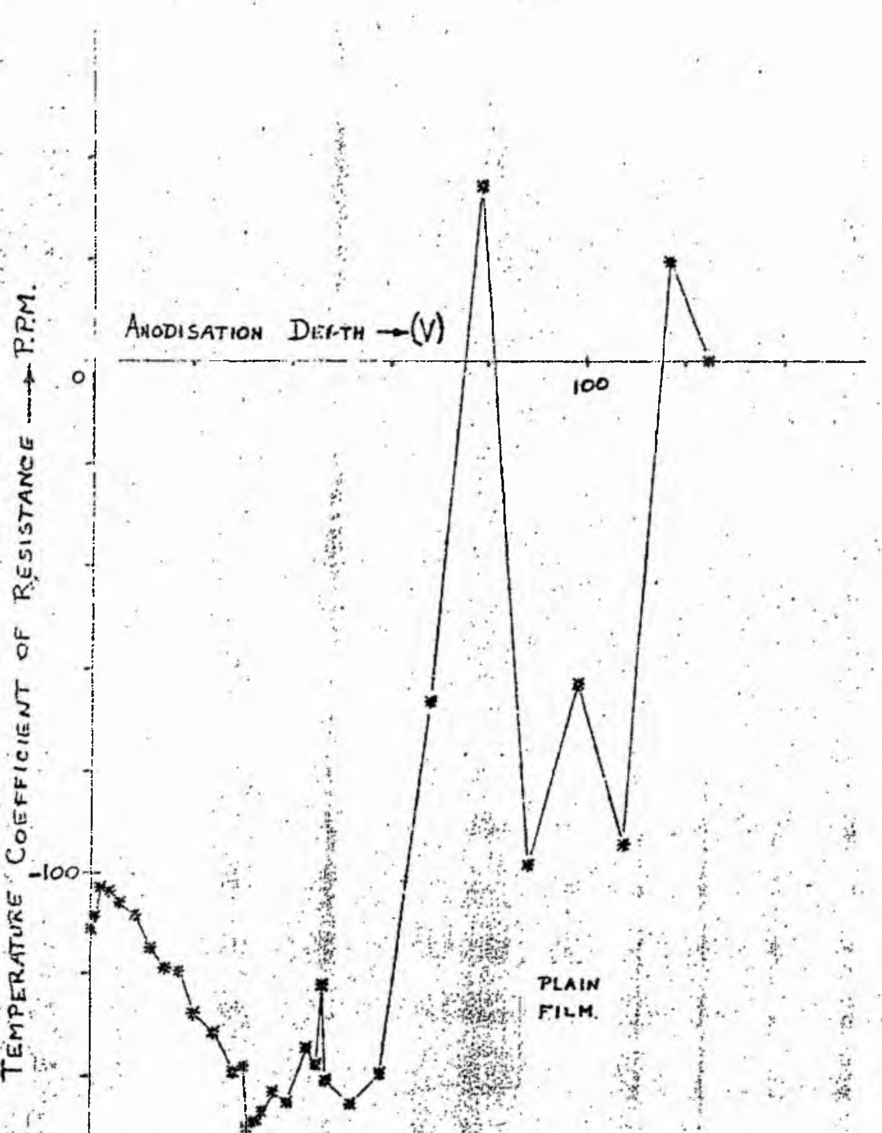

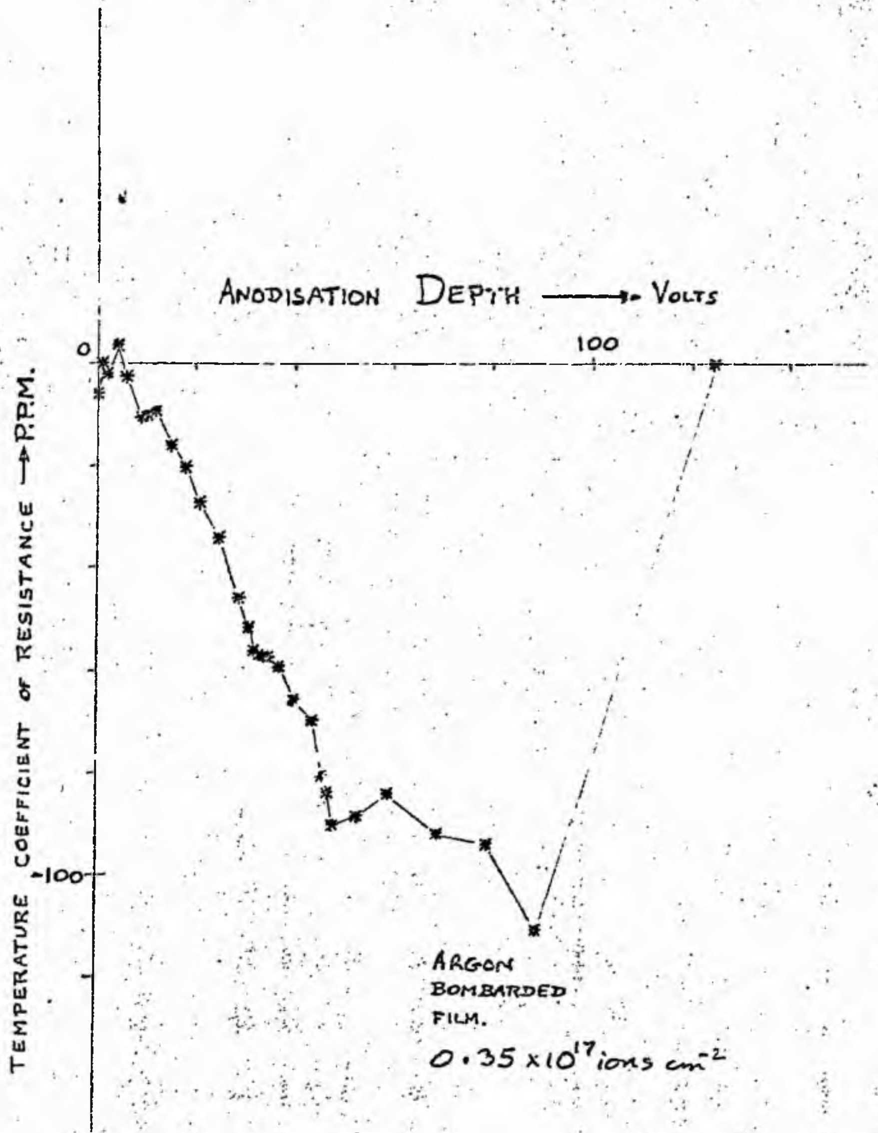

FIG. 4.28 (c)

Temperature Coefficient Of Resistance vs Anodisation Depth.

Tantalum Film. t = 800 Å.

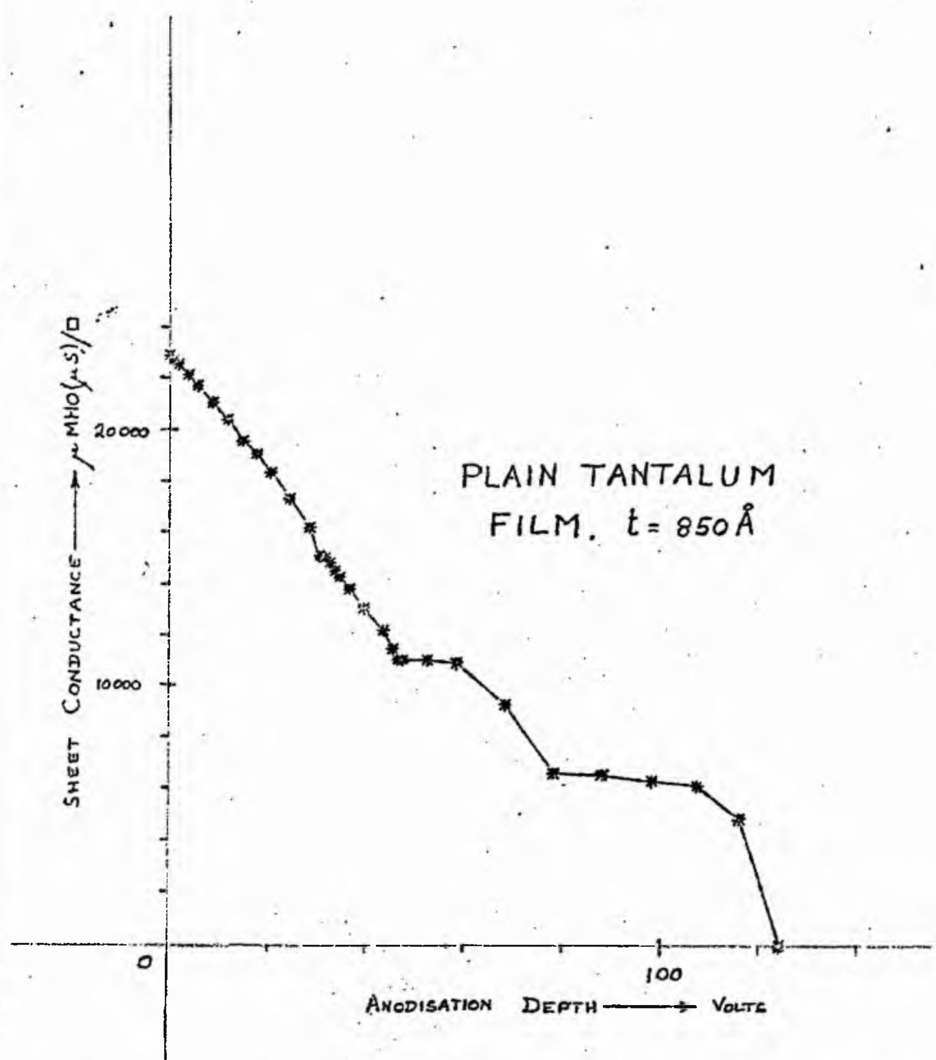

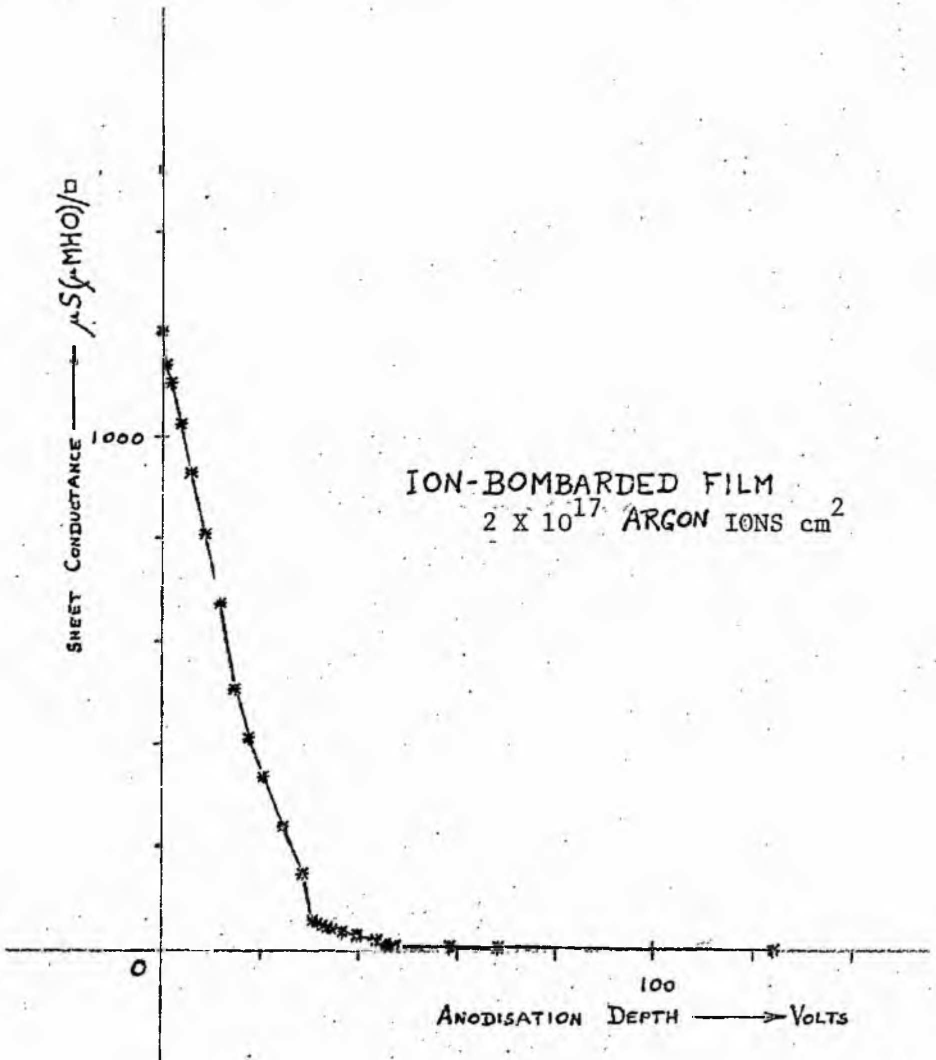

FIG. 4.29 (a)

SHEET CONDUCTANCE VS ANODISATION DEPTH

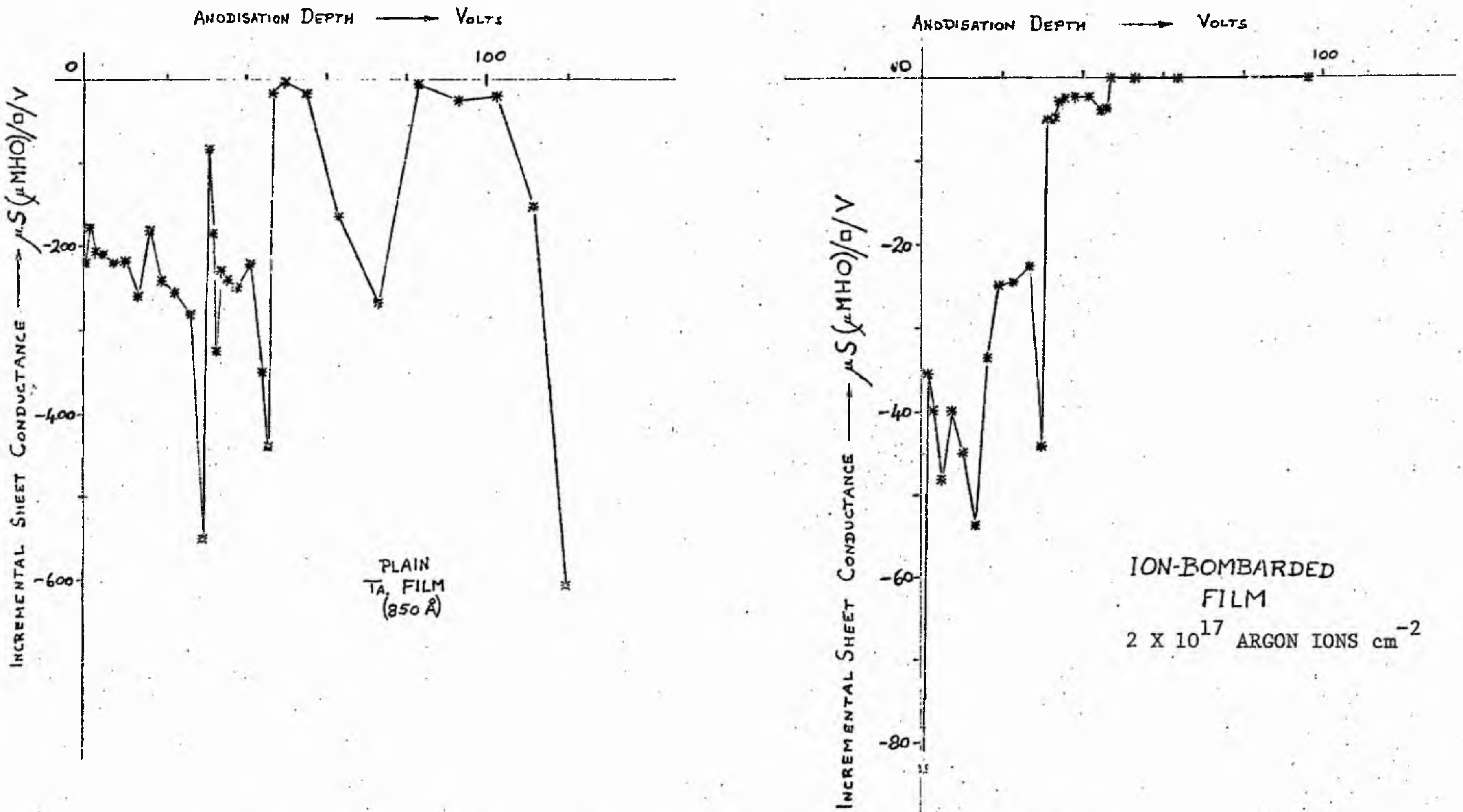

FIG. 4.29 (b)

INCREMENTAL SHEET CONDUCTANCE VS ANODISATION DEPTH

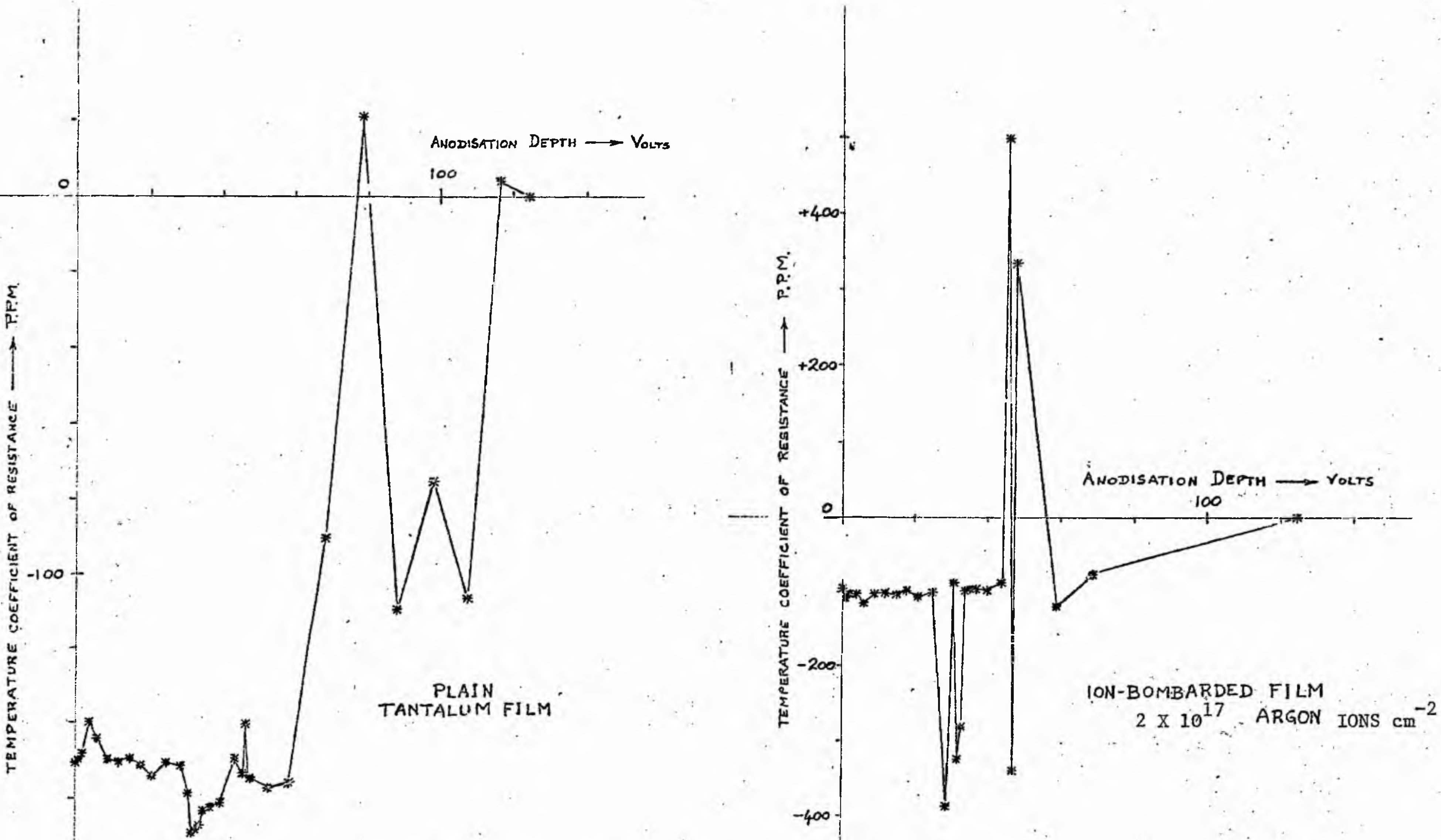

FIG. 4.29 (c)

TEMPERATURE COEFFICIENT OF RESISTANCE vs ANODISATION DEPTH

5. Discussion of the Results

5.1 Gold Films

The films examined in this section are gold films, and range in sheet resistance from 3 Ω/□ to above 4×10^4 Ω/□. Those of low resistance are films used "as deposited" and without ion bombardment, and were nominally of 200 Å thickness. The high-resistance films were evaporated as 200 Å low-resistance films and were then bombarded with argon ions until the resistance was increased to the desired value.

This inert ion bombardment of low-resistance films is the most significant difference between the films described here and those of other workers. Parker and Kirnsky[4]; and Nishiura, Yoshida and Kinbara[5] stopped short the nucleation upon reaching the particular resistance values required, and Stroud[2] bombarded already high-resistance titanium films (~400Ω) with oxygen ions - a reactive combination. Parker and Krinsky covered their films in vacuo with a thick layer of SiO_2 to prevent oxidation: all other films discussed have been left exposed to the atmosphere.

These differences make it important to examine the conduction mechanism taking place in the films, and this will be done first in the context of the strain-gauge coefficient of resistance (S.G.C.R.)

5.1.1 Strain-Gauge Coefficient (γ)

It has been shown (equn.2.6) that the strain-gauge factor of a thin film carried on a substrate should be

$$\gamma = 1 + \sigma_s + \sigma_f \frac{(1 - \sigma_s)}{(1 - \sigma_f)} + \frac{d\rho/\rho}{d\ell/\ell}$$

where σ_s and σ_f = Poisson's ratio for substrate and film, respectively,

ρ = the film resistivity,

ℓ = the longitudinal dimension of the film,

and $\varepsilon = d\ell/\ell$ = the applied strain.

Large values of gauge-factor (γ) may only be expected for correspondingly large rates of change of resistivity (ρ) with strain (ε). Two possible conduction mechanisms may be postulated for such films - an activated tunnelling mechanism whereby charge carriers cross the dielectric regions in an island structure of metal, or metallic conduction with restriction (due to edge effects) of the electron mean-free-path.

5.1.2 Tunnelling

An implication of this type of electrical conduction is the relation between γ and sheet resistance. Parker and Krinsky[4] show (by measurement) that for gold γ rises from a minimum value around 1.1, to 100 as the resistance changes between 10^2 Ω/□ and 10^5 Ω/□ , and this is attributed to an increase in the separation of metallic islands in the film. Such dependence of γ on R_s is not found to be the case here, however, since γ remained constant for all resistance values measured, i.e. up to 4×10^4 Ω/□ . Parker and Krinsky derive the following relation between S.G.C.R. (γ_t) and particle separation (s)

$$\gamma_t = 1.03\, \xi_0^{\frac{1}{2}}\, s$$

where ξ_0 is an effective electron barrier potential lying between 0 and $\emptyset$ (the metal work function).

Working backwards, to estimate the particle separation implied by the measured values of γ (average = 2.58 at 30°C), and assuming $\xi_0 = \emptyset$ = 4.9 eV for gold (P and K's choice),

$$\text{Island separation} = \frac{\gamma_t}{1.03\xi_0^{\frac{1}{2}}} = 1.13\text{Å} .$$

This separation is less than the mean atomic spacing for bulk gold (= 2.57 Å, see section 2.2), and lends support for the view against tunnelling as the conduction mechanism of the films reported here.

5.1.3 Metallic Conduction

This model is based on the assumption that conduction within the film substantially follows the value of resistivity found in bulk material, but that the proximity of the film surfaces severly limits the mean-free-path (m.f.p.) of the conduction electrons. Parker and Krinsky give the m.f.p. in most metals as lying between 200 - 800 Å.

We have already derived an expression for the conductivity (equn. 2.10), in terms of resistivity we have;

$$\frac{\rho_B}{\rho} = \frac{3t}{4\lambda_B} (1 + 2p) \left[\ell n \left(\frac{\lambda_B}{t} \right) + 0.4228 \right]$$

To a first approximation the conductance may be taken to be proportional to film thickness, so that resistance

$$R = \frac{\text{const}}{t}, \qquad \frac{dR}{R} = -\frac{dt}{t}$$

and

$$\therefore \quad \frac{d\rho}{\rho} = -\frac{dt}{t}$$

$$\frac{dt}{t} = -\sigma_f \frac{(1 - \sigma_s)}{(1 - \sigma_f)} \frac{d\ell}{\ell} \qquad \text{(See section 2.3)}$$

This leads to

$$\frac{1}{\rho} \frac{d\rho}{d\varepsilon} = \sigma_f \frac{(1 - \sigma_s)}{(1 - \sigma_f)}$$

Also, from equn.2.6, we have

$$\gamma = 1 + \sigma_s + \sigma_f \frac{(1 - \sigma_s)}{(1 - \sigma_f)} + \frac{1}{\rho} \frac{d\rho}{\varepsilon},$$

so that S.G.C.R. becomes

$$\gamma = 1 + \sigma_s + 2\sigma_f \frac{(1 - \sigma_s)}{(1 - \sigma_f)} \quad \text{- - - - - - - - - 5.1}$$

Kaye and Laby[9] give values for Poisson's ratio,

for Gold, $\sigma_f = 0.44$,

and for Glass, $\sigma_s = 0.25$ (average),

so that the predicted value of S.G.C.R. for gold film on glass is

$$\gamma \approx 2.43$$

This is in very good agreement with the observed values, the average of which is 2.58 ± 0.07 at the 95% confidence limits.

5.1.4 The Temperature Coefficient of Resistance (α)

The positive TCR of the bombarded films also indicates that metallic conduction is the predominant mechanism.

An approximate relationship between sheet-resistivity (R_s) and the TCR of the film (α_F) is derived in section 2.5 (equn.2.11);

$$\alpha_F \approx \alpha_B / \left[\mathrm{Ln} \left(\frac{\lambda_B R_s}{\rho_F} \right) + 0.4228 \right]$$

where α_B is the TCR of the bulk material, ρ_F is the resistivity of the film and λ_B the electron mean-free-path in the bulk. This assumes metallic conduction modified by the reduction of electron mean-free-path caused by the proximity of surfaces. It also assumes that the surface and defect scattering is temperature independent and that the film thickness is much less than λ_B.

This function is plotted in Figure 4.7 as the continuous curve for $\lambda_B = 800$ Å, $\rho_F = 50$ μΩcm and $\alpha_B = 40 \times 10^{-4}\ {}^0C^{-1}$.

The agreement is reasonable considering the approximations that have been made. Certainly the reduction of TCR with increasing sheet resistance is observed.

Over the range of sheet resistance from 30 $\Omega/\square$ to $10^4\Omega/\square$ measurement shows the TCR to be almost invariant, the average value at the 95% confidence level being,

$$\alpha = 11.75 \times 10^{-4} \pm 0.95 \times 10^{-4}$$

5.1.5 <u>The Temperature Coefficient of Strain-Gauge Factor</u> (β)

It has been shown (section 2.4) from the definitions of γ, α and β that the relationship $\beta = -\alpha$ should hold true.

The results for the gold films appear to confirm this prediction experimentally for the first time.

In the present work the variability of S.G.C.R. measurement makes it impracticable to arrive at reliable values of β for individual films, but, on the grounds that the S.G.C.R. is independent of sheet resistance, a simultaneous reduction of all data has been carried out. Table 4.2 and Figure 4.9 show the related S.G.C.R. and temperature values, and the result of the computations. The points on the graph of Figure 4.9 are very scattered, and the correlation coefficient is only 0.26. However, an application of Fisher's z-test[15] indicates that this is a significant correlation at well above the 95% confidence level. On the assumption, therefore, that a linear relationship holds, it is possible to calculate the mean intercept and slope, and this yields values, within the 95% probability limits,of

Intercept = mean S.G.C.R. at $0^\circ C$ = 2.71 ± 0.07, and

Slope /Intercept = mean temperature coefficient of S.G.C.R.,

$\beta = -16 \times 10^{-4} \pm 11 \times 10^{-4}$.

The limits of the temperature coefficient are seen to be extremely wide, showing the uncertainty associated with its true value. However, by using this value of temperature coefficient, the mean S.G.C.R. may be adjusted to 30°C, giving

$$\text{mean } \gamma = 2.58 \pm 0.07 \quad \text{at } 30^{\circ}\text{C}.$$

The mean value for β of -16×10^{-4} compares favourably with the mean T.C.R., α, for these same films, of 11.75×10^{-4}.

5.1.6 The Structure of the Bombarded Films

The lack of change in γ with sheet-resistance and the positive value of α indicate that metallic conduction remains the predominant mechanism.

This result is remarkable when one considers that if one assumes the very high resistivity of say 1000 μΩcm for the 40 kΩ/□ films this would infer, assuming a uniform film, that the film thickness is of the order of one monolayer. This would only be the case if the thickness change due to sputtering is extremely uniform.

It has been shown[18] that the sputtering rate of gold varies with orientation such that the surface of a polycrystalline specimen soon becomes very irregular, with low sputtering rate grains standing proud of the rest. This would lead to a network type of structure where the gold in a thin film is removed in the areas of high sputtering rate to expose the substrate. The stereoscan micrographs (Figure 4.10) reveal that a network structure is indeed formed. It appears therefore that the resistance increases with dose due to a reduction in the number of interconnecting necks, rather than an overall decrease in film thickness. This would explain the apparently very high sputtering rate. Most material will be removed around the edge of the holes due to the oblique

incidence of the beam until there is no connecting pathway between electrodes, and it appears that with our films the gaps between the islands of gold remaining on the film are too large for tunnelling type conduction.

The mean thickness of the 'necks' must stay of the order of the film thickness until the width decreases rapidly to zero, as γ does not fall to the minimum value of about 1.0 reported for many thin evaporated films where the network structure is first established.

Another explanation of the results could be that gold is implanted into the surface of the glass to form a gold-glass cermet of a similar type to that produced by sputter deposition of a mixture of gold and glass.[19]

The mechanism whereby this is done is the exchange of momentum between an argon ion and a gold atom in the film. This leads to the familiar recoil sputtering with gold ejected from the surface, and also to transmission sputtering where the gold is implanted into the glass. It has been predicted theoretically[20] and demonstrated experimentally[21] that the transmission sputtering yield can be considerably greater than the recoil sputtering yield.

5.1.7 The Resistance Ageing Effect

Inspection of the historical record of gold film number 038 (see Figure 4.5) shows that the resistance increased from about 100 Ω to 2000 Ω in the first 1000 hours after ion bombardment. Thereafter the resistance, though having still increased, did so at a reduced rate.

A similar effect is apparent with all films (Figure 4.6), though the resistance change was not always so severe.

Two mechanisms could be proposed to explain the increase and saturation of resistance with time and also the increase in resistance

on annealing. Either oxidation of the gold surface or diffusion of gold atoms to form clusters. Clustering would decrease the number of conducting pathways and therefore increase the resistance of the film. In the case of the films that go open circuit i.e. those with a resistance immediately after ion bombardment of greater than 10,000 Ω, a discontinuous island structure may be formed where the island separation is usually too large for a significant amount of conduction by tunnelling. The one film with a large negative TCR (see Table 4.2) may be of this type, with an island separation that is smaller than usual.

The initial incubation period of about one week, when little change occurs, is indicative of another mechanism that prevents diffusion, or oxidation, for this time, but we have no explanation for this behaviour at present.

As a chemical element gold is in Group 1 of the Periodic Table, Sub-group (b), which comprises Cu, Ag, and Au. Gold may be either uni- or trivalent and, although trivalency characterises most of its compounds, forms auric oxide - unstable and slightly acidic.[17]

The films reported here were all kept in closed (but not airtight) boxes, but were exposed to the atmosphere during measurement. When heated above 90°C an irreversible increase in resistance always occurred (see, for example, film 044 in Figure 4.6). Neither this nor the ageing of films at room temperature materially effected the value of S.G.C.R.

5.1.8 *The Initial Drop in Resistance for doses below 2×10^{15} ions/cm^{-2}*

There is a dramatic reduction in the resistivity of the gold films from 24 μΩ cm to 12 μΩ cm (bulk value 2.25 μΩ cm) for a dose of 1.8×10^{15} ions cm^{-2} (Figure 4.2). This effect has been observed by other workers[22,23] for other films and has been attributed to desorption of gases in the surface of the film. More recent results[6] indicate that it is more probable that the reduction in resistivity arises from re-arrangement of the film structure; a form of radiation enhanced annealing, plus possible reduction of oxides by preferential sputtering of oxygen.[24]

5.2 *Tantalum Films*

5.2.1 *The as-deposited Films*

Films above 200 Å in thickness appear to have fairly uniform properties with a resistivity of 370 μΩ cm and TCR of -150 PPM/°C (one batch has larger negative values of TCR, possibly due to a poor vacuum during deposition). These values are similar to those measured by other workers using the same deposition system[6,7,8]. From their results it seems probable that the films are b.c.c. tantalum, semi amorphous (grain size <50 Å), with 40 Å of surface oxide and an average of 30 atomic per cent of oxygen dissolved in the rest of the film.

The large negative values of TCR (and high resistivity) for $t \leq 200$ Å indicate that the first 200 Å to be deposited contain larger amounts of oxygen (due to gettering), there is therefore no continuous metallic conduction path and activated tunnelling dominates the conduction process.

The measured activiation energies for thicker films (Figure 4.17) are low because one is seeing the combined effects of metallic and activated tunnelling mechanisms. There appears to be evidence for at

least two thermally activated mechanisms one becoming evident above -130°C and the other above -35°C. The actual value of activation energy measured will depend sensitively on the balance between metallic and activated conduction and this will be greatly affected by the microstructure of the films. This would explain the large scatter in measured values of activiation energies (Figure 4.18) which can be taken as evidence for differences in microstructure (or oxygen concentration) and the trend to higher values at higher resistivity indicates the reduced contribution from metallic conduction as the oxygen concentration increases as it will do for the thinner films.

Although strain-gauge factor has been measured over a much narrower range of sheet resistance it seems clear that there is very little scatter in the value (3.02 ± 0.15). This indicates that the strain-gauge factor is less sensitive than net activation energy (and TCR) to the microstructure of the films and is probably (like the gold films) determined by relative changes in the metallic component of conduction but not by the absolute magnitude of resistance. The value of strain-gauge factor using equn. 5.1 and the value of Poisson's ratio given for bulk tantalum (0.342)[9] is; $\gamma = 2.03$. Some factor is acting to increase the strain sensitivity of our tantalum films. A possible mechanism to explain the higher value of γ is proposed in section 5.2.4.

5.2.2 The Effect of Argon Bombardment on Resistivity

The initial drop in resistivity towards values expected of bulk tantalum could be explained by preferential sputtering of oxygen (particularly in view of the vast difference in mass between oxygen and tantalum) and radiation enhanced diffusion of oxygen to the surface and re-arrangement of the film resulting in a more metallic phase being formed. This is supported by the microscope observations of other workers[6,7], by the anodic stripping results reported here (Figure 4.28), and by theoretical predictions on preferential sputtering.[24]

After passing through a minimum at 0.6 x 10^{17} ions/cm^{-2} the resistivity rises with increasing dose, but the linear rate of increase cannot be fitted to a simple sputtering theory, and there is a large scatter in values. The latter could arise from differences in microstructure that affect the balance between conduction mechanisms. The slow rise could be explained if a phase of low sputtering rate is formed by reaction with the substrate, the oxygen content increasing with increasing ion dose.

5.2.3 <u>Changes in TCR as a result of Argon Bombardment</u>

The TCR reaches a peak positive value at the same dose as the minimum in resistivity and the peak value measured (+ 400 PPM per ^{o}C) approaches the value one would expect from a very pure tantalum film[25]. This fully supports the ideas of purification and re-arrangement of the film at low doses as detailed in the last section.

It is curious that although a similar swing to a large positive TCR has been seen for in-situ measurements on oxygen bombarded tantalum films[6], no such effect has been seen for in-situ measurements for argon bombardment[6], or for later measurements (taken after removal from the target chamber) on oxygen bombarded films[8].

It must however be pointed out that the latter measurements were made on annealed (5 hr. at 250°C) films whereas the results presented here are for films which are only heated to 120°C at the start of the TCR run. Thus the apparent discrepancy could arise if the metallic phase leading to low values of resistivity and high positive TCR is a metastable phase, which changes to a more stable (oxide?) phase on annealing at higher temperatures. The wide scatter of values in the region of the TCR peak would be explained if some annealing takes place at room temperature (see section 5.2.5 below) as the time before determination of the TCR varies from sample to sample.

At high doses there is little scatter in TCR values indicating that a stable phase has been formed, and the value of TCR is similar to that measured by other workers.[6]

5.2.4 Changes in Strain-Gauge Factor as a Result of Argon Bombardment

The strain-gauge factor peaks at a similar dose to the peak in TCR and values of γ as high as 5.2 have been observed. Once more a wide scatter in the values is observed. It is not clear why this structure has a strain sensitivity greater than that of 2.03 predicted using the bulk value of Poisson's ratio. The highly metallic properties indicate that a cermet film is not formed in this case. One could postulate that when the film is strained the phase structure is such that the number of metallic conducting pathways is reduced so increasing resistance whilst retaining the dominance of metallic conduction. If this is so then bombardment induced changes in microstructure seems to enhance the effect. This process would have to be reversible as no hysteresis is observed.

At high doses where TCR measurements indicate that a stable phase is formed the gauge factor approaches the predicted value of 2.

5.2.5 Resistance Ageing

The results of ageing tests (Figures 4.26 and 4.27) support fully the models for film structure proposed above. At doses where a supposedly metastable metallic structure is formed the resistance increases by up to two orders in magnitude after two years at room temperature. The most probable mechanism for the disappearance of the metallic phase is by reaction with the oxygen that remains below the metal phase near the film/substrate interface. This model is supported by the results of other workers.[26]

At higher doses where it is proposed that a stable structure is

formed by reaction with the substrate, an extremely stable structure is indeed formed which is little affected by annealing at 130°C. These models are also supported by the results of anodic profiling.

It seems clear that while the effects of argon bombardment of gold films can be explained in terms of sputter etching, the mechanisms that determined the observed changes in electrical properties of tantalum films are changes in phase structure and chemical effects such as preferential sputtering of oxygen and reaction with the glass substrate.

6. Conclusions

6.1 Argon Bombardment of Gold Films

Many workers[2,4,5,22,23] have examined the strain-gauge properties of gold film prepared by thermal avaporation to have sheet resistances of up to a few thousand Ω/□ . Gauge factors rising to ~100 have been measured, coupled with a negative temperature coefficient of resistance(TCR). These factors have been satisfactorily explained on the basis of electrical conduction by tunnelling across the boundaries of islands of metal.

The films examined in this thesis do not, however, exhibit the same behaviour even though the sheet resistances cover much the same range (3 Ω/□ to 4×10^{4} Ω/□). The strain-gauge factor (S.G.C.R.) has been found to be invariant, and to have an average value of 2.58. The TCR has been found to be positive, and with a constant value of about 11.75×10^{-4}. The temperature coefficient of S.G.C.R. has been measured as -16×10^{-4}. All these values are inconsistent with electron tunnelling but they are consistent with metallic electrical conduction, the resistivity being presumed to have the bulk value modified by a reduction of the electron mean-free-path.

This fundamental divergence in results can only be attributed to the method of film preparation. Although the films of the other workers were also prepared by condensation at room temperature from thermally evaporated gold (the same method as was used in the present work), evaporation of the films reported here was not stopped on reaching the desired resistance, but was continued down to resistances of ~ 5Ω/□ . The films were then bombarded with argon until the resistance had been increased to the desired value. By this means the structure of the film had been made similar in effect to that of bulk metal, a feature which is evidently retained after ion bombardment.

The effect of argon bombardment of thin gold films appears to be the formation of a 'network' structure where metallic conduction is retained.

When the film eventually becomes discontinuous either by further bombardment, or by processes taking place during ageing, the island separation appears to be too great for conduction by tunnelling.

The increasing resistance during bombardment is attributed to a reduction in the number of connecting pathways rather than a reduction in their size.

Exposure to the atmosphere results in an irreversible increase in resistance. The initial 'incubation' during ageing and the ageing mechanism have yet to be fully explained.

The film quality as determined by resistivity is improved for low doses (below one quarter of the dose required to make the film go open-circuit).

6.2 Argon Bombardment of Tantalum Films

The as deposited films have electrical properties consistent with conduction by a combination of metallic and activated tunnelling mechanisms. The latter component appears to increase in importance as the oxygen content of the film increases, and there is evidence for at least two activation processes.

The strain-gauge factor appears to be determined by changes in the metallic component but is higher than predicted from bulk metal values, possibly as a result of strain altering (reversibly) the number of conducting pathways in the film, thereby changing the resistance, but not the conduction mechanism. Bombardment with argon results first in a change in electrical properties towards those expected of very pure tantalum films. This is thought to be the result of preferential sputtering of oxygen, radiation enhanced diffusion of oxygen to the surface and re-arrangement of the film to form large islands of b.c.c. tantalum. The strain-gauge factor is increased to up to 5.2 at this point, possibly because the change in phase structure has increased the effect of the conducting path way mechanism proposed above.

The tantalum phase appears to be metastable and the resistance increases markedly with time at room temperature, probably as a result of reaction with oxygen that exists near the film/substrate interface.

For higher doses of argon it appears that a single phase, stable, low sputtering rate compound is formed, probably by reaction with the glass substrate. This compound has a mixture of activated and metallic conduction with a strain-gauge factor (probably determined by the metallic component) close to that predicted for a tantalum film on a glass substrate.

To summarise the overall result of this work it appears that the phenomenon that dominates the electrical properties of argon ion bombarded

gold films is that of sputter etching, whilst for tantalum (plus oxygen) films changes in phase structure and chemical effects dominate.

7. References

1. R.G.R. Robinson, K.G. Stephens and I.H. Wilson; Thin Solid Films; 27(1975) 251.

2. P.T. Stroud; AWRE Nucl.Research Note No. 29/71.

3. I.H. Wilson, K.H. Goh and K.G. Stephens; Int.Conf. on Application of Ion Beams to Metals. Albuquerque (1973) paper V8.

4. R.L. Parker and A. Krinsky; J.of Appl.Phys. 34 (1963) 2700.

5. M. Nishiura, S. Yoshida and A. Kinbara; Thin Solid Films 15 (1973) 133.

6. I.H. Wilson, K.H. Goh and K.G. Stephens; Thin Solid Films; 33 (1976) 205.

7. K.H. Goh; Ph.D. Thesis, University of Surrey,(1976.)

8. K.G. Stephens and I.H. Wilson; Thin Solid Films; 50 (1978)

9. G.W.C. Kaye and T.H . Laby; Tables of Physical and Chemical Constants; Longmans.

10. (a) B.S. Verma; Measurement of Strain Coefficient of Resistance in Silver Films; Thin Solid Films, 7, (1971) 259-264.
    (b) B.S. Verma and H.J. Juretschke; J.Applied Phys. 41, (1970) 109.

11. G.R. Witt and T.J. Coutts; Thin Solid Films 7, (1971), R1.

12. O.S. Heavens; Thin Film Physics, Methuen.

13. R. Fuchs; Proc.Cambridge Phil.Soc., 34 (1938) 100.

14. E.H. Sondheimer; Advan.Phys., 1 (1952) 1.

15. J.C. Turner, Modern Applied Mathematics, E.U.P.

16. W.S. Johnson and J.F. Gibbons; Projected range statistics in semiconductors (1970).

17. G.R. Davies; Chemistry, article in Chambers Encyc. Vol. III.

18. I.H. Wilson and M.W. Kidd; J. of Materials Science, 6, (1971) 1362.

19. T.J. Coutts; Thin Solid Films 4 (1969) 429.

20. P. Sigmund; Phys.Rev. 184 (1969) 383.

21. J.G. Perkins and P.T. Stroud; Nucl.Instruments and Methods 102 (1972) 109.

22. B. Navinsek and G. Carter; Can.J. Phys., 46 (1968) 719

23. M. Deery, K.H. Goh, K.G. Stephens and I.H. Wilson, Thin Solid Films, 17 (1973) 59.

24. H.M. Naguib and R.Kelly; Radiat.Effects, 25 (1975) 1.

25. L.G. Feinstein and R.D. Huttemann, Thin Solid Films, 20 (1974)

26. M.R.M. Moulding, Ph.D Thesis, University of Surrey 1979.

8. Appendices

1 COMPUTER PROGRAMMES

1.1 Computation of slope of line through strain gauge data

1.2 "Free" formal input of decimal data from paper tape

1.3 Subroutine to calculate to "best fit" straight line

1.4 Graph plotting

2 EXTRA RESULTS AND CORRELATIONS (OF USE TO OTHER WORKERS)

2.1 Bending ring for 1" strain gauges

2.2 R_s vs. thickness (T_a) showing different evaporation runs

2.3 TCR vs. R_s (T_a) showing different evaporation runs

2.4 TCR vs. thickness (T_a) showing different evaporation runs

2.5 TCR vs. thickness (T_a) showing different evaporation runs

2.6 TCR vs. activation energy (T_a)

2.7 Activation energy vs. thickness (T_a)

2.8 Activation energy vs. thickness (T_a) showing different runs

2.9 Activation energy vs. R_s (T_a) showing different runs

2.10 R_s vs. $(time)^{\frac{1}{2}}$ (T_a)

2.11 R_s vs. $(time)^{\frac{1}{2}}$ (T_a)

2.12 SGF vs. R_s (T_a)

2.13 SGF vs. TCR (T_a)

2.14 Relative resistance vs. R (after 1000 hrs.), Au films.

3 END CORRECTIONS FOR IMPLANTED STRAIN GAUGES

```
PAGE    1     ENG01693

/ JOB     1001 1002                      1002      *ENG01693 01

OG DRIVE     CART SPEC     CART AVAIL    PHY DRIVE
 0000          1001          1001          0000
 0001          1002          1002          0001

 MOO    CONFIG   8K

AT VERSION D.M. SYSTEM V1 MOO

EQUAT(PAPTZ,PAPTC)

/ FOR
NAME GRAAL       COMPUTATION OF SLOPE OF LINE THROUGH STRAIN-GAUGE DATA
LIST SOURCE PROGRAM
IOCS(CARD,1132 PRINTER)
IOCS(PAPER TAPE)
ONE WORD INTEGERS
      DIMENSION X(20),Y(10),NOTE(36)                                      GRAAL   1
000   FORMAT('0'T39'DATA'// (T 2,10F8.3))                                 GRAAL   2
001   FORMAT('0'T2'SPECIMEN'T11,I3,T14',  TEMP ='T24,I2T27'DEG C,'T35'SLGRAAL   3
     1OPE ='T43,E10.3,T53',  CORR COEFF ='T69,E10.3)                      GRAAL  A3
002   FORMAT('0'T 6,36A2/)                                                GRAAL   4
003   FORMAT('1')                                                         GRAAL   5
000   FORMAT(36A2)                                                        GRAAL   6
      ILP=3                                                               GRAAL   7
      ITR=4                                                               GRAAL   8
      READ(ITR,4000)NOTE                                                  GRAAL   9
      WRITE(ILP,3002)NOTE                                                 GRAAL  10
      NUM=20                                                              GRAAL  11
      CALL GREAD(NUM,X)                                                   GRAAL  12
      IF(X(1))2,1,3                                                       GRAAL  13
      WRITE(ILP,3003)                                                     GRAAL  14
      CALL EXIT                                                           GRAAL  15
      WRITE(ILP,3000)(X(I),I=1,19,2),(X(I),I=2,20,2)                      GRAAL  16
      INO=IFIX(X(1))                                                      GRAAL  17
      ITEMP=IFIX(X(2))                                                    GRAAL  18
      K=0                                                                 GRAAL  19
      DO 6 I=4,20,2                                                       GRAAL  20
      IF(X(I-1))5,4,5                                                     GRAAL  21
      IF(X(I))5,6,5                                                       GRAAL  22
      K=K+1                                                               GRAAL  23
      X(K)=X(I-1)                                                         GRAAL  24
      Y(K)=X(I)                                                           GRAAL  25
      CONTINUE                                                            GRAAL  26
      CALL GRYLL(K,X,Y,A,B,C)                                             GRAAL  27
      WRITE(ILP,3001)INO,ITEMP,A,C                                        GRAAL  28
      GO TO 1                                                             GRAAL  29
      END                                                                 GRAAL  30

ATURES SUPPORTED
ONE WORD INTEGERS
IOCS

RE REQUIREMENTS FOR GRAAL
OMMON        0   VARIABLES      112   PROGRAM      308
```

```
AGE   1    ENG0172C

* JCB    1001 2001                       2CC1      *ENG01720

JG CRIVE   CART SPEC   CART AVAIL  PHY DRIVE
 0000        1001        1001        COCO
 0001        2001        2001        0002
                         1002        0001

? M11   CCNFIG  8K

CAT VERSION D.M. SYSTEM V1 M02
```

' FCR FREE FORMAT INPUT

```
NAME GREAC
LIST SOURCE PROGRAM
ONE WORD INTEGERS
      SUBROUTINE GREAC(IPR,N,OUT)                                        GREAC   1
      DIMENSION OUT(1 ),INPUT(72),KINC(15)                               GREAC   2
      DATA KIND/' ','/','0','1','2','3','4','5','6','7','8','9','.','-'  GREAC   3
     1,',','/                                                            GREAD   4
)     FORMAT(72A1)                                                       GREAD   5
 READ INPUT RECORC.                                                      GREAC   6
      READ(IPR,40)(INPUT(I),I=1,72)                                      GREAC   7
 TEST ARRAY SUBSCRIPT RANGE                                              GREAC   8
      IS=1                                                               GREAC   9
      IF(N)19,19,1                                                       GREAC  10
      IF(N-36)3,3,2                                                      GREAC  11
      NN=36                                                              GREAD  12
      GC TC 4                                                            GREAC  13
      NN=N                                                               GREAD  14
 INITIALIZE                                                              GREAC  15
      DO 5 I=1,NN                                                        GREAD  16
      OUT(I)=0.                                                          GREAC  17
 SEPARATE THE CATA WORDS                                                 GREAC  18
      DO 18 I=1,NN                                                       GREAC  19
 SKIP LEADING BLANKS                                                     GREAD  20
      DO 51 K=IS,72                                                      GREAC  21
      DO 51 L=2,15                                                       GREAD  22
      IF(INPUT(K)-KIND(L))51,52,51                                       GREAD  23
l     CCNTINUE                                                           GREAC  24
      GC TC 19                                                           GREAC  25
 START NEW CATA WORD                                                     GREAD  26
2     IS=K                                                               GREAC  27
      IF=IS+7                                                            GREAC  28
      IF(IF-72)7,7,6                                                     GREAD  29
      IF=72                                                              GREAD  30
      SIGN=1.                                                            GREAD  31
      IDP=C                                                              GREAD  32
      MM=0                                                               GREAD  33
 SEPARATE AND IDENTIFY DATA CHARACTERS                                   GREAD  34
      DC 16 J=IS,IF                                                      GREAC  35
      DO 8 K=1,15                                                        GREAC  36
      IF(INPUT(J)-KIND(K))8,9,8                                          GREAC  37
      CONTINUE                                                           GREAD  30
      GC TC 16                                                           GREAC  31
      IF(K-2)16,17,10                                                    GREAD  32
)     IF(K-13)13,14,11                                                   GREAD  33
l     IF(K-15)12,17,17                                                   GREAD  34
```

```
12      SIGN=SIGN*(-1.)                                                     GREAD 35
        GC TC 16                                                            GREAC 36
C BUILD CATA VALUE                                                          GREAC 37
13      OUT(I)=OUT(I)*10.+FLOAT(K-3)                                        GREAC 38
        IF(MM)16,16,15                                                      GREAD 39
14      IF(ICP)142,142,141                                                  GREAC 40
141     IDP=MM                                                              GREAD 41
142     IDP=ICP+1                                                           GREAC 42
15      MM=MM+1                                                             GREAC 43
16      CONTINUE                                                            GREAC 44
        J=J-1                                                               GREAD 45
17      IS=J+1                                                              GREAC 46
C INSERT CECIMAL PCINT ANC SIGN                                             GREAC 47
        OUT(I)=OUT(I)*SIGN*(10.**(IDP-MM))                                  GREAC 48
        IF(IS-72)18,18,19                                                   GREAD 49
18      CONTINUE                                                            GREAD 50
19      RETURN                                                              GREAC 51
        ENC                                                                 GREAC 52

FEATURES SUPPORTEC
 CNE WCRC INTEGERS

CORE REQUIREMENTS FCR GREAC
 CCMMCN       0  VARIABLES     106  PROGRAM     37C

RELATIVE ENTRY POINT ACDRESS IS C07C (HEX)

END CF CCMPILATION

// CUP

*DELETE                GREAC      2CC1
CART ID 2001   CB ACCR  1220   DB CNT    0018

*STORE       WS  UA  GREAD      2001  2001
CART ID 2001   DB ACDR  1850   DB CNT    001B
```

```
PAGE   1     E0000295

// JOB    1001 1002                           1002        *E0000295

LOG DRIVE   CART SPEC   CART AVAIL  PHY DRIVE
  0000         1001        1001        0000
  0001         1002        1002        0001

V2 M11   CONFIG  8K

CAT VERSION D.M. SYSTEM V1 M02

// FOR                         STRAIGHT-LINE OPTIMISATION
*NAME GRYLL
*LIST SOURCE PROGRAM
*ONE WORD INTEGERS
      SUBROUTINE GRYLL(K,X,Y,N,A,B,C,D,E,F)                            GRYLL   1
      DIMENSION X(1),Y(1)                                              GRYLL   2
      A=0.                                                             GRYLL   3
      B=0.                                                             GRYLL   4
      C=0.                                                             GRYLL   5
      D=0.                                                             GRYLL  A5
      E=0.                                                             GRYLL  B5
      F=0.                                                             GRYLL  C5
      AGGR=FLOAT(K)                                                    GRYLL  D5
      IF(K-2)16,16,1                                                   GRYLL   6
C INITIALISE STORAGE                                                    GRYLL   7
1     XTOT=0.                                                          GRYLL   8
      YTOT=0.                                                          GRYLL   9
      XYTOT=0.                                                         GRYLL  10
      X2TOT=0.                                                         GRYLL  11
      Y2TOT=0.                                                         GRYLL  12
      COVAR=0.                                                         GRYLL  13
      VARX=0.                                                          GRYLL  14
      VARY=0.                                                          GRYLL  15
      SUMX=0.                                                          GRYLL  16
      SUMY=0.                                                          GRYLL  17
C CENTRALISE AXES                                                       GRYLL  18
      DO 2 I=1,K                                                       GRYLL  19
      SUMX=SUMX+X(I)                                                   GRYLL  20
2     SUMY=SUMY+Y(I)                                                   GRYLL  21
      XMEAN=SUMX/AGGR                                                  GRYLL  22
      YMEAN=SUMY/AGGR                                                  GRYLL  23
      DO 3 I=1,K                                                       GRYLL  24
      X(I)=X(I)-XMEAN                                                  GRYLL  25
      Y(I)=Y(I)-YMEAN                                                  GRYLL  26
C COMPUTE TOTALS                                                        GRYLL  27
      XTOT=XTOT+X(I)                                                   GRYLL  28
      YTOT=YTOT+Y(I)                                                   GRYLL  29
      XYTOT=XYTOT+X(I)*Y(I)                                            GRYLL  30
      X2TOT=X2TOT+X(I)*X(I)                                            GRYLL  31
      Y2TOT=Y2TOT+Y(I)*Y(I)                                            GRYLL  32
3     CONTINUE                                                         GRYLL  33
C COMPUTE SAMPLE MEAN VALUES                                            GRYLL  34
      XBAR=XTOT/AGGR                                                   GRYLL  35
      YBAR=YTOT/AGGR                                                   GRYLL  36
      XYBAR=XYTOT/AGGR                                                 GRYLL  37
      X2BAR=X2TOT/AGGR                                                 GRYLL  38
      Y2BAR=Y2TOT/AGGR                                                 GRYLL  39
```

```
      DO 4 I=1,K                                                    GRYLL 40
 COVARIANCE                                                         GRYLL 41
      COVAR=COVAR+(X(I)-XBAR)*(Y(I)-YBAR)                           GRYLL 42
 VARIANCES                                                          GRYLL 43
      VARX=VARX+(X(I)-XBAR)*(X(I)-XBAR)                             GRYLL 44
      VARY=VARY+(Y(I)-YBAR)*(Y(I)-YBAR)                             GRYLL 45
 CORRELATION COEFFICIENT                                            GRYLL 46
      C=COVAR/SQRT(VARX*VARY)                                       GRYLL 47
      IF(N-2)5,6,6                                                  GRYLL 48
 SOLUTION BY X-REGRESSION                                           GRYLL 49
 SLOPE OF LINE                                                      GRYLL 50
      A=VARY/COVAR                                                  GRYLL 51
 VARIANCE OF DEVIATIONS                                             GRYLLA51
      S=(VARX-COVAR*COVAR/VARY)/FLOAT(K-2)                          GRYLLB51
 S.E. OF SLOPE                                                      GRYLLC51
      D=SQRT(S/VARY)                                                GRYLLD51
      D=D*A*A                                                       GRYLLE51
 S.E. OF INTERCEPT                                                  GRYLLF51
      E=SQRT(S*(1./AGGR+YBAR*YBAR/VARY))                            GRYLLG51
      E=-E*A                                                        GRYLLH51
      GO TO 7                                                       GRYLL 52
 SOLUTION BY Y-REGRESSION                                           GRYLL 53
 SLOPE OF LINE                                                      GRYLL 54
      A=COVAR/VARX                                                  GRYLL 55
 VARIANCE OF DEVIATIONS                                             GRYLLA55
      S=(VARY-COVAR*COVAR/VARX)/FLOAT(K-2)                          GRYLLB55
 S.E. OF SLOPE AND INTERCEPT                                        GRYLLC55
      D=SQRT(S/VARX)                                                GRYLLD55
      E=SQRT(S*(1./AGGR+XBAR*XBAR/VARX))                            GRYLLE55
 INTERCEPT                                                          GRYLL 56
      B=YBAR-A*XBAR                                                 GRYLL 57
      IF(N-2)14,14,8                                                GRYLL 58
 SOLUTION BY DOUBLE REGRESSION                                      GRYLL 59
 SUM OF SQUARES OF PERPENDICULAR DISTANCES                          GRYLL 60
      PD2=0.                                                        GRYLL 61
      DO 9 I=1,K                                                    GRYLL 62
      PD2=PD2+(A*X(I)-Y(I)+B)*(A*X(I)-Y(I)+B)                       GRYLL 63
      PD2=PD2/(A*A+1.)                                              GRYLL 64
 OPTIMISATION OF MEAN SQUARE DISTANCE                               GRYLL 65
 PERPENDICULAR DISTANCE OF CENTROID                                 GRYLL 66
0     PDCEN=(A*XBAR-YBAR+B)/(1.+A*A)                                GRYLL 67
 INTERIM VALUES                                                     GRYLL 68
      F=F+1.                                                        GRYLLA68
      STOR1=2.*AGGR/(1.+A*A)                                        GRYLL 69
      STOR2=B*XBAR-XYBAR                                            GRYLL 70
      STOR3=Y2BAR - X2BAR + B*(B - 2.*YBAR)                         GRYLL 71
 FIRST DIFFERENTIAL COEFFICIENTS                                    GRYLL 72
      GRDA=STOR1*(STOR2-(A/(1.+A*A))*(STOR3+2.*A*STOR2))            GRYLL 73
      GRDB=2.*AGGR*PDCEN                                            GRYLL 74
 SECOND DIFFERENTIAL COEFFICIENTS                                   GRYLL 75
      GRDA2=STOR1*(STOR3-2.*A*(3.+A*A)*STOR2-3.*A*A*X2BAR)/((1.+A*A)* GRYLL 76
     1(1.+A*A))                                                     GRYLL 77
      GRDB2=STOR1                                                   GRYLL 78
      GRDAB=STOR1*(XBAR-2.*A*PDCEN)                                 GRYLL 79
 INVERSION OF THE HESSIAN MATRIX                                    GRYLL 80
 DETERMINANT                                                        GRYLL 81
      DET=GRDA2*GRDB2-GRDAB*GRDAB                                   GRYLL 82
```

```
'AGE   3    E0000295

      DET=DET*(-1.)                                                    GRYLL 83
      IF(DET)11,14,11                                                  GRYLL 84
 INVERTED MATRIX                                                       GRYLL 85
1     H1=GRDB2/DET                                                     GRYLL 86
      H2=-GRDAB/DET                                                    GRYLL 87
      H3=H2                                                            GRYLL 88
      H4=GRDA2/DET                                                     GRYLL 89
 NEW VALUES OF SLOPE AND INTERCEPT                                     GRYLL 90
      AA=A+H1*GRDA+H2*GRDB                                             GRYLL 91
      BB=B+H3*GRDA+H4*GRDB                                             GRYLL 92
 NEW VALUE OF SUM OF SQUARES OF PERPENDICULAR DISTANCES                GRYLL 93
      SUM=0.                                                           GRYLL 94
      DO 12 I=1,K                                                      GRYLL 95
2     SUM=SUM+(AA*X(I)-Y(I)+BB)*(AA*X(I)-Y(I)+BB)                      GRYLL 96
      SUM=SUM/(AA*AA+1.)                                               GRYLL 97
 TEST FOR VALIDITY OF CORRECTION                                       GRYLL 98
      OPT=(PD2-SUM)/PD2                                                GRYLL 99
      IF(OPT)131,131,13                                                GRYLL100
 [illegible]PLY CORRECTIONS                                            GRYLL101
3     A=AA                                                             GRYLL102
      B=BB                                                             GRYLL103
      PD2=SUM                                                          GRYLL104
      IF(1.-(OPT*1.E04))10,14,14                                       GRYLL105
31    F=-F                                                             GRYLLA05
 REPLACE AXES                                                          GRYLL106
4     DO 15 I=1,K                                                      GRYLL107
      X(I)=X(I)+XMEAN                                                  GRYLL108
5     Y(I)=Y(I)+YMEAN                                                  GRYLL109
      B=B+YMEAN-A*XMEAN                                                GRYLL110
6     RETURN                                                           GRYLL111
      END                                                              GRYLL112

EATURES SUPPORTED
ONE WORD INTEGERS

ORE REQUIREMENTS FOR GRYLL
COMMON       0  VARIABLES      86  PROGRAM    1058

ELATIVE ENTRY POINT ADDRESS IS 0062 (HEX)

ND OF COMPILATION
```

```
PAGE   1    CCSTF675

// JOB    1001 1002                          1002     *CCSTF675

LOG DRIVE   CART SPEC   CART AVAIL   PHY DRIVE
  0000        1001        1001         0000
  0001        1002        1002         0001

V1 M00   CONFIG  8K

CCAT VERSION D.M. SYSTEM V1 M00
                                GRAPH  PLOTTING
// FOR
*IOCS(CARD,1132 PRINTER,PLOTTER)
*IOCS(CARD,TYPEWRITER,KEYBOARD,1132 PRINTER,PAPER TAPE,DISK)
*ONE WORD INTEGERS
*LIST SOURCE PROGRAM
      DIMENSION RESIS(16), RUN(16,4)  ,TITLE(6)
      DATA B/'    '/
C   READ TITLEIF BLANK  FINISH
7     READ(2,100) TITLE
      IF(TITLE(1)-B) 20,21,20

C   MOVE  PEN  TO  L.H.S. AND PAPER FORWARD

20    CALL SCALF(1.0,1.0,0.,0.)
      CALL  FPLOT(1,  7.6,13.0)
      CALL SCALF(1.0,1.0,0.,0.)

C DRAW 3 LINES TO DIVIDE GRAPHS AND GO BACK TO L.H.S.
      CALL FPLOT(1,0.0,-0.85)
      CALL FPLOT(2,8.2,-0.85)
      CALL FPLOT(1,0.0,-6.2)
      CALL FPLOT(2,8.2,-6.2)
      CALL FPLOT(1,0.0,-11.6)
      CALL FPLOT(2,8.2,-11.6)
      CALL FPLOT(1,0.0,0.0)

C   WRITE TITLE
      CALL FCHAR(1.0,-.8 ,0.2,0.2,0.0)
      WRITE(7,100)TITLE
100   FORMAT(6A4)
      CALL FPLOT(1,1.,0.)
      DO 16 L=1,2
      CALL SCALF(1.0,1.0,0.,0.)


      DO 2  I=1,16
      READ(2,102) RESIS(I),(RUN(I,K),K=1,4)

C IF FIRST RESISTANCE IS ZERO  NO COMPRESSION DATA
      IF(RESIS(1))6,7,6
C IF RESISTANCE IS ZERO STOP READING AND CALCULATE RANGE
6     IF(RESIS(I))2,3,2
2     CONTINUE
C     FIND RANGE OF RESISTANCES
102   FORMAT(F9.3,4(1X,F6.4))
3      II=I-1
```

```
      RANGE  =  RESIS(II)- RESIS(1)
      IF(L-1)14,13,14

C  TOP IS TOP OF GRAPH AREA
13    TOP =-1.
      GO TO 15
 14   TOP =-6.35
 15   CALL FCHAR(1.0,-.5+TOP,0.2,0.2,0.0)
      IF(L-1)19,17,19

C   WRITE  GRAPH DESCRIPTION
17    WRITE(7,101)
 101  FORMAT('TENSION     ')
      GO TO 18
19    WRITE(7,107)
107   FORMAT('COMPRESSION')
18    CALL SCALF(1.0,1.0,3.0,0.)
      CALL FPLOT(1,1. ,8.0)
      BACK =RANGE-(TOP*RANGE/5.)

C  CHANGE SCALE AND ORIGIN FOR PLOTTING
      CALL SCALF(1/0.02,5./RANGE,-.052,BACK)


C NOW FOR THE ACTUAL PLOTTING
      DO   4 J=1,II
      Y=RESIS(J)-RESIS(1)
       CALL FCHAR(-0.08,Y,.1,.1,0)
      IF(RESIS(J)-9999.)10,10,11
10     WRITE(7,201) RESIS(J)
201   FORMAT(F9.3)
      GO TO 12
11    WRITE(7,203) RESIS(J)
203    FORMAT(F9.2)
12    DO   4 K=1,4

C  IF X VALUE IS 1. DON'T PLOT
      IF(RUN(J,K)-1.)5,4,5
5     CALL FCHAR(RUN(J,K),Y         ,0.1,0.1,0.0)
      WRITE(7,200) K
200   FORMAT(I1)
4     CONTINUE

C    DRAW  X-AXIS
      CALL FGRID(0,-.050,0,0.05,2)
      X=-.1
      DO 9 I=1,3
      X=X+0.05
      CALL FCHAR(X-.005,         -.17*RANGE/5.,.08,.08,0)
9     WRITE(7,202) X
202   FORMAT(F5.2)

C   LINE UP FOR NEXT GRAPH
       CALL FPLOT(1,-.076, BACK)
16    CONTINUE
      GO TO 7
```

```
PAGE   3    CCSTF675

21     CALL EXIT
       END

FEATURES SUPPORTED
 ONE WORD INTEGERS
 IOCS

CORE REQUIREMENTS FOR
 COMMON        0  VARIABLES     198   PROGRAM     630

END OF COMPILATION

// DUP

*DELETE                    IHGRF
CART ID 1002    DB ADDR   440F    DB CNT    002C

*STORE        WS   UA   IHGRF        1002  1002
CART ID 1002    DB ADDR   440F    DB CNT    002C
```

BENDING RIG FOR 1" STRAIN-GAUGE SUBSTRATES

Material:- Mild Steel, Duralumin, Brass, or Stainless Steel, except where stated.

All fixing screws may be 4 B.A. or 6 B.A.

Dimensions in Millimetres.

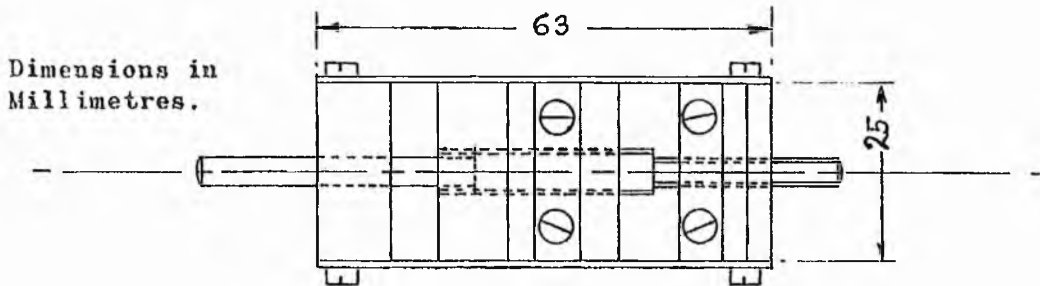

PLAN VIEW

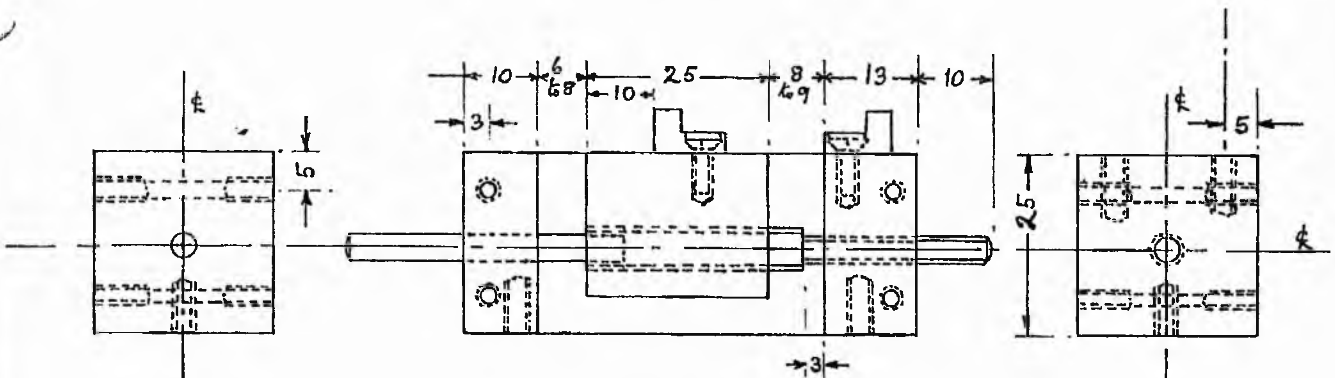

DETAIL A

Bearing Block. Reamed as a bearing for part C.

SIDE ELEVATION

Shown with one guide-plate removed.

DETAIL B

End Block. Tapped 4 B.A. to fit part C.

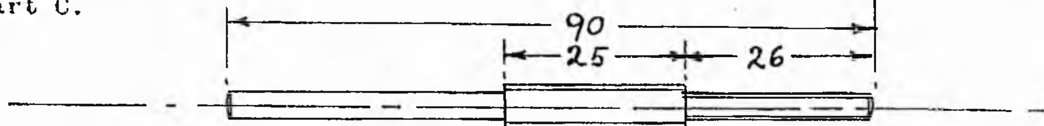

DETAIL C

Lead Screw. Material:- Silver Steel 4 mm dia., threaded 4 B.A. at one end. The sleeve, 6 mm O.D., is hard-soldered in position and threaded 0 B.A.

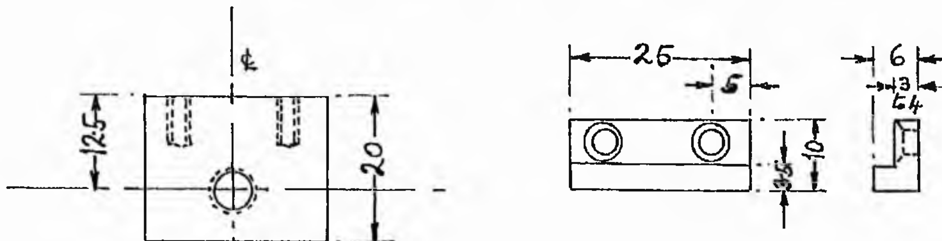

DETAIL D

Slide Block. Tapped 0 B.A. to fit part C.

DETAIL E

Work Holder. 2 off.

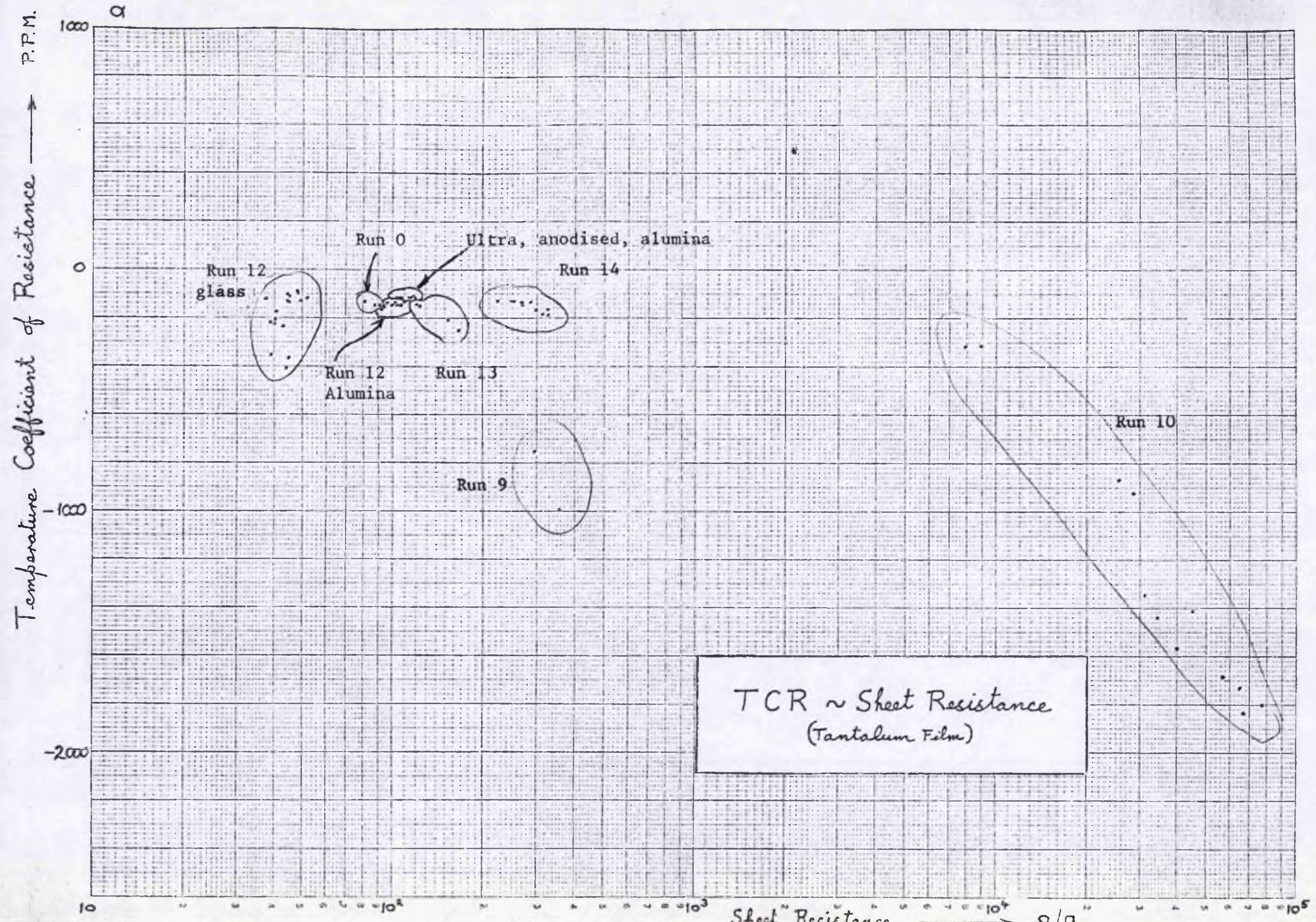
TCR ~ Sheet Resistance
(Tantalum Film)
Run 12
glass
Run 0
Ultra, anodised, alumina
Run 14
Run 12
Alumina
Run 13
Run 9
Run 10
α
1000
0
-1000
-2000
Temperature Coefficient of Resistance
P.P.M.
10
10²
10³
10⁴
10⁵
Sheet Resistance
Ω/□

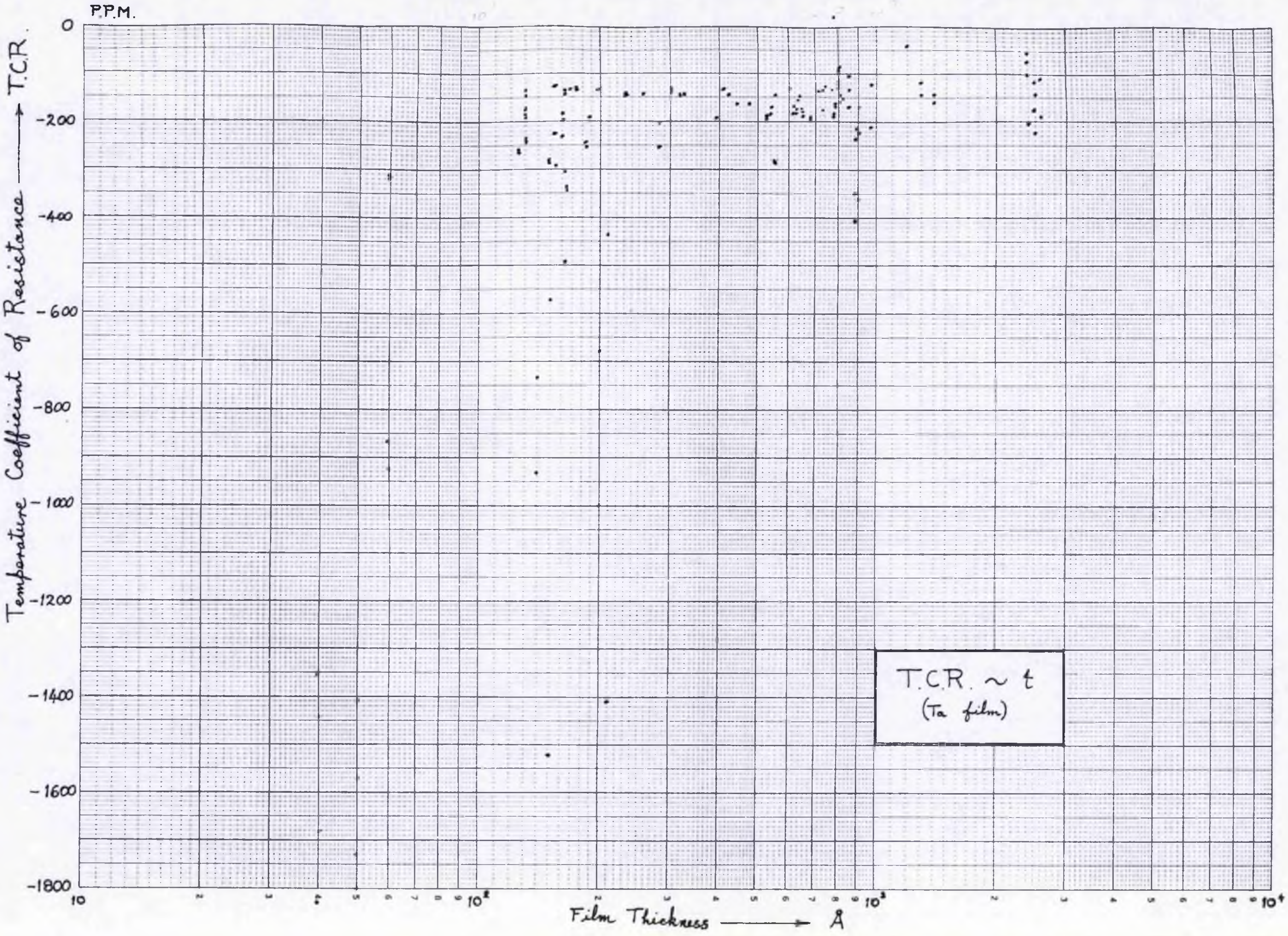
P.P.M.
Temperature Coefficient of Resistance → T.C.R.
0
-200
-400
-600
-800
-1000
-1200
-1400
-1600
-1800
10
10^2
10^3
10^4
Film Thickness → Å
T.C.R. ~ t
(Ta film)

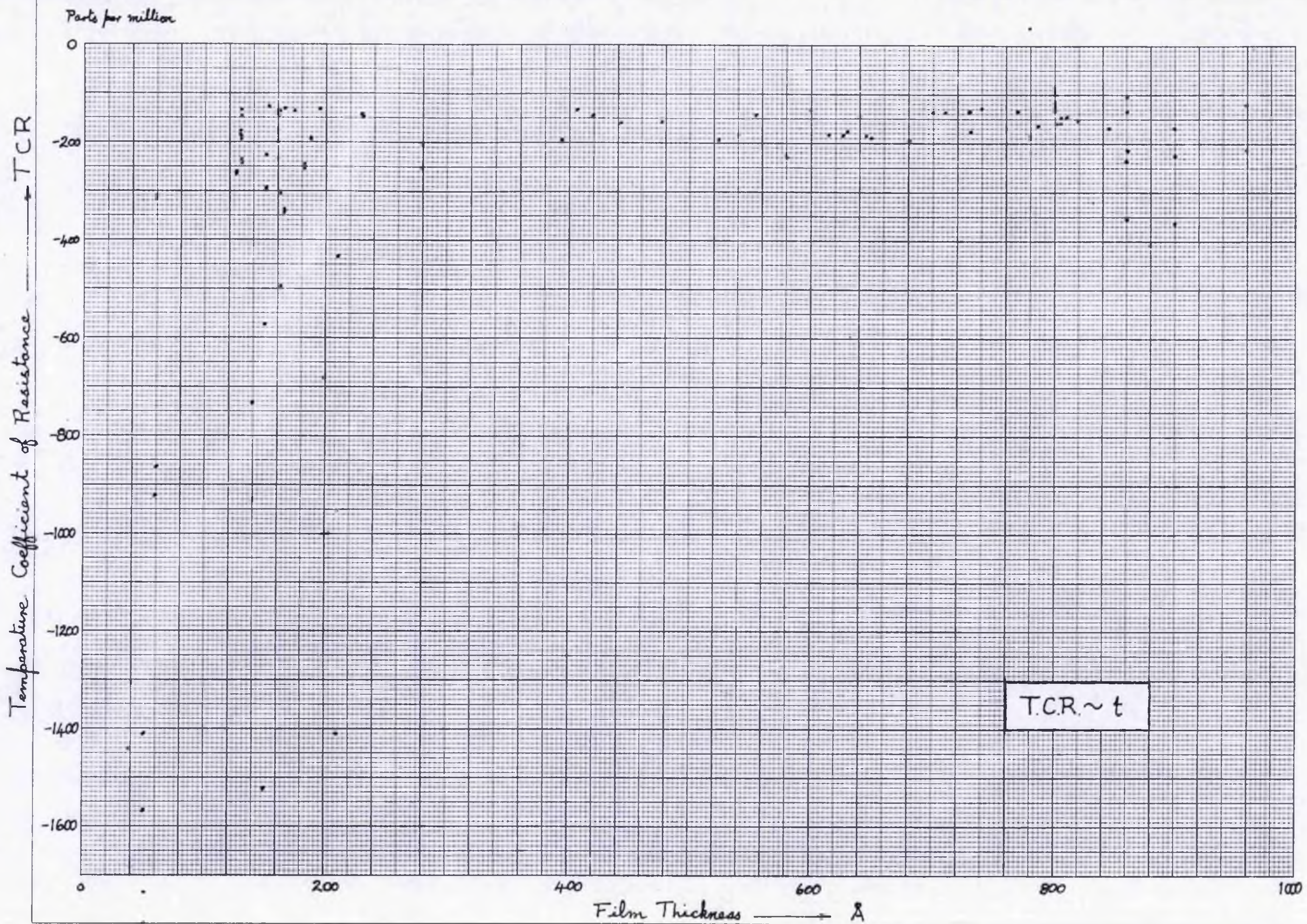
Parts per million
0
-200
-400
-600
-800
-1000
-1200
-1400
-1600
Temperature Coefficient of Resistance → TCR
T.C.R. ~ t
0
200
400
600
800
1000
Film Thickness → Å

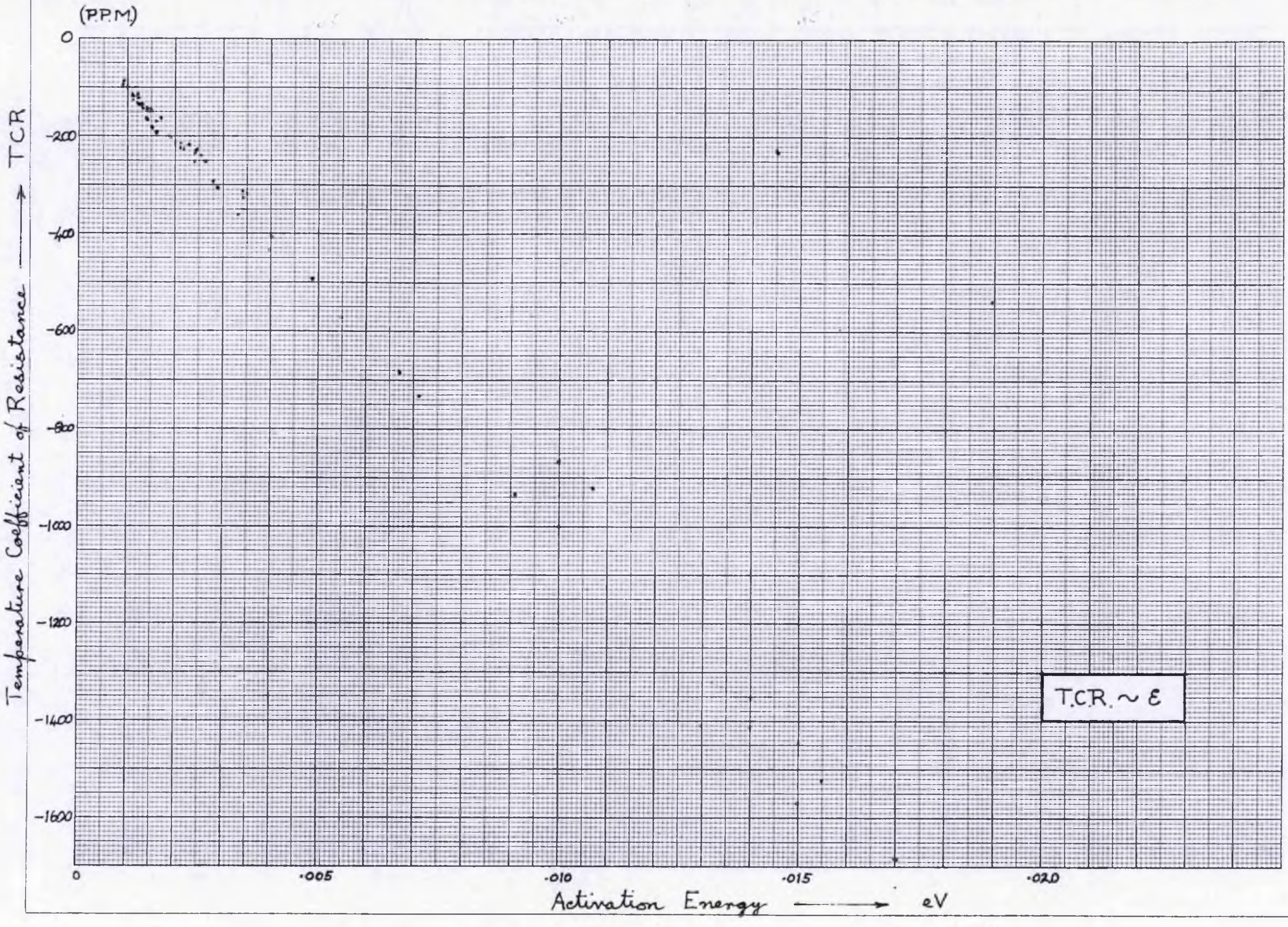
(P.P.M.)
Temperature Coefficient of Resistance ——→ TCR
0
-200
-400
-600
-800
-1000
-1200
-1400
-1600
T.C.R. ~ ε
0
·005
·010
·015
·020
Activation Energy ——→ eV

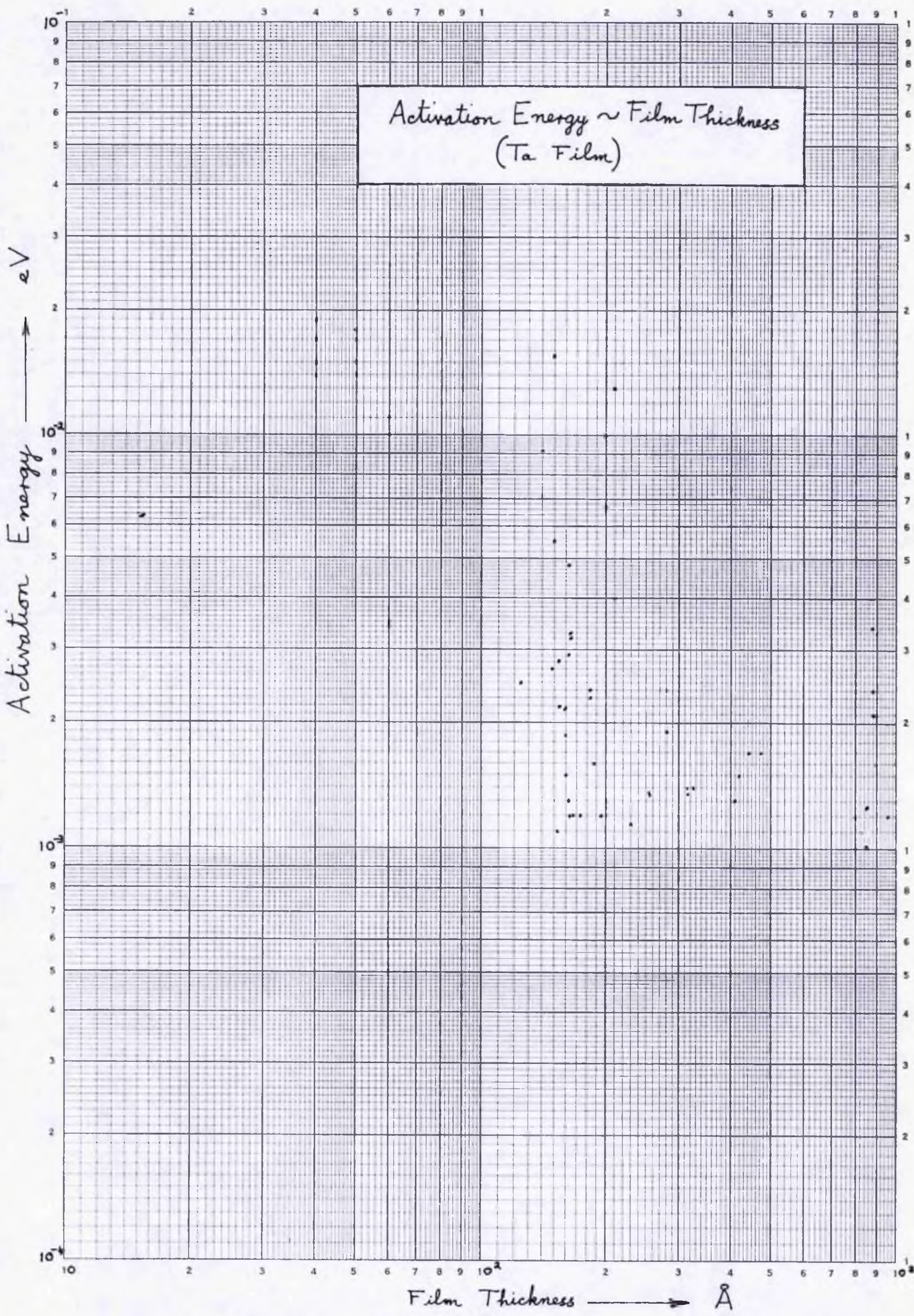

Activation Energy ~ Film Thickness
(Ta Film)
Activation Energy ——→ eV
Film Thickness ——→ Å
Log 3 Cycles x 2 Cycles
Graph Data Ref. 5932
WELL

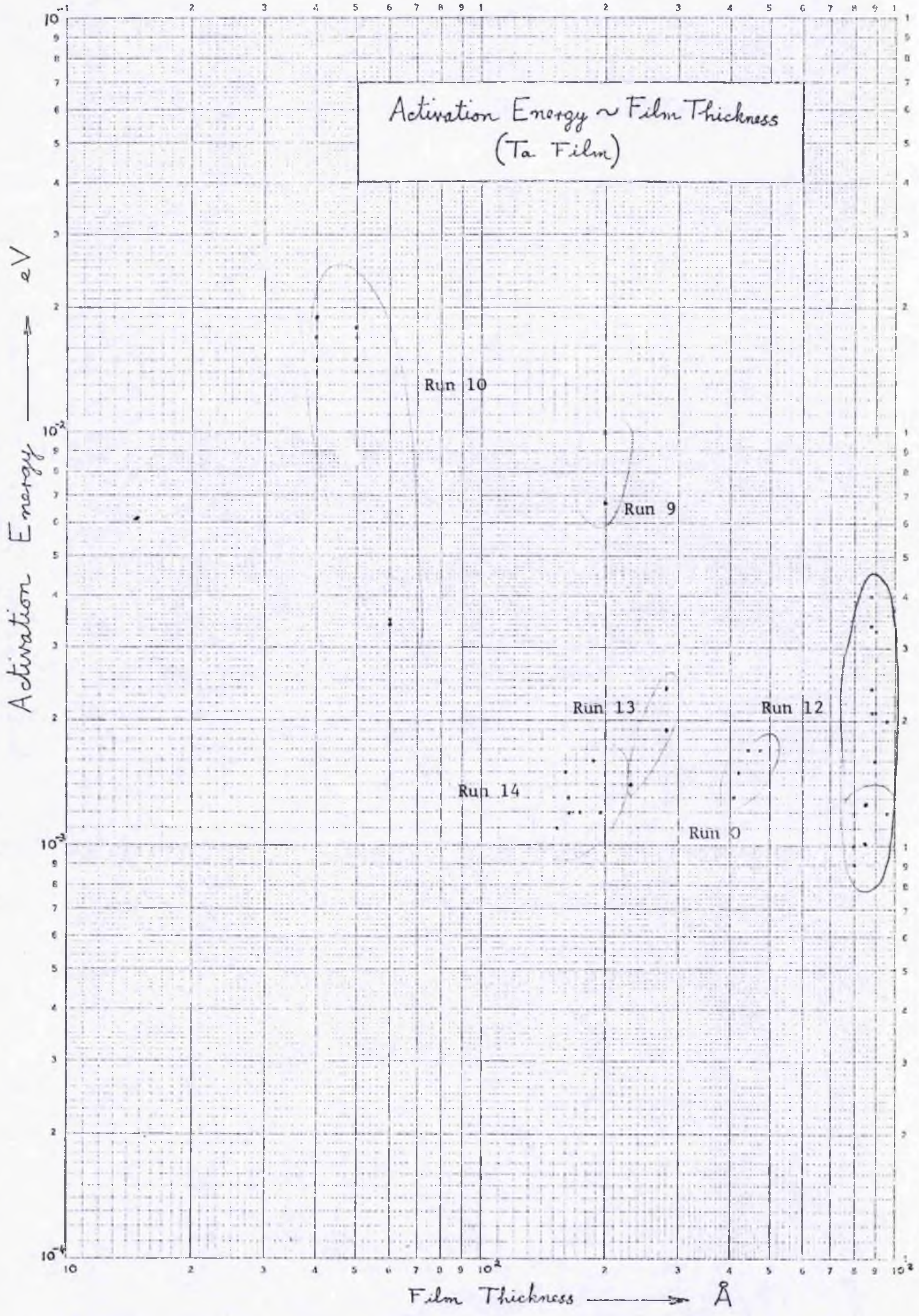

Activation Energy ~ Film Thickness
(Ta Film)
Run 10
Run 9
Run 13
Run 12
Run 14
Run 0
Activation Energy ——→ eV
Film Thickness ——→ Å
Log 3 Cycles x 2 C
Graph Data Ref. 5032

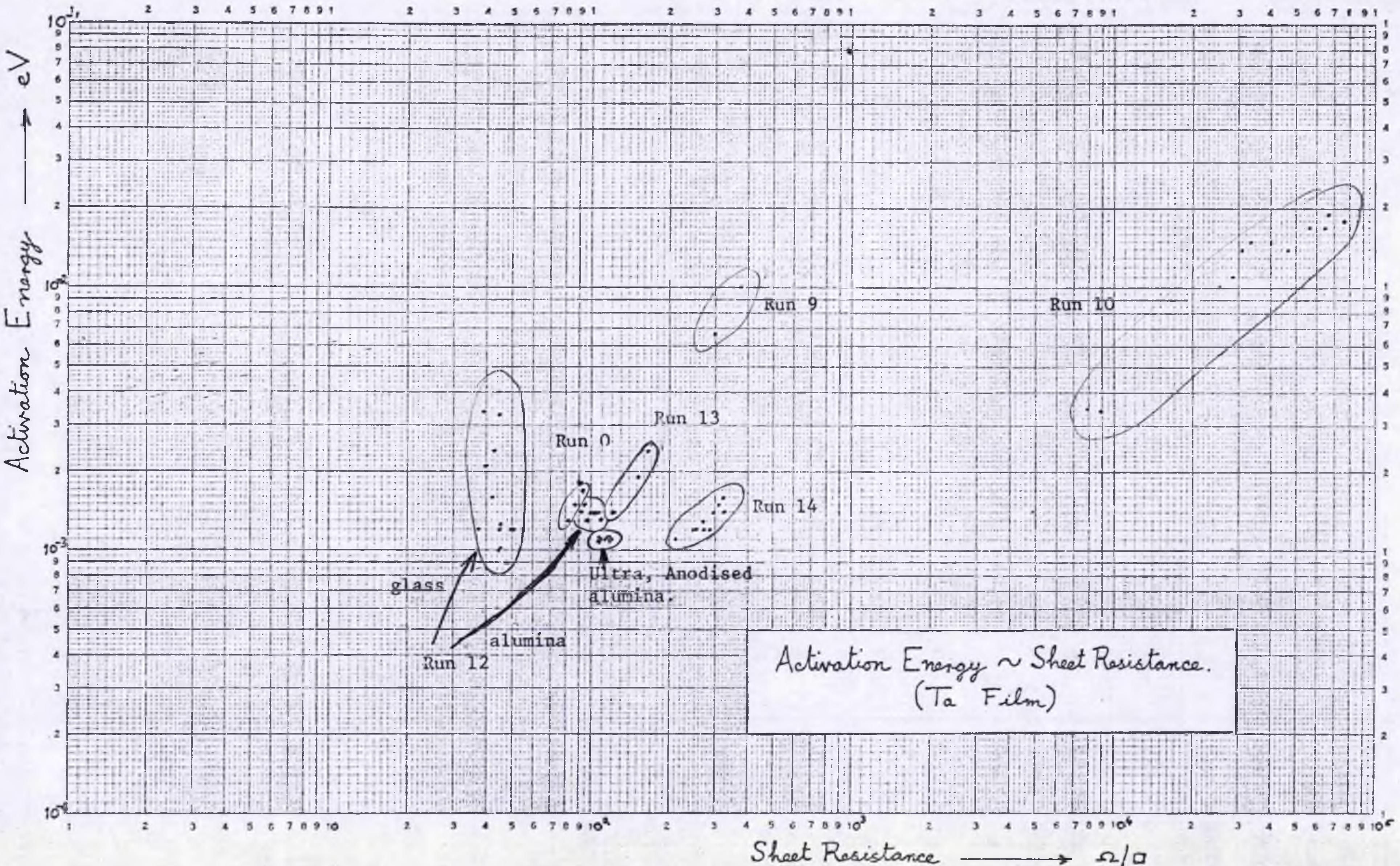
Graph Data Ref. 5935
Log 3 Cycles x 5 Cycles
Activation Energy ~ Sheet Resistance.
(Ta Film)
Run 9
Run 10
Run 13
Run 0
Run 14
Ultra, Anodised alumina.
glass
alumina
Run 12
Activation Energy → eV
Sheet Resistance → Ω/□

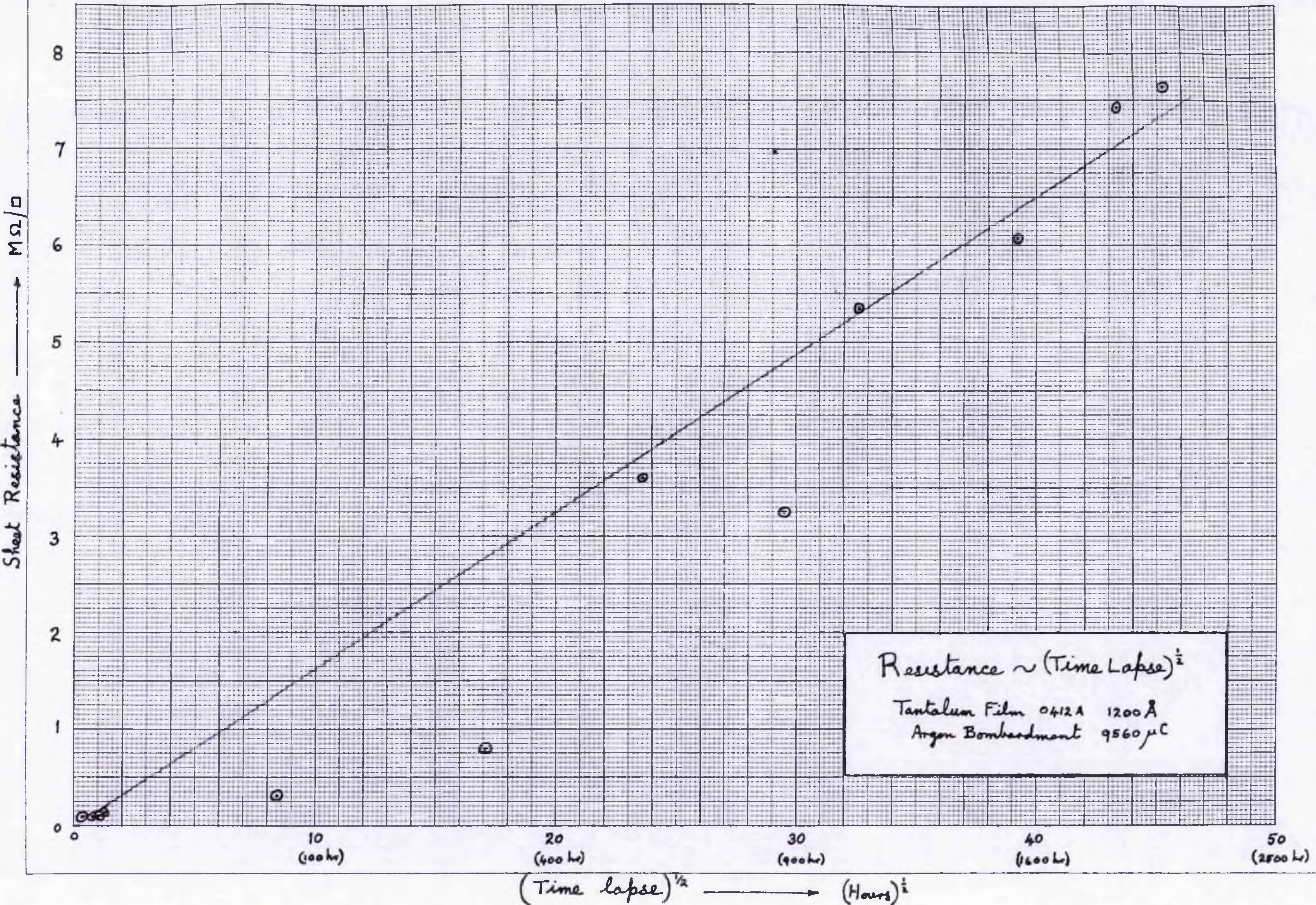

Resistance ~ (Time Lapse)^½
Tantalum Film 0412A 1200 Å
Argon Bombardment 9560 μC
Sheet Resistance → MΩ/□
0
1
2
3
4
5
6
7
8
(Time lapse)^½ → (Hours)^½
0
10 (100 hr)
20 (400 hr)
30 (900 hr)
40 (1600 hr)
50 (2500 hr)

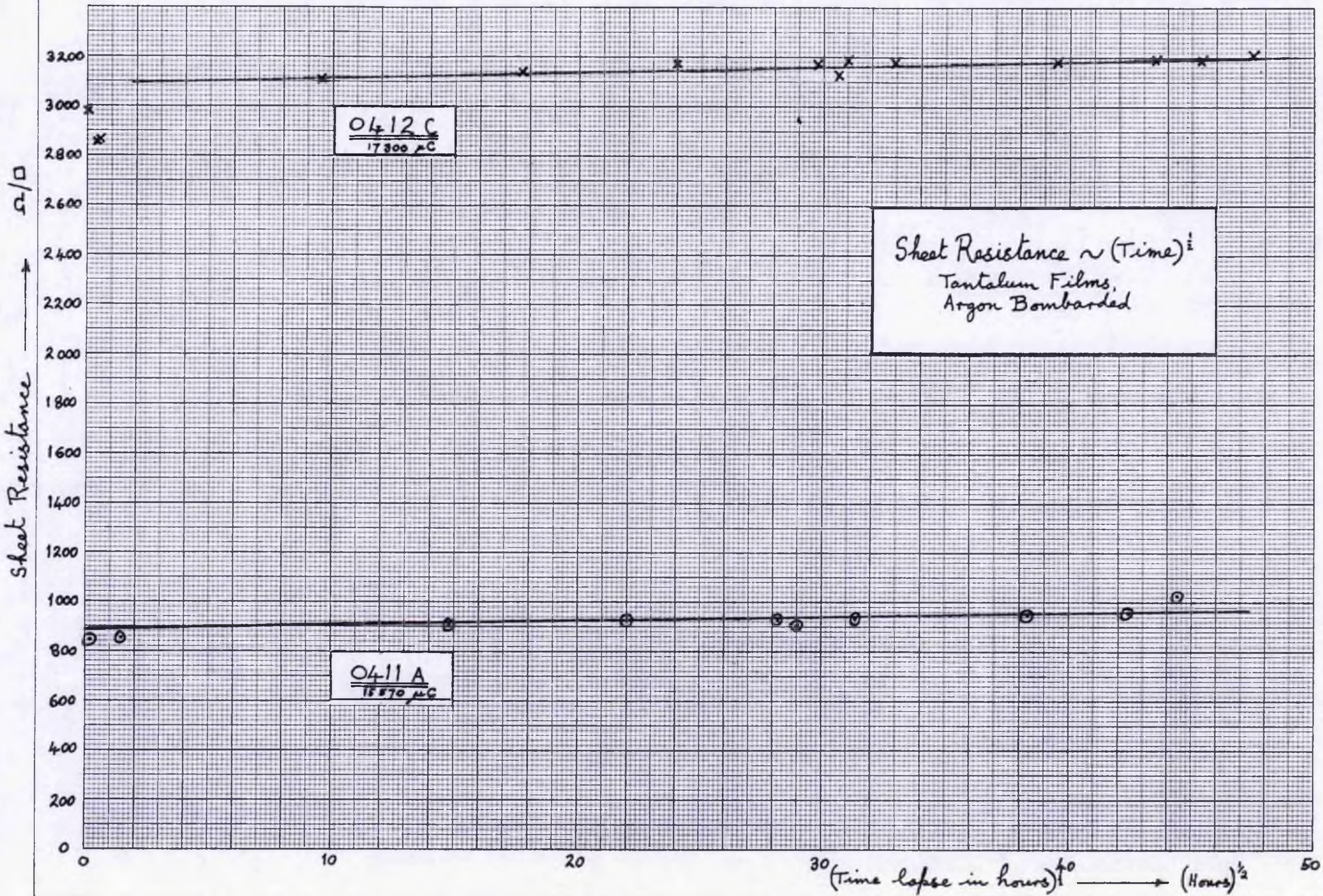

Sheet Resistance ~ (Time)^½
Tantalum Films,
Argon Bombarded
0412 C
17300 μC
0411 A
15570 μC
Sheet Resistance → Ω/□
(Time lapse in hours)^½ → (Hours)^½
0
200
400
600
800
1000
1200
1400
1600
1800
2000
2200
2400
2600
2800
3000
3200
10
20
30
40
50

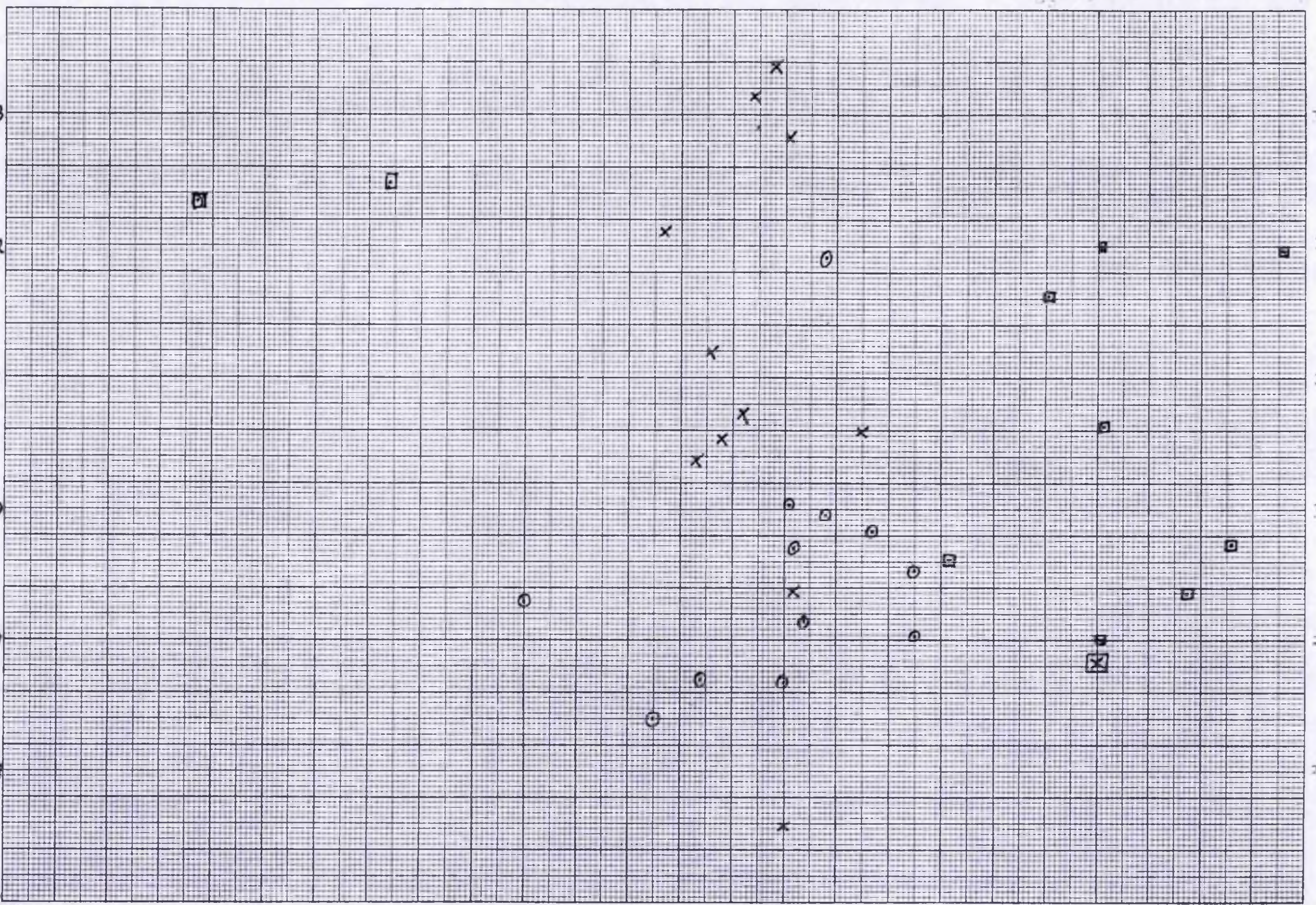

γ
before bomb
3.3
3.2
3.1
3.0
2.9
2.8
2.7
Strain - gauge factor
25
30
35
40
45
50
Sheet Resistance
Ω/□

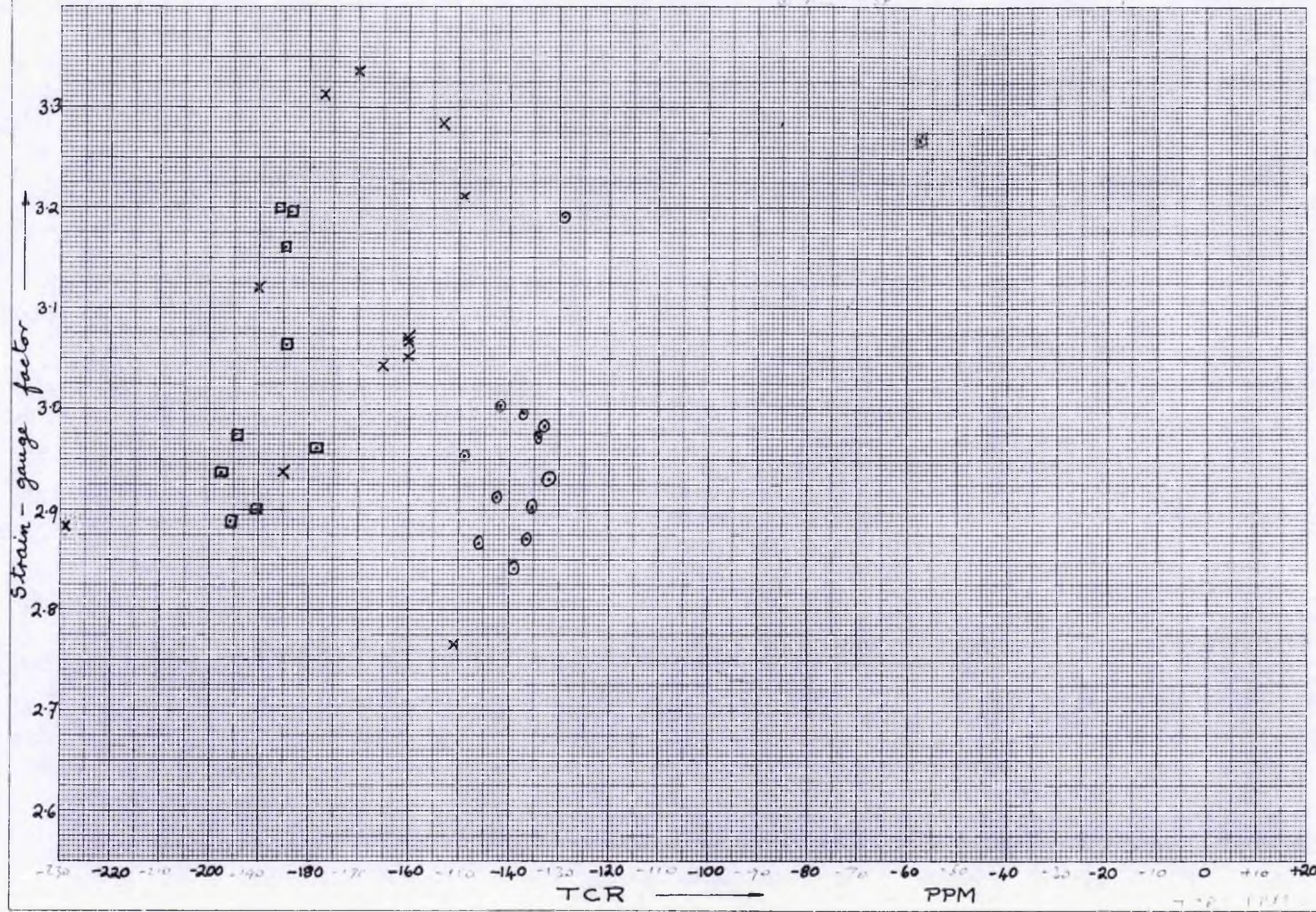
γ
3.3
3.2
3.1
3.0
2.9
2.8
2.7
2.6
Strain - gauge factor
-220
-200
-180
-160
-140
-120
-100
-80
-60
-40
-20
0
+20
TCR
PPM

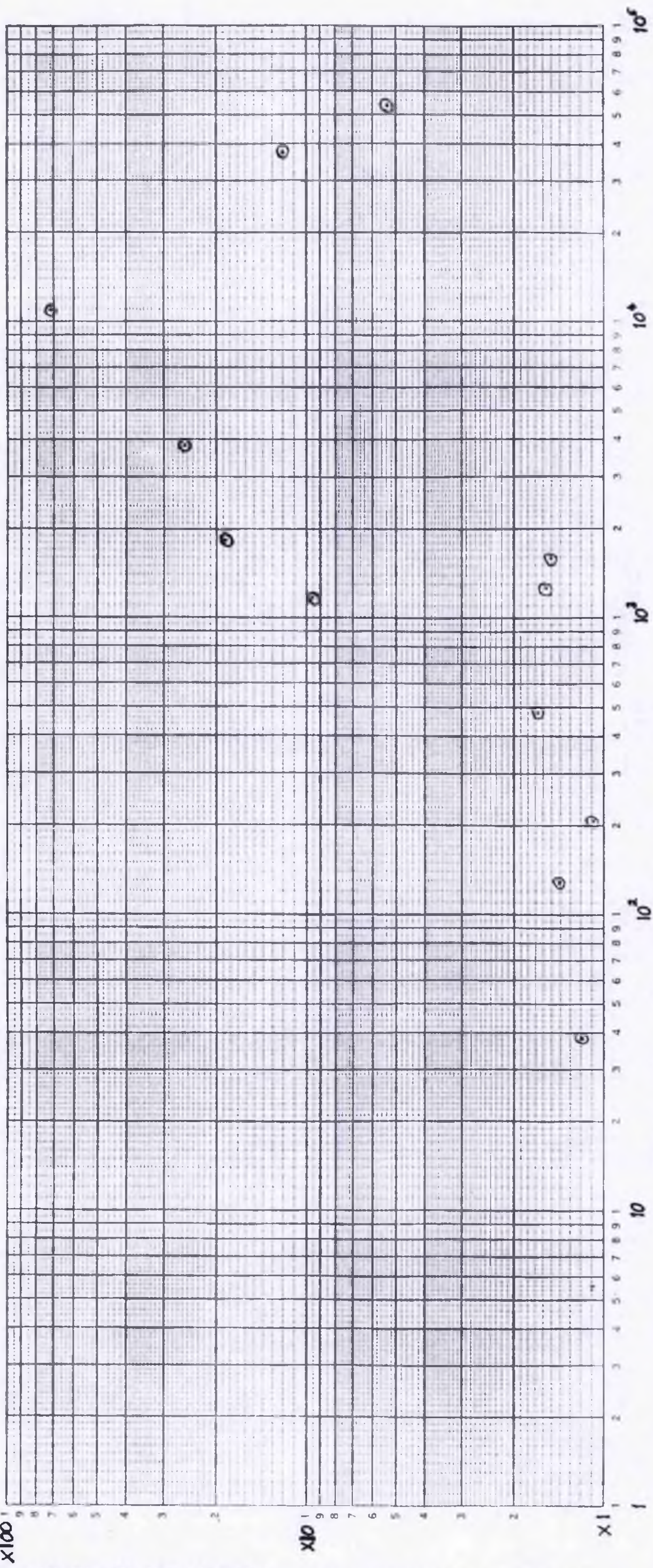

Relative Resistance ~ Resistance after 1000 Hours.
Gold Film.
Film Resistance after 1000 Hours —— Ω
Relative Resistance = Resistance after 1000 Hours / Resistance at bombardment.
X100
X10
X1
1
10
10²
10³
10⁴
10⁵
Graph Data Ref. 5925
Log 2 Cycles x 5 C

APPENDIX 3

STRAIN GAUGE FACTOR CORRECTION CALCULATIONS

(i) Virgin Gauge

$$\gamma_{REAL\ LONG} = \gamma_{APP\ LONG} \times \frac{\gamma_{APP\ SHORT}}{\gamma_{APP\ LONG}} \times \frac{\gamma_{REAL\ SHORT}}{\gamma_{APP\ SHORT}}$$

where: $\gamma_{REAL\ LONG}$ = Real strain gauge factor of virgin film

$\gamma_{APP\ LONG}$ = Strain gauge factor of virgin film assuming four point bending

$\frac{\gamma_{APP\ SHORT}}{\gamma_{APP\ LONG}}$ = Result of strain measurements on virgin film which had gold electrodes extended to bombardment area. Four point bending assumed.

$\frac{\gamma_{REAL\ SHORT}}{\gamma_{APP\ SHORT}}$ = Result of the calibration of the short geometry with micro-measurements strain gauge.

Evaluating we have:-

$$\gamma_{REAL\ LONG} = \gamma_{APP\ LONG} \times 1.06 \times 0.766$$

OR

$$\gamma_{REAL\ LONG} = \gamma_{APP\ LONG} \times 0.814$$

(ii) Implanted Film

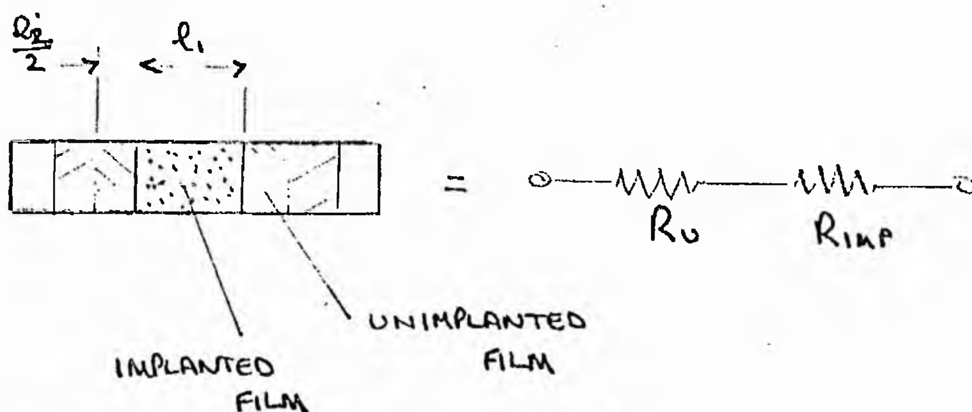

Now,

$$R_T = R_u + R_{IMP} \qquad \text{.........................} \quad (i)$$

where R_T = total resistance of compound film

R_u = resistance of unimplanted film

R_{IMP} = resistance of implanted film

Let the specimen be strained in the bending rig then:-

$$\Delta R_T = \Delta R_u + \Delta R_{IMP}$$

OR

$$\Delta R_T = R_u \gamma_u \varepsilon_2 + R_{IMP} \gamma_{IMP} \varepsilon_1 \qquad \text{.........................} \quad (ii)$$

where R_u = resistance, γ_u = strain gauge factor, ε_2 = strain } of the unimplanted film

R_{IMP} = resistance, γ_{IMP} = strain gauge factor, ε_1 = strain } of the implanted film

Now if we assume a relationship between the two strain levels:-

$$\varepsilon_2 = K\varepsilon_1 \qquad \text{.........................} \quad (iii)$$

substituting (iii) into (ii):-

$$\Delta R_T = R_u \gamma_u K \varepsilon_1 + R_{IMP} \gamma_{IMP} \varepsilon_1$$

thus:-

$$\frac{\Delta R_T/R_T}{\varepsilon_1} = \frac{R_u\gamma_u K + R_{IMP}\gamma_{IMP}}{R_u + R_{IMP}} \quad \text{.........................} \quad \text{(iv)}$$

Now:-

$$\gamma_{T(app)} = \frac{\Delta R_T/R_T}{\varepsilon_{app}} \quad \text{.........................} \quad \text{(v)}$$

where $\gamma_{T(app)}$ = apparent strain gauge factor of the combined gauge assuming 4 point bending

ε_{app} = apparent strain in specimen assuming 4 point bending.

But:-

$$\gamma_{T(app)} = \frac{\Delta R_T/R_T}{\varepsilon_1} \times \frac{\varepsilon_{real\ short}}{\varepsilon_{app\ short}} \quad \text{.........................} \quad \text{(vi)}$$

where $\frac{\varepsilon_{real\ short}}{\varepsilon_{app\ short}}$ = result from central region strain calibration $(= \frac{1}{0.766})$

thus substituting (iv) into (vi) we have:-

$$\gamma_{T\ APP} = \frac{R_u\gamma_u K + R_{IMP}\gamma_{IMP}}{R_u + R_{IMP}} \times \frac{1}{0.766} \quad \text{.........................} \quad \text{(vii)}$$

Determination of K

Now,

$$\ell_T = \ell_1 + \ell_2 \quad \text{.........................} \quad \text{(viii)}$$

where ℓ_T = total gauge length

ℓ_1 = length of implanted gauge

ℓ_2 = length of unimplanted gauge

Hence:-

$$\Delta\ell_T = \Delta\ell_1 + \Delta\ell_2$$

OR

$$\varepsilon_T\ell_T = \ell_1\varepsilon_1 + \ell_2\varepsilon_2 \quad \text{.........................} \quad \text{(ix)}$$

where ε_T = integrated strain over ℓ_T

ε_1 = integrated strain over ℓ_1

ε_2 = integrated strain over ℓ_2

From equation (ix):-

$$\varepsilon_2 = \frac{\varepsilon_T\ell_T - \ell_1\varepsilon_1}{\ell_2}$$

thus:-

$$K = \frac{\varepsilon_2}{\varepsilon_1} \quad \frac{(\varepsilon_T/\varepsilon_1)\ell_T - \ell_1}{\ell_2} \quad \text{.........................} \quad \text{(x)}$$

evaluating:-

ℓ_T = 1.3 cm

ℓ_1 = 0.67 cm

ℓ_2 = 0.63 cm

$$\frac{\varepsilon_T}{\varepsilon_1} = \frac{\varepsilon_{long}}{\varepsilon_{short}} = \frac{1}{1.06} \quad \text{(from part (i))}$$

therefore,

$$\underline{\underline{K = 0.879}}$$

Substituting this value of K into equation (vii)

$$\gamma_{T\,APP} = \frac{R_u \gamma_u\ 0.879 + R_{IMP} \gamma_{IMP}}{(R_u + R_{IMP})} \times \frac{1}{0.766}$$

and

$$\gamma_{IMP} = \frac{\gamma_{T\,APP} R_T\ 0.766 - R_u \gamma_u\ 0.879}{R_{IMP}}$$

Note

R_u can be determined from:-

$$R_u = \frac{\ell_2}{\ell_T} R_{B1}$$

where R_{B1} = resistance of gauge before implantation